To the Graduate Council:

I am submitting herewith a dissertation written by Sangeetha Rajagopalan entitled "Functional analysis of Chromodomain helicase DNA binding protein 2 (CHD2) mediated genomic stability." I have examined the final electronic copy of this dissertation for form and content and recommend that it be accepted in partial fulfillment of the requirements for the degree of Doctor of Philosophy, with a major in Life Science.

Sundaresan Venkatachalam, Major Professor

We have read this dissertation
and recommend its acceptance:

Bruce Mckee

Ranjan Ganguly

Mariano San Jose-Labrador

Seung J. Baek

Accepted for the Council:

Carolyn R. Hodges

Vice Provost and Dean of the Graduate School

(Original signatures are on file with official student records)

Functional Analysis of Chromodomain Helicase DNA Binding Protein 2(CHD2) mediated Genomic Stability

A Dissertation Presented for the

Doctor of Philosophy

Degree

The University of Tennessee, Knoxville

Sangeetha Rajagopalan

May 2010

ACKNOWLEDGEMENTS

First I would like to thank the Genome Science and Technology program at University of Tennessee for admitting me and giving me an opportunity to work on my doctoral studies in this prestigious university. I greatly appreciate the financial support provided by Dr. Cynthia Peterson, former Director of the Genome Science and Technology program during the duration of my doctoral studies.

I extend my sincere thanks to my PhD advisor, Dr. Sundar Venkatachalam, for giving me an excellent opportunity to work on such an exciting project. I extend my appreciation to Dr. Bruce Mckee, Dr. Ranjan Ganguly, Dr. Mariano Labrador and Dr. Seung Baek for serving in my thesis committee and giving constructive and insight suggestions which greatly aided in the progress of my project.

A special thanks to Dr. Prabakaran Nagarajan, a former post-doctoral associate in Dr. Venkatachalam's laboratory for training me initially in many of the molecular and cell culture techniques. I would like to thank George Samaan and under-graduate students Michelle Chi, Justin Nepa and Nathan Stebbins for helping me with some of the experiments. I would like to thank Savannah Arnold for editing and proofreading the thesis, Ryan Rickels for his assistance with some of the graphical works in the thesis and Richard Giannone for providing the necessary reagents and troubleshooting the problems faced in the proteomics work. I would like to thank Dr. Hayes McDonald and Appliedbiomics for performing the mass spectrometric analysis. I would also like to thank Dr. Karla J. Matteson and her laboratory staff for helping me with the cytogenetic work.

I would like to express my gratefulness to all my friends who have constantly supported and encouraged me during the course of the program. I would also like to thank my husband, parents, in-laws and sister. Without their support and encouragement I would not have reached till here. Special thanks to my husband, Vasudevan Hariharan who patiently tolerated all my emotional outbursts and supported me through all the ups and downs during the program.

ABSTRACT

Histone modifying enzymes and chromatin remodeling complexes play an important regulatory role in chromatin dynamics that dictate the interaction of regulatory factors involved in processes such as DNA replication, recombination, repair and transcription, with DNA template. The CHD (Chromodomain Helicase DNA Binding Protein) family of proteins is known to be involved in the regulation of gene expression, recombination and chromatin remodeling via their chromatin specific interactions and activities. Phenotypic analysis of the *Chd2* mutant mouse model developed by our laboratory indicates that the Chd2 protein plays a critical role in tumor suppression as the heterozygous mutant mice develop spontaneous lymphomas. In this study we demonstrate that mutation of *Chd2* renders cells susceptible to inefficient DNA repair and genomic instability. Homozygous and heterozygous *Chd2* mutant mouse embryonic fibroblast accumulates higher levels of gamma-H2AX after DNA damage. *Chd2* mutant cells show inefficiency in DNA repair of DNA lesions induced by X-rays and UV irradiation as assessed by single cell gel electrophoresis assays. These cells also exhibit increased chromosomal aberrations after treatment with low doses of X-ray irradiation (2 Gy) and show increased radiosensitivity in a clonogenic survival assay. At the molecular level, endogenous CHD2 protein level is induced after exposure to X-ray radiation. In addition, we have also demonstrated in this study that CHD2 is phosphorylated after DNA damage and is a potential substrate for phosphoinositide 3-kinase-related kinases (PIKK) - ATM/ATR. Additionally, mass spectrometric analysis showed possible association of CHD2 with the paraspeckle family of proteins known to be involved in an array of cellular processes specifically in RNA processing and DNA repair. An *in vivo* splicing assay demonstrated that CHD2 played a role in modulation of pre-mRNA splicing event. Collectively, our findings suggest that CHD2 is a multi-functional protein working with the paraspeckle protein complex to facilitate both the pre-mRNA splicing process and the initial DNA repair process. CHD2 may also be involved in the later stages of DNA damage response pathway by influencing p53's transcriptional activity.

Table of Contents

Chapter I 1

General Introduction 1

Structure of Chromatin 1

Histone modifying complexes 1

Histone acetylation 2

Histone methylation and demethylation 3

Histone phosphorylation 4

Chromatin remodeling complexes 4

The class of SWI/SNF 5

The class of ISWI 6

The class of INO80 7

The class of CHD proteins 8

Chromodomain helicase DNA binding protein 1 (CHD1) 9

Chromodomain helicase DNA binding proteins 3 and 4 (CHD3 and CHD4) 12

Chromodomain helicase DNA binding protein 5 (CHD5) 14

Chromodomain helicase DNA binding protein 6 (CHD6) 15

Chromodomain helicase DNA binding protein 7 (CHD7) 15

Chromodomain helicase DNA binding protein 8 (CHD8) 16

Chromodomain helicase DNA binding protein 9 (CHD9) 17

Chapter-II 19

Characterization of Chromodomain Helicase DNA Binding Protein 2 (Chd2) in mice 19

Introduction 19

Materials and Methods 21

cDNA synthesis and reverse transcriptase (RT)- polymerase chain reaction (PCR) 21

cDNA synthesis and Real time RT-PCR 22
Generation of polyclonal Chd2 antibodies 23
Immunofluorescence microscopy 23
Western blot analysis to confirm specificity of anti-Chd2 antibody 23
Results and Discussion 24
1.1 Analysis of expression pattern of mouse Chd2 transcript 24
1.2 Polyclonal antibody production and immuno-localization of CHD2 24
1.3 Mouse models of Chd2 25
1.4 Analysis of Chd2 expression in the N-terminal mutants 29
Significance of the study 29
Chapter III 34
Analysis of genomic stability and DNA repair process in *Chd2* 34
mutant cells 34
Introduction 34
The direct reversal pathway 34
The mismatch repair (MMR) pathway 35
The nucleotide excision repair (NER) pathway 35
The base excision repair (BER) pathway 36
The homologous recombination (HR) pathway 36
The non-homologous end joining (NHEJ) pathway 37
Chromatin remodeling and DNA repair 37
Chromodomain helicase DNA binding proteins and DNA repair 39
Material and Methods 40
Generation of Chd2 mouse embryonic fibroblast cells (MEFs) 40
Immortalization of Chd2 MEFs 40
Strand break detection using the alkaline comet assay 41
Analysis of metaphase chromosomes 41

MTT assay 42
Clonogenicity assay 43
Statistical analysis 43
Results 43
3.1. *Chd2* mutant cells are inefficient in repair of IR induced DNA damage. 43
3.2. Mutation in *Chd2* promotes chromosomal instability. 44
3.3. Metaphase analysis of spleenic and thymic lymphomas obtained from heterozygous mice. 46
3.4. Mutation in *Chd2* does not affect cell viability after DNA damage. 49
3.5. Clonogenic survival of SV40 immortalized Chd2 MEFs is affected after DNA damage. 50
Discussion 53
Chapter IV 58
Determination of molecular changes in CHD2 in response to DNA damage 58
Introduction 58
ATM/ATR and Chromatin remodeling proteins 59
Materials and Method 61
Generation of polyclonal Chd2 antibodies 61
Gel Electrophoresis and Immunoblots for detection of CHD2 61
cDNA synthesis and reverse transcriptase (RT)- polymerase chain reaction (PCR) 62
Generation of Chd2 with a hemagglutinin epitope tag (HA tag) at the c-terminus 63
Generation and expression of Tandem affinity purification (TAP) tagged Chd2 63
Transfection and Immunoprecipitation 64
Immuno blot analysis of phosphorylated SQ/TQ motifs 64
Co-immunoprecipitations of CHD2 and ATR from nuclear extracts 65
Results 66
4.1. X-ray induced DNA damage increases endogenous CHD2 protein levels 66
4.1.1 Induction of CHD2 post DNA damage regulated by posttranslational events 66
4.2. CHD2 is a potential ATM/ATR substrate 66

4.3. Phosphorylation of CHD2 by ATM/ATR kinase in response to DNA damage 68
4.4. Physical interaction between ATR and CHD2 70
Discussion 70
Chapter V 76
Determination of interaction of Chd2 with p53 and other proteins involved in genomic stability and DNA repair 76
Introduction 76
Materials and Methods 80
Co-immunoprecipitations of CHD2 and p53 from whole cell lysate 80
Generation of full length recombinant Chd2 81
Tandem affinity purification (TAP) of CHD2 protein complex 81
Single step purification of CHD2 protein complex using Ni-NTA beads 83
Co-immunoprecipitations of CHD2 and PSP1 from whole cell lysate 84
In vivo splicing assay 85
Results 86
5.1. CHD2 interacts with p53 86
5.2. Tandem affinity purification (TAP) of CHD2 complex and mass spectrometric analysis 87
5.3 Identification of CHD2 interacting proteins through single step purification using Ni-NTA beads 89
3.4 Effect of CHD2 on alternative splicing 91
5.5 Interaction of CHD2 and PSP1 92
Discussion 95
Conclusion: “CHD2 a multi-function protein?” 101
References 105
Vita 121

List of Figures

Figure 1.Structural domains of CHD proteins 10
Figure 2.Schematic representation of mouse Chd2 protein..... 20
Figure 3. Distribution of Wt-Chd2 transcript in mouse tissues..... 25
Figure 4.Specificity of anti-Chd2 Ab..... 26
Figure 5.Immunofluorescent localization of CHD2 in U2OS cells..... 26
Figure 6.Gene traps vector insertion in the Chd2 gene..... 28
Figure 7.Analysis of *NChd2* mRNA transcripts by real-time quantitative RT-PCR using the 2-Δ ΔCt method..... 32
Figure 8.Role of Chd2 in repair of DNA damage..... 45
Figure 9.*Chd2* mutant cells have an impaired ability to repair damaged DNA 46
Figure 10.Repair of DNA damage induced by UV..... 47
Figure 11.Role of Chd2 in genomic stability..... 48
Figure 12. Mutation in *Chd2* promotes chromosomal instability..... 49
Figure 13.Cell viability of Chd2 MEFs after X-ray induced DNA damage..... 51
Figure 14.Cell viability of Chd2 MEFs after UV induced DNA damage..... 52
Figure 15. Cell viability of Chd2 MEFs after DNA damage with MMS 53
Figure 16. Clonogenicity assay of Chd2 MEFs..... 54
Figure 17.Induction of CHD2 in OSU2 cells following DNA damage 67
Figure 18.Effect of X-ray treatment on *CHD2* mRNA expression determined by RT-PCR 68
Figure 19.Potential ATM target sequences in Chd2..... 69
Figure 20.CHD2 is phosphoylated at the SQ site 71
Figure 21.Generation of recombinant HA tagged Chd2 peptide..... 72
Figure 22. CHD2 phosphorylation by ATM/ATR kinase(s)..... 72
Figure 23. Interaction of CHD2 and ATR 73
Figure 24. Endogenous interaction of CHD2 with p53..... 86
Figure 25. Interaction of recombinant p53 and CHD2..... 88

Figure 26. TAP purification of ChdkthRR-3 (1395 a.a clone) stable clone 88
Figure 27. Identification of CHD2 associated proteins 90
Figure 28. CHD2 affects the splicing pattern of E1A minigene 93
Figure 29. Co-immunoprecipitation of PSP1 and CHD2 94
Figure 30. A model illustrating a role of CHD2 in DNA damage response 103
Figure 31.Role of CHD2 in transactivation of p53 dependent target genes 104

Chapter I

General Introduction

Structure of Chromatin

Organization of DNA within the eukaryotic nucleus is a complex process. The organization of DNA involves its folding into a highly compact structure called chromatin. The basic structure of chromatin consists of the nucleosome, which contains 146 base pairs of DNA wrapped around the histone octamer. A histone octamer is composed of two molecules each of the histones H2A, H2B, H3 and H4[1]. The nucleosomes are arranged in a sequential manner by linker DNA of variable length to form a structure known as "beads-on-a-string". This 10 nm "beads-on-a-string" fiber is further condensed into a 30 nm diameter helical structure by linker histone H1[2]. The highly compact structure of the chromatin blocks access to the naked DNA for various nuclear factors involved in cellular processes such as replication, repair, recombination, and transcription. Accessibility to the DNA needs to be positively and negatively regulated in order to ensure smooth functioning of the cell. Some factors such as histone modifying and chromatin remodeling complexes help to open up the chromatin structure thereby allowing accessibility to the DNA template during replication, repair, recombination, and transcription. Other factors such as the chromatin assembly factor-I (CAF) help to restore the original structure of chromatin once the necessary cellular processes are completed [1].

Histone modifying complexes

Histones are the basic organizational unit of the chromatin. Histones play an important role in the regulation of gene expression by modifying chromatin structure. Each of the core histones (H2A, H2B, H3 and H4) contains a N-terminal tail, which protrudes outside the compact chromatin structure and thus is susceptible to a variety of covalent post-translational modifications [3]. These covalent modifications act as an “epigenetic code” for chromatin remodeling factors or transcription factors to regulate

gene expression [4]. The post-translational modifications include phosphorylation, acetylation, methylation, ubiquitination, sumoylation, ADP ribosylation, glycosylation, biotinylation and carbonylation[2]. Phosphorylation, acetylation and methylation are some of the best understood and well-studied post-translational modifications.

Histone acetylation

Acetylation occurs at specific lysines on the core histones' tail which neutralize the positive charge of the epsilon amino group of the lysine residues. This modification weakens the interaction between the histones and the negatively charged DNA, resulting in an open chromatin structure [5-6]. Recent studies suggest histone acetylation patterns dictate a variety of downstream processes including transcription, DNA repair, and telomere silencing. For example, acetylation of histone H3K56 helps in maintaining genome stability. Acetylation of phospho-H2Av by the Drosophila dTip60 complex facilitates removal of phospho-H2Av after DNA damage repair [7]. Histone H4K16 Acetylation is associated with formation of high-order chromatin structure in *D.melanogaster* and histone H4K12 acetylation is associated with the repression of transcription in *S.cerevisiae* and *D.melanogaster* [5]. Two classes of enzymes are involved in the regulation of histone acetylation: histone acetyl-transferases (HATs) and histone deacetylases (HDACs). Histone acetyl-transferases (HATs) activity is possessed by many transcriptional coactivators such as Gcn5/PCAF, CBP/p300, and SRC-1. Acetylation of histones is reversed by histone deacetylases (HDACs), which promotes the condensation of the nucleosomal fiber [8]. Transcriptional corepressors possessing histone deacetylases such as mSin3a, NCoR/SMRT, and NURD/Mi-2 are responsible for restoring the native chromatin structure [5]. A disturbance in the balance between the HATs and HDACs activities result in the origin of a variety of cancers [6].

Histone methylation and demethylation

The process of methylation can occur on both lysine and arginine residues. Mono or dimethylation occurs on the 17th arginine residue in histone H3 and on the 3rd arginine residue in histone H4 [9-10]. Lysine 4, 9, 27, 36 and 79 of histone H3 and lysine 20 of histone H4 are mono, di or trimethylated. Histone H3K4 and H3K36 methylation is associated with transcription activation while methylation of H3K9, H3K27, H3K79 and H4K20 signals for the silencing of transcription [11]. Histone methylation is brought about by histone methyltransferases (HMTs). HMTs transfer the methyl group from s-adenosylmethionine (SAM) to the side-chain nitrogen of lysine or arginine residues [6]. There are three classes of HMTs : arginine methyltransferases, SET domain containing lysine methyltransferases, and Dot1-like lysine methyltransferases [6]. Histone arginine methylation is carried out by the coactivator arginine methyltransferase (CARM1) and the protein arginine methyltransferase (PRMT1) [5]. SET domain containing lysine methyltransferases methylate specific lysines on histone H3 and H4. Some examples of SET domain containing lysine methyltransferases include Ezh2, PR-Set7, Set1, Set2, Suv4-20h1, and Suv4-20h2 [6]. Dot1 (disruptor of telomeric silencing-1) -like lysine methyltransferases need a nucleosomal substrate and thus cannot methylate free histones. An example of Dot1-like lysine methyltransferases is Dot1 which mono, di, or trimethylates H3K79. This methylation is required for telomere-associated gene silencing [5]. Methylation of histones is counterbalanced by reversing the process through histone demethylation. Two classes of enzymes, amine oxidases such as LSD1(lysine specific demethylase1) and hydrolases of the JmjC (Jumonji) family have recently been found to demethylate a specific lysine on histones [12]. LSD1 is capable of demethylating mono- or di- methylated H3K4, thus functioning as a transcriptional repressor [6]. JmjC family members can demethylate lysine of H3K4, H3K9, H3K27, and H3K36 [5]. Arginine methylation is reversed by arginine deiminase, PADI4/PAD4 (peptidyl arginine deiminase 4), which converts the methyl-arginine residue into citrulline. This deimination process is associated with silencing of the oestrogen-controlled gene, pS2 [12].

Histone phosphorylation

Phosphorylation of histones occurs at specific sites on serine and threonine and it is associated with different processes such as transcriptional activation and chromosome condensation during meiosis and mitosis [4]. The onset of metaphase in mitosis marks the phosphorylation of histone H3S10 by aurora kinase B which abolishes methylation of histone H3K9 and removes HP1(heterochromatin protein 1) from chromosomes [13]. By contrast, during prophase aurora kinase B comes back to phosphorylate histone H3S28 causing chromosome condensation. Similarly, phosphorylation of H2B at serine 14 by Mst1 (mammalian sterile twenty) kinase is correlated with chromosome condensation during meiosis. Phosphorylation of histone H3S10 by MSK1/2(mitogen and stress-activated protein kinase 1 and 2) initiates transcription of mitogen-stimulated immediate-early response genes [4-5]. Another well studied phosphorylated histone is histone H2AX which can be mediated by any of the following: phosphatidylinositol-3-OH kinase-related kinase (PIKK) family- ataxiatelangiectasia mutated (ATM), ataxia telangiectasia related (ATR) or DNA-dependent protein kinase (DNA-PK). Histone H2AX phosphorylation occurs on serine 139 and is triggered by the formation of DNA double-strand breaks (DSBs) after DNA damage [14]. H2AX phosphorylation (γ-H2AX) acts as an initial signal for the recruitment of DNA damage checkpoint and repair proteins to the damaged regions [14]. γ-H2AX also helps in recruiting cohesins to the damaged regions. Cohesins keep the sister chromatids together, thus helping in homologous recombination to repair the damaged DNA strand with the undamaged DNA strand serving as the template. After completion of the repair process, protein phosphatase 2A (PP2A) dephosphorylates chromatin-associated γ-H2AX and removes it. The mechanism by which PP2A removes the dephosphorylated γ-H2AX is not known. The removal of γ-H2AX facilitates segregation of sister chromatids [15].

Chromatin remodeling complexes

The proteins present in this group are also known as ATP-dependent chromatin remodeling factors. These proteins, as the name suggests, utilize the energy derived

from ATP hydrolysis to modulate chromatin fluidity [16-17]. All ATP-dependent chromatin remodeling factors contain a highly conserved ATPase subunit belonging to the Swi2/Snf2 ATPase superfamily. There are four classes of the ATPase subunit- SWI (switching)/ SNF (sucrose non-fermenting), ISWI (imitation switch), CHD (Chromodomain helicase DNA binding), and INO80. All of the ATP-dependent chromatin remodeling factors are classified under the aforementioned classes, depending upon which type of ATPase subunit they possess [17].

The class of SWI/SNF

This class of ATP-dependent chromatin remodeling factors includes the yeast SWI (switching)/ SNF (sucrose non-fermenting) complex, the yeast RSC (remodels the structure of chromatin) complex, *Drosophila melanogaster* brahma complex, and the mammalian BRG1 and BRM complex. The Swi2/Snf2-like ATPase subunits present in these complexes exhibit DNA-dependent ATPase activity. Other conserved motifs between these proteins include the presence of a C-terminal bromodomain and two other conserved regions (domains I and II) of unknown function [16]. The yeast SWI (switching)/ SNF (sucrose non-fermenting) complex was the first ATP-dependent chromatin remodeling factor to be discovered [18-19]. The genes were named SWI / SNF, as they were discovered during a genetic screen for factors needed for mating-type switching and use of sucrose as a carbon source [20]. The SWI/SNF complex is required for inducing transcription of both the homothallic switching (HO) endonuclease and the sucrose hydrolyzing enzyme (SUC2) genes [17]. Studies elucidating the functions of SWI/SNF complex show that this complex can bind to both DNA and nucleosomes. The complex alters the position/structure of nucleosomes on arrays increasing the access to DNA for transcriptional activators or repressors [21]. The yeast RSC (remodels structure of chromatin) complex contains 15 ATPase subunits. Four out of the fifteen [Sth1 (for Snf2 homolog), Rsc8/Swh3 and Rsc6] are homologous to SWI/SNF subunits [16]. Unlike the SWI/SNF subunits, the four homologous subunits of RSC complex are essential for mitotic growth and necessary for cell viability [22].

Localization of the RSC complex to Pol III and Pol II promoters shows its involvement in the regulation of transcription [23]. Its involvement in chromatin remodeling includes the transferring of histone octamers from one DNA to another [16, 22]. Unlike the yeast system, *Drosophila melanogaster* contains only one Swi2/Snf2- like ATPase, the brahma (BRM) protein. D.brahma is an activator of homeotic genes and is required for cell viability. BRM has been shown to associate with RNA polymerase II and hyperacetylated chromatin, suggesting a functional role of BRM in gene activation [24]. Human/mammalian cells have two SWI2/SNF2 homologs, BRG1 and human BRM. Both of these proteins form separate complexes and in vitro studies show that both are involved in alteration of nucleosome structures [22]. BRG1 has been shown to associate with tumor-suppressor proteins retinoblastoma (pRB) and BRCA1. Both BRG1 and BRM demonstrate a role in the tissue differentiation process [17]. A BRG1-containing coactivator complex, E-RC1 (EKLF coactivator-remodeling complex 1) creates an open chromatin structure to facilitate EKLF-dependent transcription of the human β-globin gene [16].

The class of ISWI

Drosophilia ISWI (imitation switch) complexes are the founding members of this class. The members of the ISWI class posses the SLIDE domain, and the HAND-SANT domain in addition to the ATPase domain. The SLIDE domain which resembles a myb-like DNA binding domain is known to play an important role in nucleosome recognition and the HAND-SANT domain is known to interact with histone tails [25]. ISWI is the only member of this class in *Drosophilia* and is part of three chromatin remodeling complexes: NURF (nucleosome remodeling factor), ACF (ATP-utilizing chromatin assembly and remodeling factor), and CHRAC (chromatin accessibility complex). These complexes use ATP hydrolysis to alter chromatin by creating regularly spaced nucleosomal arrays [24]. *Drosophilia* ISWI is the involved in maintenance of the male X chromosome structure and is also found to be essential for cell viability[16]. Co-localization studies of ISWI with RNA polymerase II show no interaction, speculating a

negative role of ISWI in transcription regulation [26]. Isw1 and Isw2 are two members of yeast ISWI which, along with other proteins form two distinct complexes involved in ATP-dependent nucleosome disruption. Isw2 complex and Isw1/Ioc3 complex are known to be involved in displacement of the basal transcription machinery to silence gene expression, whereas Isw1/Ioc4/Ioc2 complex regulates transcription elongation and termination [27]. Isw2 complex is also involved in formation of a 'nuclease-inaccessible chromatin structure in vivo'[17]. The mammalian system contains two ISWI proteins; SNF2H and SNF2L. The SNF2H forms a part of the RSF (remodeling and spacing factor) along with p325 in humans, which is involved in nucleosomal spacing and transcription initiation. SNF2H is also found as a subunit in WICH complex (WSTF [Williams's syndrome transcription factor] −ISWI chromatin remodeling complex) which is required for DNA replication. SNF2H has also been purified as a subunit from human CHRAC complex and SNF2L from human NURF complex[25].

The class of INO80

The INO80 complex was first isolated in a genetic screen for yeast mutants defective in transcriptional activation in response to inositol depletion [28] . This class possesses a unique ATPase called Ino80p/Swr1 ATPase, which splits into two because of the presence of a spacer between the domains [29]. The INO80 class consists of two complexes: INO80 remodeling complex (INO80.com) and SWR1 remodeling complex (SWR1.com). The INO80 complex consists of Ino80, Rvb1, Rvb2, Arp4 (actin-related protein 4), Arp5, Arp8, actin, Nhp10 (nonhistone protein 10), Anc1/Taf14, Ies1 (ino eighty subunit 1), Ies2, Ies3, Ies4, Ies5 and Ies6. The human INO80.com consists of the Gli-Kruppel zinc finger transcription factor Yin Yang 1 (YY1), the deubiquitylating enzyme Uch37 and nuclear factor related to kB (NFRKB) as its subunits. *Drosophila* INO80 complex has subunits similar to the human INO80 complex [28]. INO80 complex is involved in positive and negative regulation of transcription through its ATP-dependent chromatin remodeling activity [28]. Studies have also demonstrated INO80's important role in DNA repair. INO80.com is recruited to DNA double strand break (DSB)

sites via its interaction with γ-H2AX and helps in recruiting DNA repair proteins through its chromatin remodeling activities [30]. INO80.com along with another chromatin remodeler, Iswip helps in fork movement during DNA replication through remodeling of nucleosomes[28]. The SWR1 remodeling complex is composed of the subunits: Swr1, Swc2/Vp372, Swc3, Swc4/Eaf2/God1, Swc5/Aor1, Swc6/Vps71, Swc7, Yaf9, Bdf1, Act1/actin, Arp4, Arp6, Rvb1 and Rvb2. SWR1.com functions as a replacement apparatus by replacing the H2A–H2B dimer in the nucleosome with H2AZ–H2B. Other functional studies on SWR1.com demonstrate a similar role as INO80.com in DNA repair process [29].

The class of CHD proteins

The Chromodomain helicase DNA binding proteins(CHD) are a group of highly conserved proteins sharing sequence motifs and functional domains such as chromo (chromatin organization modifier) domains, SNF2-related helicase/ATPase domains, specific DNA binding domains, and the C-terminal helicase domains associated with regulation of chromatin structure and gene transcription [31]. CHD proteins regulate ATP-dependent nucleosome assembly via their chromodomains and SNF2-related helicase/ATPase domains [32-33]. The CHD family of proteins is present in eukaryotic organisms like Caenorhabditis *elegans*, yeast, *Drosophila,* mice, and humans [34]. According to The Human Genome Organization, the mammalian CHD family contains nine members. The family can be further subdivided into three subfamilies according to the presence of additional functional domains and the type of chromodomains (CDs) present (http://www.gene.ucl.ac.uk/nomenclature/) (Fig.1). CHD1 and CHD2 belong to subfamily I. CHD3 and CHD4 belong to the second subfamily. The third subfamily is comprised of the CHD proteins five through nine. The CHD1 and CHD2 subfamilies both contain chromodomains of subclasses 0 and H. These two proteins share CDs and Myb DNA binding domains, which are identical to each other. The CHD3 and 4 subfamilies contain CDs of subclasses P and J and also contain a pair of N-terminal PHD Zn-fingers that are not present in other CHD sub-families. The CHD-6 subfamily

contains CD subclasses Q and I with BRK and/or SANT DNA binding domains in the C-terminal region [35].

The shared domains of CHD family:

The chromodomain: The chromodomain (chromatin organization modifier) is a domain of 40-50 amino acids present in proteins involved in chromatin remodeling and regulation of gene expression in eukaryotes during development. The best studied examples of such proteins are found in *Drosophila melanogaster*. This includes Heterochromatin Protein 1(HP1), the histone acetyltransferase MOF, Polycomb, and Suppressor of variegation and their homologues in other organisms [35]. The chromodomain binds to methylated histones and has been found to act as recognition motifs for methylated lysine-9 of histone H3. Chromodomains are shown to interact with RNA and also self-associate with one another[16].

The SNF2-related helicase/ATPase domain: This domain is ~400 amino acids long and consists of two subdomains: “a conserved N-terminal subdomain I required for ATP binding and hydrolysis and a C-terminal subdomain involved in energy transduction” [34]. The SNF2 related ATP dependent helicase domain functions to processively move along DNA templates and destabilize protein-DNA interactions[31]. SNF2/SWI2 is the ATPase of the *S.cerevisiae* SWI/SNF complex. The SWI/SNF complex is also known to remodel chromatin structure to facilitate binding of gene specific transcription factors. SNF2 also participates in a number of DNA related processes including DNA repair, chromatin remodeling, recombination and transcription [16, 36-37].

Chromodomain helicase DNA binding protein 1 (CHD1)

Mouse Chd1 was the first chromdomain helicase DNA binding protein to be characterized by Delmas et al. in 1993 [36]. Subsequently, Woodage et al. mapped the human *CHD1* gene to 5q15-q21 by PCR screening of the CEPH YAC library [31]. Human CHD1 encodes a 1,709-amino acid protein and shares a 95% homology to the mouse Chd1 [31]. CHD1 protein has two chromodomains near the N-terminus, a

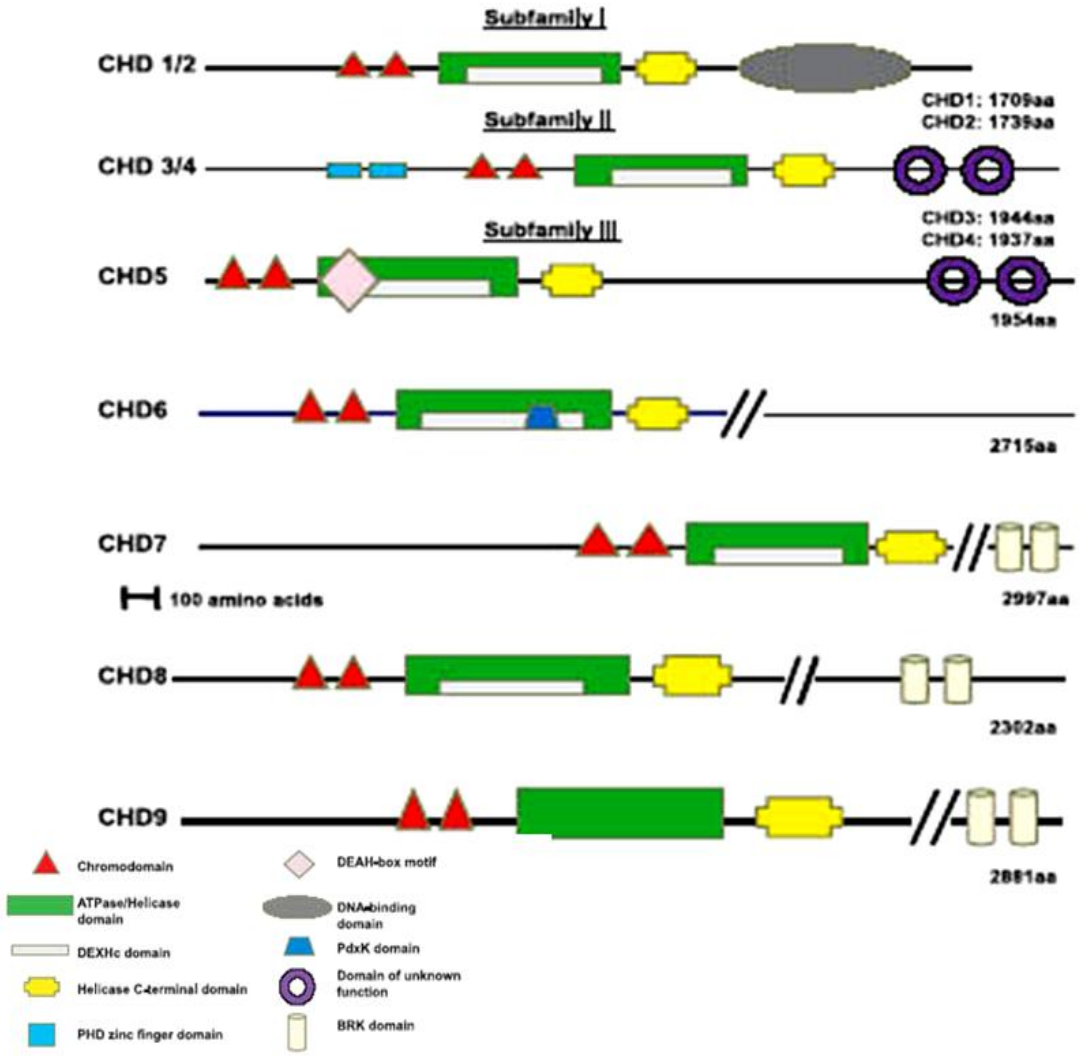

Figure 1.Structural domains of CHD proteins

Schematic representation of the structural domains present in CHD subfamilies (adapted from Hall and George, 2007)

centrally located Snf2-related helicase/ATPase domain and a Myb-related DNA binding domain at the C-terminus [36]. A search for proteins that bind a DNA promoter elements led to the identification of murine Chd1 , which was found to bind to immunoglobulin promoter sequences [36]. Following the above findings, Stokes and Perry showed that Chd1 binds to (A+T)-rich DNA via minor-groove interactions [38]. It was demonstrated that Chd1 has a “cell cycle –related localization pattern” as it localized to the cytoplasm at the beginning of mitosis and then became part of the chromatin during telophase-cytokinesis. Chd1 was designated as “constituent of bulk chromatin” and had to be treated with salt and micrococcal nuclease to purify from the nucleus [38]. Characterization of the *Drosophila melanogaster* Chd1 homologue was also reported in 1996 [39]. The expression of the protein was localized to interbands on polytene chromosomes and a functional role for Chd1 in chromatin remodeling was speculated [39]. *In vivo* chromatin assembly studies in *Drosophila* provide evidence that Chd1 is a factor involved in assembly of histone variant H3.3 containing nucleosomes and it interacts with *Drosophila* histone chaperone HIRA [40]. *Drosophila* Chd1 co-localizes with elongating RNA polymerase II, but is not required for RNA polymerase II’s association with chromatin[41]. *Drosophila* Chd1 is an important factor for female and male fertility [41]. The orthologos of CHD1 and the nuclear protein *s*tructure-*s*pecific *r*ecognition *p*rotein 1(SSRP1) were found to interact and the two proteins were shown to co-localize in Drosophila polytene chromosomes [42]. SSRP1 is part of the FACT (fa<u>c</u>ilitates <u>c</u>hromatin <u>t</u>ranscription) complex in mammals. SSRP1 interacts with Rad54 and plays an important role in the HR-mediated DNA damage response [43]. *Saccharomyces cerevisiae* Chd1 was shown to interact with Rtf1, a component of the Paf1 complex The Paf1 complex associates with RNA polymerase II and regulates transcription elongation. Chd1 also interacts with components of two elongation factors Spt4-Spt5 and Spt16-Pob3 [44]. Other functional studies of CHD1 suggest a role for the protein in active chromatin assembly and as a component of yeast SAGA (Spt-Ada-Gcn5 acetyltransferase) and SLIK (SAGA-like) histone acetyltransferase complex [45-46].

Saccharomyces cerevisiae Chd1 has been found to have a role in the regulation of the ADH2 (alcohol dehydrogenase 2) gene and is required for ADH2 promoter nucleosome organization [47]. Yeast Chd1 plays an antagonistic role to yFACT (yeast facilitates chromatin transcription) complex in regulation of TBP (TATA binding protein) binding at promoters in yeast [48]. Set2(a histone methyltransferase that methylates K36 of histone H3) and Chd1 negatively regulate DNA replication possibly through negative regulation of DNA replication factors recruited by yFACT to stabilize the replication fork [49]. Comparative analysis of yeast and human CHD1 showed that only the chromodomains of human CHD1 interacts with methylated lysine 4 on histone H3 [33, 50]. Mouse Chd1 has been suggested to have a functional role in the repression of gene expression by virtue of its interaction with NCoR, a co-repressor of nuclear hormone receptor transcription factor [51]. CHD1 is also associated with histone deacetylase activity and has a role in pre-mRNA splicing [51]. CHD1 has been proposed to function as a recruiter of U2 snRNP and FACT/PAF to the first nucleosome. This recruitment has been shown to boost the efficiency of pre-mRNA splicing and transcript elongation [52]. Recent studies on *Bombyx mori* follicle development, led to the identification of the silkmoth chromo-helicase/ATPase-DNA binding protein 1 (Chd1) ortholog [53]. The silkmoth ortholog of Chd1 binds to the chorion gene promoter element and repositions the nucleosomes. This repositioning allows accesses to C/EBP and TFIID to the promoter elements which initiate transcription [53]. More recently, *Chd1* has been reported as an essential gene for maintaining both pluripotency and an open chromatin structure in the embryonic stem cells [54].

The focus of this thesis is Chromodomain helicase DNA binding protein 2(CHD2), which will be discussed in chapter II of the thesis.

Chromodomain helicase DNA binding proteins 3 and 4 (CHD3 and CHD4)

CHD3 and CHD4 belong to the second subfamily. These proteins are also called Mi-2α and Mi-2β. Mi-2 proteins were first identified as autoantigens in the connective tissue disease dermatomyositis [55-56]. The domain unique to this subfamily is a PHD (plant

homeo domain) Zn-finger-like domain also known as LAP [57]. The PHD or leukemia associated protein (LAP) domain is a ~60 amino acid domain found in proteins mainly involved in transcriptional regulation. Mutations in the PHD domain of genes such as recombination activating gene 2 (RAG2), Inhibitor of Growth (ING), nuclear receptor-binding SET domain-containing 1 (NSD1) and Alpha Thalassaemia and Mental Retardation Syndrome, X-linked (ATRX) have been connected to diseases such as α-thalassemia, head and neck squamous cell carcinoma, Williams's syndrome and myeloid leukemias [58-59]. Mi-2α and Mi-2β form a "multi-subunit protein complex containing both histone deacetylase and nucleosome-dependent ATPase subunits", known as the NuRD(nucleosome remodeling deacetylase) complex [57]. The NuRD complex consists of seven polypeptides including histone deacetylases 1 (HDAC1) and HDAC2, H4 interacting proteins-retinoblastinoma-associated proteins 46 and 48 (RbAp46/48), methyl-CpG-binding domain-containing protein 3 (MBD3), metastasis-associated protein family members (MTA1 to MTA3), and CHD3/4 [60]. The NuRD complex has been recognized in mammals and *Xenopus,* and homologs of NuRD subunits have been identified in *Drosophila*, *Caenorhabditis elegans*, and *Arabidopsis* [61]. CHD3/4 in the NuRD complex utilizes ATP to remodel nucleosomes, giving access to HDAC1 and HDAC2 to deacetylate the histone tails. The deacetylated histones form a compacted nucleosomal structure, thus negatively regulating transcription [62]. An example of this type of negative regulation is the MTA3-containing NuRD complex. This complex acts as a corepressor for BCL-6 to regulate expression of MHC class II through repression of Blimp-1in B lymphocyte [63]. In addition, CHD3 and CHD4 interact with pericentrin, which is an integral centrosomal component. The interaction recruits pericentrin to the centrosome, affecting microtubule and spindle function. Pericentrin levels increase during mitosis and fall upon entry into the G1 phase. The pericentrin levels are positively regulated by CHD3, which remains associated with pericentrin throughout mitosis. Pericentrin levels are negatively regulated by CHD4, which dissociates from the centrosome during mitosis. The mechanism as to how CHD3/CHD4 controls the levels of pericentrin is not known. But it

is speculated that CHD3 “acts as a structural anchor for pericentrin” and CHD4 is “responsible for regulating the removal of pericentrin from the centrosome” [64]. The two homologs of Mi-2 in *Caenorhabditis elegans,* Let-418 and Chd3, play an important role in vulval cell fate determination through regulation of the Ras signaling pathway and Notch signaling [65]. The Chd3 homolog, *PICKLE* (*Pkl*), in *Arabidopsis* is involved in repression of seed-associated genes through facilitating trimethylation of histone H3 lysine 27 [66]. Drosophila Chd4/dMi-2 and dChd3 are involved in ATP-dependent remodeling of nucleosomes and colocalize with RNA polymerase II on the transcriptionally active region of polytene chromosomes [67].

Chromodomain helicase DNA binding protein 5 (CHD5)

CHD5 was identified during the course of mapping genes deleted in 1q36.3 region in human neuroblatomas by Thompson et al. [68]. CHD5 contains two PHD zinc-finger domains and a DEAH-box-type helicases domain in addition to the common structural domains found in the CHD family [68]. DEAH-box-type helicases are RNA-dependent ATPases shown to unwind RNA duplexes [69]. CHD5 was shown to be highly expressed in fetal brain and cerebellum while negligible expression was seen in a panel of neuroblastoma cell lines [68]. Chromosome engineering was used to identify the mouse chromosomal region D4Mit190-51 as the region involved in the regulation of proliferation, senescence, and apoptosis. The region was also shown to regulate p53 activity via $p19^{Arf}$. Chd5 was identified as the gene in the D4Mit190-51 region accountable for the aforementioned tumor-suppressive functions. Mouse D4Mit190-51 maps to human chromosome 1p36 [70]. CpG island hypermethylation was observed in the CHD5 promoter in human cancer cell lines. The hypermethylation was seen to be associated with the loss of CHD5 expression and CHD5 expression was restored upon treatment with demethylating agents in these cancer cell lines [71]. Somatic heterozygous missense CHD5 mutations and promoter methylation of CHD5 were identified in some of the ovarian cancer. These observations lead to the speculation that biallelic inactivation of CHD5 would lead to ovarian cancers [72].

Chromodomain helicase DNA binding protein 6 (CHD6)

CHD6 contains the additional structural domains SANT (for 'switching-defective protein 3 (Swi3), adaptor 2 (Ada2), nuclear receptor co-repressor (N-CoR), transcription factor (TF)IIIB')) and TCH/BRK (Breast tumor kinase) domains [73]. The SANT domain is a 50 amino acid motif found in many chromatin-remodeling complexes. SANT domains are very similar in sequence to DNA-binding domains (DBD) of Myb-related proteins [Myb DBDs]. SANT domains are thought to function as “histone-binding modules” [74]. CHD6 was found to interact with Nrf2, a transcription factor needed for cellular redox homeostasis by a yeast two-hybrid screen [75]. Recently CHD6 has been shown to exhibit DNA-dependent ATPase activity, co-localize with phorsphorylated forms of RNA polymerase II, and is present in loci of mRNA synthesis [76]. CHD6 is part of the PRIC (PPARα-interacting cofactor)-complex and associates with the transcription factor Nrf2, implicating a role of CHD6 in gene activation [75, 77].

Chromodomain helicase DNA binding protein 7 (CHD7)

CHD7 has been identified as the gene mutated in a congenital syndrome called CHARGE syndrome. The congenital anomalies of the syndrome include choanal atresia and malformations of the heart, inner ear, and retina. Seven stopcodon mutations, two missense mutations and one mutation at an intron-exon boundary in the CHD7 have been identified in 17 patients with CHARGE syndrome [78]. Seven heterozygous mutations, two splice and five missense CHD7 mutations, were observed in another developmental disorder called Kallmann syndrome (KS). Kallmann syndrome is characterized by impaired olfaction and hypogonadism [79]. CHD7 belongs to the third subfamily of the CHD proteins and contains two chromodomains, two helicase domains, a SANT domain, and two BRK domains [80]. The BRK or the TCH domain is a 50 amino acid stretch of unknown function that is also found in the brahma/BRG1 family of chromatin remodeling enzymes. The presence of BRK domains in chromatin remodeling proteins in higher eukaryotes suggest that they play a role in regulation of chromatin structure specific to higher eukaryotes [81]. Mouse models with mutations in

the *Chd7* gene show phenotypes similar to CHARGE syndrome such as cleft palate, choanal atresia, septal defects of the heart, haemorrhages, prenatal death, vulva and clitoral defects, and keratoconjunctivitis sicca [82]. More recently, homozygous mice generated from a mouse model carrying *Chd7* deficient gene trapped lacZ reporter alleles exhibited prenatal lethality, indicating an important role of CHD7 in mammalian development [83]. Recently, chromatin immunoprecipitation on tiled microarrays (ChIP-chip) studies showed localization of CHD7 to discrete locations along chromatin that were specific to each cell type used in the study. The study also shows that CHD7 binding correlates with the location of methylated lysine4 of histone H3, speculating a role of CHD7 in enhancer mediated transcription [80].

Chromodomain helicase DNA binding protein 8 (CHD8)

The DNA-binding transcription factor CTCF (CCCTC binding factor) mediates enhancer blocking insulation at sites throughout the genome. CTCF is involved in gene regulation, specifically at the chicken b-globin locus and the imprinted IGF2/H19 locus in mice and humans [84]. Yeast two-hybrid screens performed to identify proteins interacting with CTCF to elucidate essential mechanisms of CTCF insulator in chromatin, revealed interaction of CTCF with CHD8 [85]. CHD8 like its other members of CHD subfamily III contains a SANT domain and two BRK domains in addition to the structural domains common to the CHD family. CHD8 was found at the known CTCF target sites, “such as the differentially methylated region (DMR) of H19, the locus control region of *b*-globin, and the promoter region of BRCA1 and c-myc genes”[85]. Knockdowns of CHD8 highlight its important role in CTCF-dependent insulator function and in epigenetic modifications at CTCF binding sites adjacent to heterochromatin. Loss of CHD8 resulted in CpG hypermethylation and histone hypoacetylation at CTCF binding sites [85]. A transcription factor called selenocysteine tRNA-activating factor (Staf) activates transcription of the human U6 small nuclear RNA from a preassembled chromatin. Studies have identified CHD8 as the chromatin remodeling protein needed for the efficient Staf mediated transcription of U6[86]. CHD8 is also required for

transcription of a Pol II-transcribed gene-IRF3. The study also demonstrated the ability of CHD8 to bind to di and trimethylated histone H3lysine 4 [86]. Another CHD8 interaction study demonstrates interaction of this chromatin remodeling protein with β-catenin, an essential component of the "canonical" Wnt signaling pathway. The results of the study show that CHD8 is recruited to the promoter regions of several β-catenin-responsive genes and negatively regulates the expression of these genes. Similar results were seen with *kismet*, the *Drosophila melanogaster* ortholog of Chd8 [87]. Duplin (axis duplication inhibitor) a shorter form of CHD8 expressing 749 amino acids of the protein was disrupted in mice by homologous recombination. *Duplin*$^{-/-}$ embryos exhibited growth retardation followed by massive apoptosis at E7.5. This mouse model highlights the indispensible role of CHD8 in mammalian development [88]. Follow up studies to determine the molecular basis for the apoptosis in *Chd8-/-* embryos led to the unearthing of CHD8 interaction with the tumor suppressor protein p53 [89]. CHD8 was found to bind to both p53 and histone H1. The formation of this trimeric complex resulted in recruitment of histone H1 to the promoter of p53 target genes, thus suppressing their expression. These observations suggested that CHD8 expression regulates p53-mediated apoptosis [89]. A recent transcriptomic analysis of CHD8-depleted cells showed that CHD8 "controls the expression of cyclin E2 (*CCNE2*) and thymidylate synthetase (*TYMS*), two genes expressed in the G1/S transition of the cell cycle" [90]. The results of the study show that CHD8 binds to the 5' region of both *CCNE2* and *TYMS* genes and also with the elongating form of RNAPII, thus speculating CHD8's involvement in transcription elongation [90].

Chromodomain helicase DNA binding protein 9 (CHD9)

The last member of the subfamily III, CHD9, is also known as CReMM (chromatin-related mesenchymal modulator). It is found to be expressed in mesenchymal progenitors and binds to skeletal tissue-specific promoters CBFA1, biglycan, osteocalcin (OC), collagen-II, and myosin in a differential manner. It was also found to bind to A/T-rich DNA [91-92]. CReMM is highly expressed in osteoprogenitors and co-

localizes with GR (glucocorticoid receptor) in osteoblastic cells [93], suggesting its role in osteogenic cell differentiation [94].

Chapter-II

Characterization of Chromodomain Helicase DNA Binding Protein 2 (Chd2) in mice

Introduction

CHD2 is a poorly characterized CHD protein. The human *CHD2* gene has been mapped to chromosome15q26 [31]. This region is associated with rare genetic disorders that lead to growth retardation, cardiac defects, and early post natal lethality [95-96]. The human CHD2 is predicted to be an 1828-amino acid polypeptide. It shares a 58.6% identity and a 69.5% similarity overall with mouse Chd1. The human CHD2 shares 95.9% identity with mouse Chd2. The mouse chromodomain helicase DNA binding protein 2 is mapped to chromosome 7 D1 and the protein is predicated to contain 1827 -amino acids (NCBI Accession: XP_145698). Chromodomain helicase DNA binding protein 2 has the same domain organization as CHD1. CHD2 has two chromodomains at the N-terminus, a centrally located Snf2-related helicase/ATPase domain, a DEAD-like helicase domain within the Snf2-related helicase domain, a helicase domain at the C terminus and a HMG-I domain (A+T hook) at the C terminus (Fig.2). However, it has four putative bipartite nuclear localization signals (one at the N-terminus and three at the C-terminus). This is unlike CHD1 which has one nuclear localization signal. The DEAD-like helicase belongs to the DEAD box family of helicases. DEAD box proteins are found in all eukaryotes and most prokaryotes [97]. The DEAD box proteins have RNA-dependent ATPase and ATP-dependent RNA helicase activities and are involved in various aspects of RNA metabolism [97-98]. The HGM-I domain (A+T hook), which are also present in the high mobility group (HMG) proteins are known to facilitate various DNA related activities such as transcription, replication, recombination, and repair. They bind to AT rich regions of DNA and chromatin, and induce short and long range changes in structure of their binding sites [99].

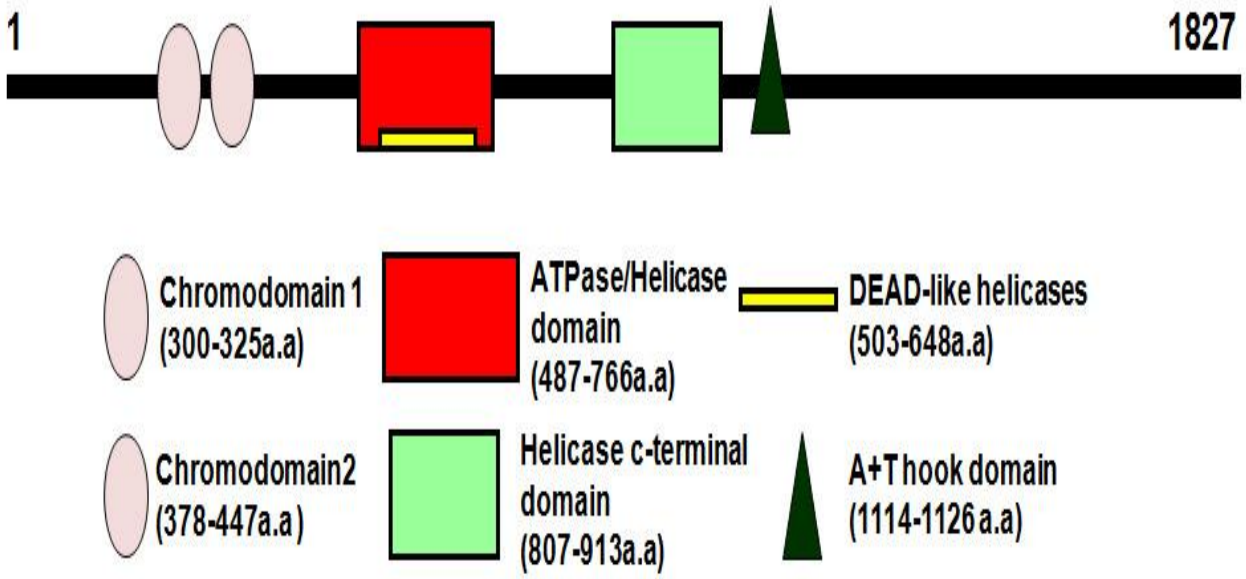

Figure 2.Schematic representation of mouse Chd2 protein.
The structural domains of the Chd2 protein are shown. The domains are represented by different shapes and colors according to the key at the bottom of the figure. The length of each domain is also shown in the key.

There are only a few reports in the literature describing possible functions of CHD2. A micro-array study attempting to map chromosomal aberrations for congenital diaphragmatic hernia (CDH) identified *CHD2* as of one of the three genes with a missense mutation in samples obtained from patients with CDH [100]. A cDNA microarray gene profile of blood cells from urinary bladder cancer patients showed downregulation of *CHD2* when compared to healthy controls [101]. Gene expression data showed a 1.7 fold decrease in *Chd2* gene expression in C57BL/6J $p53^{+/-}$ mammary glands when compared to BALB/c $p53^{+/-}$ mammary glands [102]. A homozygous deletion at 15q26.2 was found in a Hodgkin's lymphoma cell line – HDLM2 by array comparative genomic hybridization (aCGH). This region contains only two known genes, *RGMA* and *CHD2* [103]. A transcriptional profile study of fibroblasts grown in relaxed collagen lattices showed a 3.6 fold inductions in *CHD2* expression in relaxed fibroblast compared with mechanically stressed fibroblasts [104]. Recently Marfella et al showed that Chd2 is important for mouse development and survival. The phenotypic analysis of Chd2-mutant mice showed impaired kidney function [105-106]. Fluorescence anisotropy binding assays with methylated histone peptide (H3K4me3) show that the human CHD2 chromodomain has a 30-fold weaker interaction compared to that of the human CHD1 chromodomain [107]. Our observations with the Chd2 mutant mice show that the haploinsufficiency of Chd2 causes scoliosis [108] and the Chd2 protein appears to play a critical role in the development, hematopoiesis and tumor suppression [109].

Materials and Methods

cDNA synthesis and reverse transcriptase (RT)- polymerase chain reaction (PCR)

Total RNA was isolated from different mouse tissues using TRIzol reagent (Invitrogen) according to the manufacturer's protocol. Genomic DNA was removed by incubating RNA samples with 2U of RNase-free deoxyribonuclease I (Promega) per 3µg of RNA for 30 minutes at 37^0C. First strand cDNA synthesis was performed with 3µg of

total RNA using random hexamers and M-MLV reverse transcriptase (Promega). As a negative control, samples containing RNA but no reverse transcriptase were also included. 2µl of cDNA was used for PCR. The primer sequences for Chd2 are: GGTGGTGATGGCAAGTCTTCAAGT (exon 33); AGGCAAATGAGGCTTCTGAGGATG (exon 36). The primer sequences for housekeeping gene L38 (ribosomal protein L38) are: TTCGGTTCTCATCGCTGTGAGTGT (forward); TCTTGACAGACTTGGCATCCTTCC (reverse). The PCR conditions for Chd2 exons 33-36 were initial denaturation at 94^0C for 2 min, followed by 30 cycles at: 94^0C for 30 sec, 58^0C for 30 sec, 72^0C for 40 sec with a final extension at 72^0C for 5 mins. The conditions for the house keeping gene, ribosomal protein L38 were 94^0C for 2 min, followed by 30 cycles at: 94^0C for 30 sec, 58^0C for 30 sec, and 72^0C for 10 sec. PCR products were resolved by agarose gel electrophoresis and stained with ethidium bromide.

cDNA synthesis and Real time RT-PCR

Total RNA was extracted using Trizol according to the manufacturer's instructions (Invitrogen) from wild type MEFs and mutant MEFs (E14.5). First strand cDNA synthesis was performed as mentioned before. Real time PCR was performed using 1µl of the 1:10 diluted cDNA using the ABI PRISM 7300 instrument (Applied Biosystems). Real time RT-PCR was done in a final volume of 25 µl comprising 1× Master Mix of Absolute SYBR Green (Thermo Scientific) and 0.1nM of forward and reverse primers for *Chd2* (Fwd: GGTGGTGATGGCAAGTCTTCAAGT; Rev: AGGCAAATGAGGCTTCTGAGGATG), housekeeping gene ribosomal protein L38 (*Rpl38*) (Fwd: TTCGGTTCTCATCGCTGTGAGTGT; Rev: TCTTGACAGACTTGGCATCCTTCC). Data were analyzed by averaging triplicates C_t (cycle threshold). Levels of *Chd2* RNA expression was determined according to the $2^{-\Delta\Delta ct}$ method by normalizing to the internal control *Rpl38.*

Generation of polyclonal Chd2 antibodies

Commercially available cDNA clones that contain various segments of Chd2 were used to generate an N-terminal portion of CHD2. cDNA fragment encoding the first 313 amino acids of *Chd2* were generated by restriction enzymes or PCR and then inserted into the Pet30A bacterial expression vector, which contains a histidine tag at the N-terminus. Synthesis of fusion protein was induced for 24 hrs at 20^0C with 1mM isopropyl-β-D-thiogalatoside. His-Chd2 fusion protein was isolated by affinity chromatography on a nickel column. A single rabbit was immunized with a His-Chd2 fusion protein encoding the first 183 amino acids of Chd2. The serum obtained from the rabbit was tested for its specificity against recombinant Chd2 peptides.

Immunofluorescence microscopy

U2OS cells were cultured in Lab-Tek chamber slides (Nunc, Thermo Fisher Scientific) and then fixed for 15 min at room temperature in 3.7% formaldehyde in phosphate-buffered saline (PBS). CHD2 was detected by indirect immunofluorescent staining with polyclonal anti-Chd2 antibody (1:3000) followed by incubation with a fluorescein isothiocyanate-conjugated goat anti-rabbit immunoglobulin secondary antibody (1:500) (Jackson ImmunoResearch). Mounted slides were viewed with Axioplan microscope (Carl Zeiss Inc.) and images were captured with a high resolution charge-coupled device camera (Roper Industries). The images were analyzed using MetaMorph software (MDS Analytical Technologies).

Western blot analysis to confirm specificity of anti-Chd2 antibody

U2OS cells at 90% confluency were transfected with the expression plasmid construct containing 1395 amino acid Chd2 recombinant peptide with the tandem affinity (TAP) tag (ChdkthRR). Whole cell lysates were prepared using cold TAP lysis buffer (50mM Tris pH 8.0, 150mM NaCl, 0.1% NP-40, 10 mM β-mercaptoethanol, 50 µg/ml avidin, 50mM NaH2PO4, and 10mM imidazole and protease inhibitors). The cell lysates were sonicated for 20 seconds in ice. The sonicated lysates were spiked with

3mM $MgSO_4$ and 1mM $CaCl_2$ and treated with 1µl of 50units/µl of micrococcal nuclease for 20 min at room temperature. Protein concentrations were determined using a BCA kit (Pierce). The lysates were eluted via AcTEV digest (3x 80U; Invitrogen) for 30min at 37°C. Straight lysates and TEV elutes were subjected to SDS-PAGE and immunoblotted with 1:1000 dilution of rabbit anti-6X His tag (Rockland) antibody and rabbit anti-Chd2 antibody (1:4000).

Results and Discussion

1.1 Analysis of expression pattern of mouse Chd2 transcript

Chd2 was first characterized by Woodage et al in 1997 [31]. The authors [31] mapped the human *CHD2* to the 15q26 region of chromosome 15 by PCR screening of the Genebridge4 RH mapping panel and showed the presence of an 11kb *Chd2* transcript in different tissues by northern blot. In skeletal muscle the northern blot revealed an extra 7.5-kb band as well as the 11-kb band [31]. To determine the expression pattern of mouse *Chd2* in different mouse tissues, total RNA was isolated from each tissue and treated with DNase I, and subjected to RT-PCR amplification with *Chd2* or *RPL38* primers. The gene encoding the ribosomal proteinL38 (*Rpl38*) served as the internal control. The highest *Chd2* expression was seen in the thymus, whereas liver and testis showed the least amount of *Chd2* transcript expression (Fig.3)

1.2 Polyclonal antibody production and immuno-localization of CHD2

Protein sequence analysis of Chd2 shows the presence of four putative nuclear localization signals. Thus, to further localize Chd2 protein expression in the cell, we generated a polyclonal rabbit antibody against Chd2. Histidine-Chd2 fusion protein encoding the first 183 amino acids of Chd2 was produced and used to immunize the rabbits. The serum obtained from the rabbits was tested for its specificity by Western blot analysis with histidine tagged recombinant Chd2 protein expressed in U2OS cells (Fig.4). To investigate the localization pattern of CHD2 in cells, indirect

immunofluroscence technique was utilized. As shown in figure 5, anti-Chd2 immunoreactivity is predominantly seen in the nucleus of the U2OS cells.

1.3 Mouse models of Chd2

In order to study the biological effect and role of CHD2, *Chd2* mutant mice were generated by our laboratory using the Baygenomics genetrap ES cell resource [108]. The gene trap was shown to be inserted within intron 27 upstream of the A+T hook and three of the four putative nuclear localization signals. Analysis of the mutant mice indicated that the mutation of *Chd2* lead to neonatal lethality in homozygous mice and enhanced lymphoma formation in heterozygous mice [110]. The study of growth kinetics on MEFs (mouse embryonic fibroblasts), derived from embryos obtained by crosses of *Chd2* heterozygous males and females, shows low growth potential of mutant MEFs compared to wild type. In addition, an aberrant DNA damage response in *Chd2* mutant cells was noticed. [109].

Figure 3. Distribution of Wt-Chd2 transcript in mouse tissues.
Total RNA isolated from each tissue was treated with DNase I and subjected to RT-PCR amplification with *Chd2* or *Rpl38* primers. No products (*Chd2*/*RPL38*) were seen when total RNA in the absence of reverse transcription was subjected to PCR amplification (RT-). B.M refers to bone marrow. The internal control *Rpl38* refers to the ribosomal protein L38

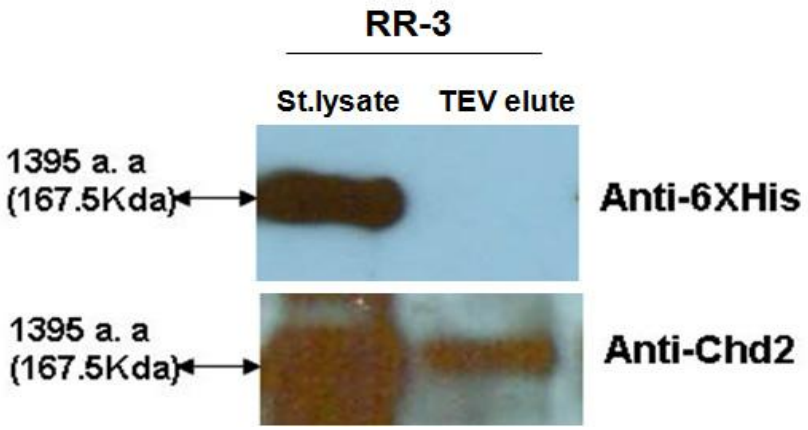

Figure 4.Specificity of anti-Chd2 Ab
The anti-Chd2 Ab could specifically recognize the recombinant Chd2 protein (1395 a.a) stably expressed in U2OScells (RR-3). Note the anti-Chd2 Ab also showed immunoreactivity with cell lysates treated with TEV protease to cleave the histidine tag (TEV elute). The anti-6XHis Ab showed no immunoreactivity with the TEV elutes, further supporting the specificity of the Chd2 Ab.

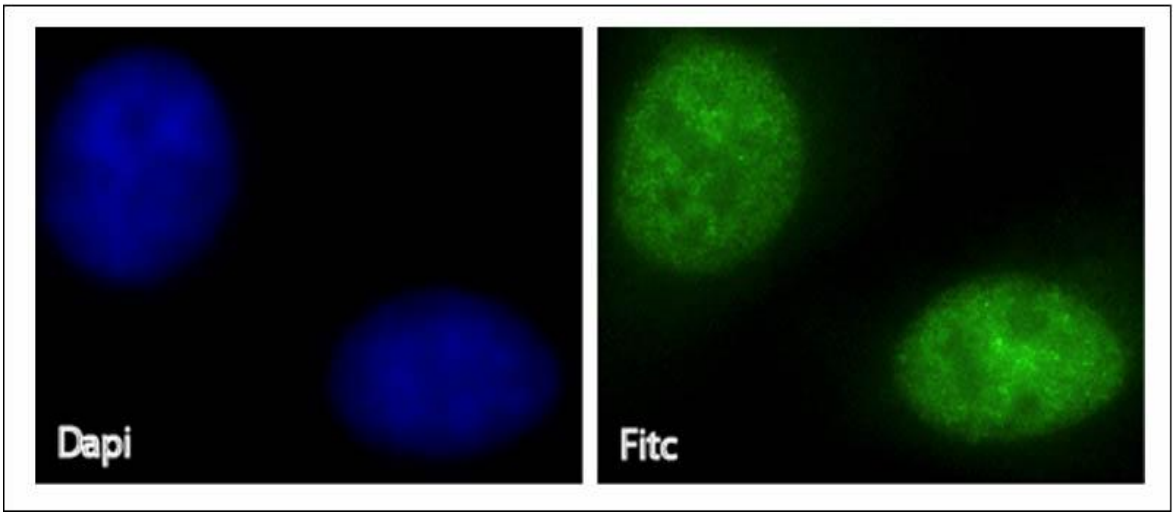

Figure 5.Immunofluorescent localization of CHD2 in U2OS cells
Indirect immunofluorescence using the anti-Chd2 antibody and a FITC conjugated secondary antibody shows localization of CHD2 to the nucleus

The C-terminal Chd2 mutant mouse model retains a substantial portion of the protein and has a truncation of the last 583 amino acids of the 1827 amino acid long wild type protein. One caveat relating to the C-terminal mutant mouse model we developed initially is the fact that it retains a substantial portion of the protein even though it has a truncation of 583 amino acids at the C-terminus. This brings about a possibility that the Chd2 mutant protein (fused to the β-galactosidase-neomycin fusion gene) may sequester additional transcription/DNA repair factors in to a non-functional complex or have dominant negative or gain of function effects leading to the observed phenotypes. To test the possibility of dominant negative effects of the fusion peptide, we analyzed the inter-molecular interactions between recombinant Chd2 peptides that contained 6x-His and HA epitope tags. Reciprocal immuno-precipitation analysis of recombinant Chd2 peptides showed that they were able to interact with each other (data not shown). These results suggested that the Chd2-β-gal-neomycin fusion protein may either sequester the wild type Chd2 protein to the cytoplasm or compete with the native protein for its binding partners.

Therefore, to rule out any indirect or dominant-negative effects of the mutant protein, a N-terminal mutant mouse model that is defective in the expression of 95% of the protein was generated. An N-terminal gene trapped ES cell line with the gene trap shown to be inserted in the intron 1 was identified (Fig.6). This insertion results in truncation of the protein after the first 20 amino acids. <u>The homozygous C-terminal Chd2 mutant mouse model was designated as *Chd2 m/m* and the N-terminal was designated as *NChd2m/m.*</u> From a total of 9 chimeric mice (7 males and 2 females) generated from the *Chd2* mutant ES cells, three males were determined to be germ line chimeras. Heterozygous intercrosses aimed at generating homozygous mutants indicated that there was partial lethality in the heterozygous and nullizygous mutants (Table 1). More importantly, unlike the C-terminal mutant mouse model, a fourth of the nullizygous *NChd2* animals (*NChd2m/m*) survived at weaning (Table 1, last column). These results indicate the C-terminal gene trap mutant exhibits a more drastic phenotype that is possibly due to dominant-negative function effects of the Chd2-beta-galactosidase fusion gene product.

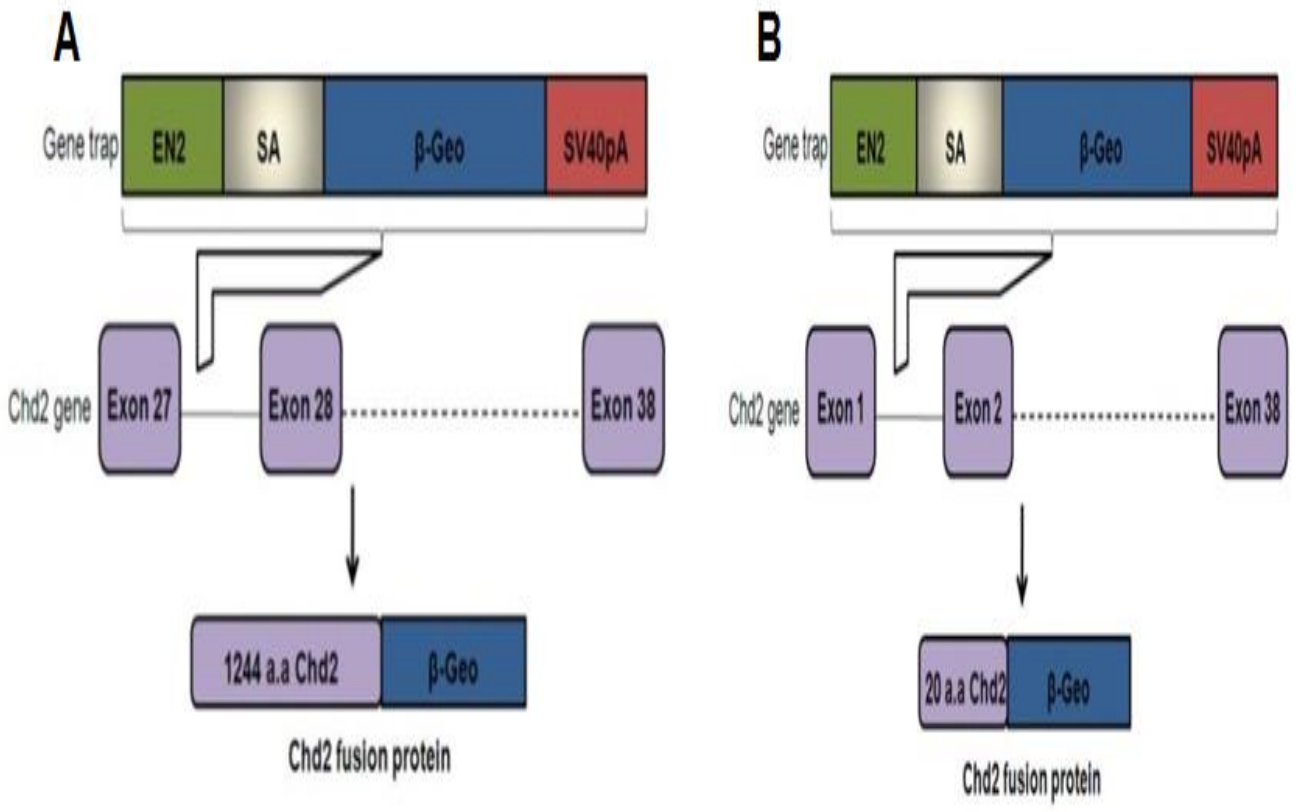

Figure 6.Gene traps vector insertion in the Chd2 gene

The gene trap vector, composed of a part of the *engrailed 2* intron 2 (*en2* intron2), a splice acceptor (SA), a beta-galactosidase/neomycin resistance fusion cDNA (β-geo), an SV40 polyadenylation signal (SV40pA),**(A)** was inserted between exons 27 and 28 of the *Chd2* gene for the C-terminal model,**(B)** between exons 1 and exons 2 for the N-terminal model.

Further analysis of *NChd2* heterozygous mice (*NChd2+/m*) indicated that the loss of a single copy of the *Chd2* gene leads to a decrease in the lifespan of the mice. Histological analysis of the tissues obtained from moribund *NChd2+/m* mice showed that they were succumbing primarily to lymphomas and the incidence of the lymphomas was higher than the incidence observed in the C-terminal mutant mice.
While the lymphoma, lymphoid hyperplasia, and extra medullary hematopoiesis phenotypes were retained in the N-terminal mutant, there was significant reduction in the nephropathy and heart inflammation phenotypes indicating tissue specific differences in a subset of the phenotypes between the two mouse models. Furthermore, the N-terminal mutants exhibited an increase in the incidence of other tumor types (sarcomas and adenomas, 16.6% versus 5%) in comparison to the C-terminal mutants (Table-2). Animals were monitored for tumors, morbidity, or spontaneous death over a period of 120 weeks. Of the 30 animals analyzed for each group, all of the heterozygous mutants died in comparison to 10 deaths for the wild-type controls. The median lifespan of the *NChd2+/m* mice was 59.35 weeks in comparison to 91.3 weeks in the wild type littermate controls. All mice were of mixed in-bred C57BL/6X129/Sv background.

1.4 Analysis of Chd2 expression in the N-terminal mutants

NChd2+/+, *NChd2+/m*, and *NChd2m/m* mouse embryonic fibroblast cells lines (MEFs) were derived from embryos obtained from crosses of *NChd2* heterozygous males and females. In order to quantify the wild-type and the mutant transcript in the homozygous mutant MEFs, real time RT-PCR was performed. *NChd2m/m* MEFs showed a reduced expression of about ~9% of the wild-type transcript (Fig.7).

Significance of the study

ATP-dependent chromatin remodeling proteins are known to be involved in the regulation of gene expression, recombination, replication and chromatin remodeling via their chromatin specific interactions and activities [17, 22]. These protein factors also play a part in the process of DNA repair, a role which has been increasingly recognized

for these factors. Some of the well documented examples include the role of ATP-utilizing chromatin assembly and remodeling factor (ACF) in the repair of 6-4PD(6-4 photoproducts) lesions on the DNA[111] and the interaction of INO80 with DNA damage induced phosphorylated histone H2A (γ-H2AX) [28, 30].

Deregulation of DNA repair is known to contribute to genomic instability and tumor formation [16, 112]. Interestingly, now there are numerous reports which link the alterations in the ATP-dependent chromatin remodeling proteins to the development of cancer. For example mutations in SNF5, BRG1 or BRM have been associated with the development of tumors [113]. Recently, somatic heterozygous missense mutations and promoter methylation of CHD5 were observed in some ovarian cancers [72]. In our study *Chd2* mutant mouse model studies, we have shown that mutation in one copy of *Chd2* results in enhanced lymphoma formation and reduced life span [110]. The emerging evidence supporting the role of ATP-dependent chromatin remodeling proteins in genomic instability and tumorigenesis along with our phenotypic observations of the *Chd2* mutant mice has led us to **hypothesize that the Chd2 protein is involved in maintaining genomic stability via its involvement in DNA Damage responses.**

The following three chapters of this thesis describe the three main objectives proposed to prove the aforesaid hypothesis. The first objective is to determine whether Chd2 plays any role in the process of DNA damage response. Experiments were conducted to determine if loss of Chd2 increased the susceptibility of cells to DNA damage and genomic instability.

The second objective involves the analysis of DNA damage induced post-translational modifications within the CHD2 protein. Protein phosphorylation is one of the commonly occurring post-translational modifications known to play a key role in DNA damage response. Phosphorylation of proteins allow their timely activation to respond to the DNA damage signal [114].

Table-1: Lethality of N-terminal Chd2 mutant mice. A total of 83 offspring were analyzed from 17 intercrosses. The genotype analysis of the offspring obtained from F1 intercrosses were performed using Chd2 specific primers in PCR assays.

Intercross	***NChd2 +/+***	***NChd2 +/m***	***NChd2 m/m***
Het.♂ X Het.♀	*36*	*39*	*10*
Expected Medelian ratio	*1*	*2*	*1*
Observed Mendelian ratio	*1*	*1.08*	*0.27*

Table-2: Distribution of pathological conditions in Chd2 mutant (N-terminal mutant) mice. Tissues from a total of 30 mice (*NChd2+/m*) were analyzed to determine the reasons for morbidity.

Pathological Conditions	**Percentage affected**
Lymphoma	53% (16 of 30)
Lymphoid hyperplasia	36.6% (11 of 30)
Extra Medullary Hematopoiesis (EMH)	56.6% (17 of 30)
Glomerulo-nephropathy	10% (2 of 19)
Inflammation of heart/artery	11% (1 of 9)
Other cancers	16.6% (5 of 30)

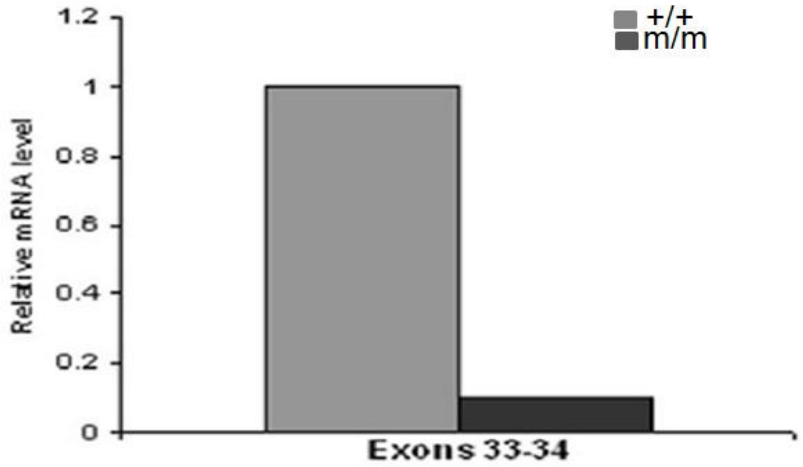

Figure 7.Analysis of *NChd2* mRNA transcripts by real-time quantitative RT-PCR using the 2-Δ ΔCt method
Each bar represents the relative *Chd2* mRNA level in *NChd2* (m/m) mutant MEFs compared with wild-type *NChd2* (+/+) MEF after normalization to RPL38. The wild-type Chd2 transcript was detected in MEFs by RT-PCR using primers for exons 33-34.

ATM (ataxia telangiectasia-mutated) and ATR (ATM and Rad3-related) are members of the phosphatidylinositol 3-kinase (PI-3) superfamily and are activated in response to DNA damage. Activated ATM /ATR phosphorylate many proteins, all of which have a role in DNA damage response pathway [115]. Analysis of the protein sequence of mouse Chd2 showed the presence of ten SQ (serine residue that precede glutamine residue) motifs. These motifs are potential sites for ATM/ATR mediated phosphorlyation, thus opening the gates of speculation that CHD2 would be a good substrate candidate for ATM/ATR mediated phosphorylation. Thus the second objective of the study was to test whether CHD2 is phosphorlyated after DNA damage and whether this phosphorlyation is brought about by ATM/ATR kinases.

The third objective focuses on the identification of CHD2 interacting proteins in response to DNA damage. DNA damage triggers the activation of phosphoinositide 3-kinase-related kinases (PIKK). Activated PIKK phosphorylates and activates H2AX,

checkpoint kinases (CHK1, CHK2), p53, MDM2, and BRCA1. All of these activated proteins then mediate the DNA damage response pathway (DDR) [116]. The tumor suppressor protein- p53 plays a crucial role in the signaling cascade known as the “DNA damage response (DDR)”. Activated p53 stimulates the transcription of target genes required for cell growth arrest as well as for efficient DNA repair. If the damage is unrepairable , p53 activates transcription of target genes involved in apoptosis[117]. Interestingly, ATP-dependent chromatin remodelers such as the SWI/SNF complex and CHD8 have been shown to interact with p53 and regulate the expression of p53 dependent target genes [89, 118]. Our preliminary analysis of Chd2 deficient thymocytes shows that these cells are defective in their ability to induce the p53-dependent pro-apoptotic gene, PUMA (George Samaan and Venkatachalam, unpublished observations). Thus we seek to determine whether CHD2 interacts with p53 and regulates the transcription of p53 dependent target genes in the third objective of this study. In addition to that, we want to determine whether CHD2 interacts with any other DNA damage response proteins through a tandem affinity purification approach coupled with mass spectrometry analysis.

Chapter III

Analysis of genomic stability and DNA repair process in *Chd2* mutant cells

Introduction

DNA in living cells is subjected to damage everyday from both endogenous and exogenous sources. About 10,000 DNA lesions occur every day due to normal metabolic processes and environmental factors [119]. It is imperative that these lesions be corrected quickly and efficiently in order to prevent deleterious mutations, genomic instability or cell death. The DNA repair machinery complex in the cell thus forms the most vital component involved in the repair of these deleterious lesions. Discrete biochemical DNA repair pathways exist in prokaryotes and eukaryotes to prevent the fixation of DNA damage in to heritable mutations. These repair pathways are divided into various subclasses based on the type of DNA lesion they repair. The major repair pathways include 1) the direct reversal pathway, (2) the mismatch repair (MMR) pathway, (3) the nucleotide excision repair(NER) pathway, (4) the base excision repair (BER) pathway, (5) the homologous recombination (HR) pathway, and (6) the non-homologous end joining (NHEJ) pathway [120].

The direct reversal pathway

Alkylating agents such as N-methyl-N-nitrosourea or N-ethyl-N-nitrosourea react with bases to transfer methyl or ethyl groups to a guanine, forming alkylation products such as O6-alkylguanine. This modified guanine base does not pair up with cytosine properly during DNA replication causing G: C → A: T mutations by anomalous base pairing[121]. O6-alkylguanine adducts are removed through the direct reversal pathway by the enzyme O6-methylguanine-DNA methyltransferase (MGMT) in mammals and the enzyme Ada in *Escherichia coli* (*E. coli*). Both enzymes transfer the alkyl group from the oxygen in the DNA to a cysteine residue in its active site enabling the removal of the adduct [120]. AlkB, a dioxygenase present in *E. coli* is involved in the direct reversal

repair of 1-methyladenine (1meA) and 3-methylcytosine (3meC). Mammalian AlkB homologues, ABH2 and ABH3 are also shown to have similar repair properties [120].

The mismatch repair (MMR) pathway

This repair pathway is activated in response to the presence of mismatched nucleotides/ DNA insertion-deletion loops formed due to DNA replication errors [121-122]. The error rate occurring during this process is approximately 107 per bp per genome [122]. The different proteins involved in the MMR pathway present in E.coli include MutS, MutL, MutH, γ-δ Complex, β-Clamp, Helicase II, ExoI, ExoX, RecJ, ExoVII, DNA pol III, SSB and DNA ligase. Homologs of the E.coli MMR proteins have been recognized in the eukaryotic system also. These different proteins in the pathway perform different tasks such as recognition of the mismatch, excision of the mismatch, DNA resynthesis and gap filling with the newly synthesized DNA [122]. A defective MMR pathway results in the instability of the genome at microsatellite regions consisting of mono- and di-nucleotide repeats. Hereditary non-polyposis colorectral cancer is the most common disease that arises from a defective MMR pathway in humans [123].

The nucleotide excision repair (NER) pathway

NER is a complex multistep DNA repair process involved in the repair of DNA lesions caused by UV radiation, mutagenic chemicals, or chemotherapeutic drugs that form bulky DNA adducts. About 30 mammalian proteins and 3 prokaryotic proteins have been identified as key players of the NER pathway [124-125]. Two types of NER pathways are the global genome NER (GG-NER) and the transcription-coupled NER (TC-NER). The XPC–RAD23B and DDB1–DDB2/XPE proteins detect lesions in the GG-NER pathway whereas the cockayne syndrome group A (CSA) (ERCC8) and CSB (ERCC6) proteins mediate the recognition in the TC-NER pathway [120, 126]. GG-NER detects and removes lesions throughout the genome whereas TC-NER repairs only actively transcribed genes [120]. The NER pathway involves recognition of the DNA lesion, dual incision of the damaged site by the incision complex (RPA [replication

protein A], XPA [xeroderma pigmentosum, complementation group A], XPG, and XPF/ERCC1), lesion removal, gap filling, and ligation by RPA, RFC [replication factor C small subunit], PCNA [proliferating cell nuclear antigen], DNA polδ and ε, and DNA ligase I [121]. Xeroderma pigmentosum (XP), Cockayne syndrome (CS), and trichothiodystrophy (TTD) are three common syndromes associated with defective NER [126].

The base excision repair (BER) pathway

DNA base damage occurring primarily from oxidative processes is repaired via the BER pathway. The two sub-pathways, short-patch BER and long-patch BER, involve removal of the damaged base by the enzyme DNA glycosylase leading to generation of an apurinic or apyrimidinic (AP) site [121, 127]. The AP site is removed by the endonuclease APE1. The short-patch BER pathway replaces a single nucleotide in the AP site and is mediated by DNA polymerase-β (Polβ). The long-patch BER pathway replaces 2-13 damaged nucleotides with the help of Polβ and/or Polε or δ. Nucleotide replacement is followed by strand ligation performed by the XRCC1/ligase III (LigIII) complex. Defective functioning of the glycosylase MUTYH results in G: C→T: A mutations leading to MUTYH-associated polyposis (MAP), an autosomal recessive disorder characterized by multiple colorectal adenomas and carcinomas [120].

The homologous recombination (HR) pathway

DNA double strand breaks (DSBs) are considered one of the most serious forms of DNA damage caused by exposure to ionizing radiation (IR), chemotherapeutic drugs, reactive oxygen species, and mechanical stress. Physiological DSBs also arise due to rearrangements of the immunoglobin loci in B cells, the rearrangement of the T-cell receptor loci in T cells, and during meiotic recombination [112, 128]. Repair of double strand breaks occur via the homologous recombination and the non-homologous end-joining (NHEJ) pathways [129].

The initial step of the homologous recombination (HR) pathway begins with the 3' DSB end processing by the NBS1/MRE11/RAD50 complex. This is followed by binding of RAD51-BRCA2 complex to 3' single-strand DNA. The RAD51 complex facilitates the invasion of 3' single-strand DNA into the homologous DNA double duplex which is then followed by strand extension by DNA polymerase. The resulting DNA crossovers called 'Holliday junctions' are subsequently resolved resulting in error-free DNA DSB repair [121, 130]. DNA DSBs occurring in germline tissues and those occurring during S and G2 phases of the cell cycle are repaired mainly by the HR pathway [121]. Defects in the HR pathway is associated with increased cell death, cell-cycle arrest, telomere defects, genomic instability, meiotic defects, immunodeficiency, and cancer [120].

The non-homologous end joining (NHEJ) pathway

The NHEJ pathway mainly acts to repair damaged DNA during the G1 phase of the cell cycle in somatic cells. It involves joining the broken ends of the DNA ,sometimes resulting in loss/gain of nucleotides and thus is error prone [131]. The process involves a complex interplay of various enzymes and proteins. The Ku70/80 heterodimer protein complex binds to the ends of the damaged DNA promoting the recruitment of the DNA-dependent protein kinase catalytic subunit (DNA-PKCS) to the DSB. DNA-PKCS phosphorylates many DNA repair proteins and recruits them to the damaged site. The repaired DNA ends are then ligated by the ligase IV/XRCC4 complex [132-133]. Mutations in the key players of NHEJ pathway result in increased chromosomal instability, increased cell death, cell-cycle arrest and increased incidence of tumors. Examples of disorders associated NHEJ repair pathway include Nijmegen Breakage syndrome (NBS) and Ataxia Telangiectasia-like disorder (ATLD) [121].

Chromatin remodeling and DNA repair

Compact nucleoprotein organization denies access to various regulatory factors involved in processes such as DNA-replication, -recombination, -repair, and -transcription. Histone modifying and chromatin remodeling complexes help to loosen up

the chromatin, giving passage to the regulatory factors to act on the naked DNA. ATP-dependent chromatin remodelers such as the Swi2/Snf2 related ATPase are key players in the DNA repair process [111, 134]. These chromatin remodelers alter the chromatin structure either through nucleosome displacement or histone exchange, increasing the access to the DNA lesion. For example, the ATP-utilizing chromatin assembly and remodeling factor (ACF), moves the nucleosomes, enhancing the activity of NER proteins to repair 6-4PD(6-4 photoproducts) lesions on the DNA [111].

The yeast SNF2-related ATPase complex, INO80, is another commonly studied ATP-dependent chromatin remodeling factor that aids in DNA repair. The complex contains 15 subunits which includes Swi2/Snf2-like ATPase subunit Ino80 and two proteins related to the bacterial RuvB DNA helicase [135]. The INO80 complex is recruited to the DSB at the yeast MAT (mating-type) locus induced by the homothallic switching (HO) endonuclease [136]. Mutations in genes encoding the ATPase subunits of the INO80 complex result in sensitivity to hydroxyurea, methyl methane sulfonate (MMS), UV and ionizing radiation, highlighting the role of the chromatin remodeler in DNA repair [135]. INO80 interacts with DNA damage induced phosphorylated histone H2A (γ-H2AX) at the DSB site further proving its important contribution to the DNA repair pathway [30]. The yeast RSC complex is also recruited to the DSB at the MAT locus along with the MRX (Mre11/Rad50/Xrs2) complex. The MRX complex then repairs the broken ends through the NHEJ pathway[111]. TIP60 possess both ATPase and histone acetyltransferase activity. TIP60 functions paradoxically in DNA repair pathway, first it acetylates histone H4 at the DSB acting as a signal for recruitment of HR repair proteins and second it catalyzes the exchange of phosphorylated histone H2Av for unmodified H2Av to cease the DSB signal after the completion of the repair process [137].

Swi2/Snf2 related ATPase containing SWR1 is another chromatin remodeler involved in histone exchange. SWR1 exchanges H2A-H2B dimers in nucleosomal arrays for H2AZ-H2B dimers. The presence of H2AZ histones loosen up the chromatin, increasing the accessibility to the DNA template. Yeast *Swr1* null mutants are sensitive

to DNA damaging agents, highlighting the role of SWR1 in the DNA repair process [111]. The Swi2/Snf2-related Rad54 protein is a key player in the HR repair pathway. Rad54 helps recruitment of Rad51 to the 3' single-stranded DNA and later aids in the branch migration of the Holliday junction [138]. A study trying to elucidate the role of the SWI/SNF complex in DSB repair showed increased binding of the SWI/SNF complex to chromatin upon DNA damage. Cells with inactive SWI/SNF complex showed decreased induction of γ-H2AX and inefficient DSB repair after DNA damage. Further analysis showed interaction of the SWI/SNF complex with γ-H2AX, suggesting a role of the SWI/SNF complex in DSB repair pathway [139].

Chromodomain helicase DNA binding proteins and DNA repair

There is no concrete evidence showing an association of CHD proteins with DNA repair processes. But there are some related studies which provide a clue to the involvement of CHD proteins in the DNA damage response pathway. One of the earlier studies done while trying to clone the SNF2/SWI2 helicase-related genes from the fission yeast Schizosaccharomyces pombe showed that the *Hrp1+* gene (helicase-related gene from S. pombe) exhibited a lower transcription rate upon treatment with DNA damaging agents such as MMS, MNNG, and UV. Protein sequence analysis of Hrp1 suggested that Hrp1 is a *S. pombe* homolog of mouse Chd1 [140]. A cDNA microarray study identified *CHD6* as up-regulated after 0.5 Gy of gamma-ray irradiation in AHH-1 lymphoblastoid cells as well as in A549 cells and HeLa cells. The induction of *CHD6* mRNA was dose-dependent and time dependent. *CHD6* transcript levels increased up to 8hrs after treatment with low dose (0.5, 1 & 2Gy) irradiation and decreased after 12hrs. In addition, high doses (4 & 8Gy) of radiation did not increase *CHD6* levels. Silencing of *CHD6* in the cells increased the resistance of A549 cells to low dose radiation whereas radiosensitivity was unchanged in response to doses larger than 4 Gy suggesting a mechanistic role of CHD6 in cellular responses to low dose radiation [141]. Ataxia telangiectasia mutated (ATM) and Rad3-related (ATR) proteins belong to a family of phosphatidylinositolkinase (PIK)-related kinases that play an

important role in the detection of DNA damage and activation of DNA repair pathway. Co-immunoprecipitation studies showed association of ATR, CHD4, and HDAC2 (histone deacetylase-2) in Hela cell lysates [142].

The limited literature evidence supporting the role of chromatin remodeling proteins in DNA repair process and the lymphoma phenotype seen in the *Chd2* mutant mice prompted us to examine the role of Chd2 in the repair of DNA damage and maintaining genomic stability. In this section we provide evidence that the Chd2 protein is required for maintaining genomic stability and for efficient repair of DNA damage. Results from the metaphase analysis, comet assay and the clonogenicity assay show that the *Chd2* mutation renders cells susceptible to genomic instability and inefficient DNA repair.

Material and Methods

Generation of Chd2 mouse embryonic fibroblast cells (MEFs)

MEFs were derived from 13.5-day-old *NChd2+/+, NChd2+/m* and *NChd2m/m* embryos. After removal of the head and intestinal organs, each embryo was washed with PBS and minced using 18 gauge needles. Cells were cultured in Dulbecco's modified Eagle medium with high glucose (HyClone, South Logan, Utah, USA) supplemented with 2mM L-glutamine, 1X antibiotic-antimycotic, 1µl/ml of fungizone (Invitrogen, Carlsbad, CA) , and 15% heat-inactivated fetal bovine serum (Gibco). Primary cells were frozen in aliquots after the first passage.

Immortalization of Chd2 MEFs

NChd2+/+, *NChd2+/m* and *NChd2m/m cells* were immortalized by transforming the cells with SV-40 (simian vacuolating virus 40) large T antigen containing plasmid pBSSVD2005 (gift from Dr. David Ron, Skirball Institute of Biomolecular Medicine). PrimaryNChd2 passage 1 MEFs were plated at 50% confluency in a 100mm plate and cells were transiently transfected with pBSSVD2005 using Lipofectamine 2000 reagent (Invitrogen, Carlsbad, CA) according to the manufacturer's instructions. When the cells

were just confluent, they were split at a dilution of 1/10. The cells were continued to be split at 1:10 dilutions till passage 5. This type of splitting ensured a strong negative selection against non-transformed cells.

Strand break detection using the alkaline comet assay

Low passage *NChd2+/+*, *NChd2+/m*, and *NChd2m/m* MEFs were seeded in 60mm dishes 1 day prior to treatment with 4Gy radiation, such that they were 75-80% confluent on the day of the treatment . $2X10^5$ cells were harvested at 10min, 30min, and 120mins post treatment. Cells were also harvested from untreated controls. DNA damage was determined by single cell gel electrophoresis performed under alkaline conditions using the comet assay kit (Trevigen, Gaithersburg, MD) according to the manufacturer's instructions. Dried samples stained with SYBR Green I was imaged by epifluorescence microscopy. At least 100 nuclei per experiment were quantified and the amount of DNA damage present in the individual nuclei was measured by Olive tail moment [tail length X (tail fluorescence / (head + tail fluorescence)], using CometScore (http://www.autocomet.com/). At least two independent clones of MEF cell lines were analyzed for the assay. For UV-C treatment, growth media was removed from the cells, rinsed with PBS and were irradiated with UV-C light at a dose rate of $0.60J/m^2$ per second. Thereafter, growth media was added to the cells and incubated for the appropriate time periods. $2X10^5$ cells were harvested at 1hr, 2hrs, 4hrs and 6hrs post treatment and comet assay was performed.

Analysis of metaphase chromosomes

Wild-type, heterozygous and homozygous *NChd2* MEFs ($1X\ 10^6$) were seeded in a 100mm plate a day before the experiment. The next day, actively growing cells were treated with 500ng (0.0625µg/ml) demecolcine (colcemid) to arrest the dividing cells in the metaphase. After 3 hr incubation with the colcemid, cells were trypsinized and collected as a pellet. The cell pellet was treated with 5ml of hypotonic solution (3:1 mixture of 0.566%potassium chloride and 0.8% sodium citrate) at 37°C for 15 minutes.

Following 15 min hypotonic treatment, cells were fixed in methanol: glacial acetic acid (3:1). Subsequently the cell suspension was dropped onto a microscope slide, and chromosomes were visualized with a light microscope after staining with Giemsa solution. Fifty metaphase spreads per genotype were scored for numerical as well as structural chromosome abnormalities.

Tumors derived from spontaneous thymic and spleenic lymphomas of male and female heterozygous *NChd2* mice were characterized for chromosomal abnormality. To characterize the chromosomal abnormality associated with these lymphomas, single-cell suspensions were prepared from hyperplastic spleens and thymus and the cells were resuspended in Dulbecco's modified Eagle medium with high glucose (HyClone, South Logan, Utah) supplemented with 2mM L-glutamine, 1X antibiotic-antimycotic, 1µl/ml of fungizone (Invitrogen, Carlsbad, CA) , 10% heat-inactivated fetal bovine serum (Invitrogen), and 20µM β-mercaptoethanol [143]. Metaphase preparations were done according to the protocol provided by Dr. Bassing's laboratory. Briefly, 5ml of freshly isolated lymphoma cells were cultured for 2hrs at 37^0C in the presence of 25µl of colcemid (KaryoMax, Invitrogen) and 25µl of 2.8mg/ml BrdU (in HBSS). Cells were then transferred to a room temperature hypotonic solution (40.2mM KCl, 0.5373mM EDTA.Na_2 and18.44mM HEPES.Na) for 25min at 37^0C and fixed by two changes of cold 3:1 methanol-acetic acid. Metaphase chromosome preparations were adhered to slides and sent to Dr. Bassing's laboratory for further processing for spectral karyotyping (SKY) analysis.

MTT assay

For the MTT [3-(4,5-dimethylthiazolyl-2)-2,5-diphenyltetrazolium bromide; ATCC, Manassas, VA] assay, low passage *NChd2*+/+, *NChd2+/m* and *NChd2m/m* MEFs were placed in a 96-well plate at 6000 cells/well 1day prior to UV, X-ray and MMS treatment. The cells were left untreated or treated with the addition of 0.025% MMS and 0.05% MMS or exposed to 10 & 20 J/m^2 UV radiation or to 5, 10, 15 and 20Gy dose of X-ray radiation. After 48hrs of culture, cells were treated with 10µl of MTT for 3hrs at 37°C,

allowing metabolic transformation of the MTT by the mitochondria and subsequent formation of an intracellular purple formazan. After solubilization of this precipitate, the absorbance was measured at 570 nm. Experiments were performed in quadruplets and results were normalized to control levels. At least two independent clones of MEF cell lines were analyzed for the assay.

Clonogenicity assay

SV-40 immortalized *NChd2+/+*, *NChd2+/m* and *NChd2m/m*($1X10^3$) cells were seeded in complete media and treated with 10 & 20 J/m^2 UV radiation or exposed to 2 & 4 Gy dose of X-ray radiation after 24hrs. After ~10-12 days, the plates were stained with coomassie blue and colonies were counted using a stereomicroscope. The colonies from the various treatments were normalized to the control. For each treatment, the cells were plated in four $60mm^2$ plates. The whole experiment was repeated three times.

Statistical analysis

Data was analyzed using GraphPad software (La Jolla,CA). Statistical significance was found using student's t-test and a P value < 0.05 was considered to be statistically significant.

Results

3.1. *Chd2* mutant cells are inefficient in repair of IR induced DNA damage.

The susceptibility of *Chd2* heterozygous mutant mice to lymphomas and the accumulation of high levels of γH2AX after DNA damage in *Chd2* mutant cells lead us to hypothesize that Chd2 is involved in DNA damage responses [109]. To test if the *Chd2* mutant cells are defective in their ability to repair DNA damage, we performed alkaline single-cell agarose gel electrophoresis (comet assay) with *NChd2+/+*, *NChd2+/m*, and *NChd2m/m* MEFs to quantify DNA damage after exposure to X-ray radiation (IR) and UV radiation. Cells from all three genotypes showed an extended

migration of fragmented DNA in comet tails after 10 min of exposure to 4Gy X-ray radiation. Interestingly, wild-type *Chd2* cells exhibited a recovery from DNA damage after 2 hours of IR exposure, with the comet tail moment comparable to that of the untreated controls. However the heterozygous and the homozygous mutant *Chd2* MEFs showed an inefficient DNA repair with the migration of fragmented DNA in comet tails still remaining higher even by 2 hours post exposure (Fig.8). Representative comet images of wild-type, heterozygous and homozygous *Chd2* mutant MEFs obtained at different time intervals after exposure to 4Gy of X-ray radiation are shown in figure-9.

To analyze the UV induced DNA damage response of *Chd2* cells, *NChd2+/+*, *NChd2+/m*, and *NChd2m/m* MEFs were exposed to varying doses of UV-C and harvested 6 hrs later for comet assay. As shown in figure-10A, *NChd2+/m* and *NChd2m/m* cells accumulated significantly increased amounts of DNA damage with increasing UV doses, as compared to wild-type cells. To assess the repair kinetics of UV induced damage a time course experiment was performed. As shown in figure-10B, 1hr after UV-C exposure *NChd2+/+*, *NChd2+/m* and *NChd2m/m* MEFs displayed increased OTM (Olive Tail Moment). Analysis of data collected at subsequent time points post UV-C exposure showed that OTM of heterozygous cells and homozygous mutant remained greater than that for wild-type at all exposure times. In contrast to the heterozygous and homozygous mutant cells, the wild-type cells showed a recovery from DNA damage with OTM significantly decreasing 6 hrs post-incubation periods.

3.2. Mutation in *Chd2* promotes chromosomal instability.

Genetic instability refers “to a range of genetic alterations from point mutations to chromosome rearrangements” [144]. Instability results from replication errors, defective DNA repair or error-prone translesion DNA synthesis [144]. Because *Chd2* mutant cells showed inefficient DNA repair, we wanted to examine the genomic stability of these cells. Metaphase spreads were prepared from low passage wild type, heterozygous and homozygous mutant MEFs treated with 4gy X-ray radiation. The metaphases were stained with Giemsa stain and scored for numerical and structural abnormities.

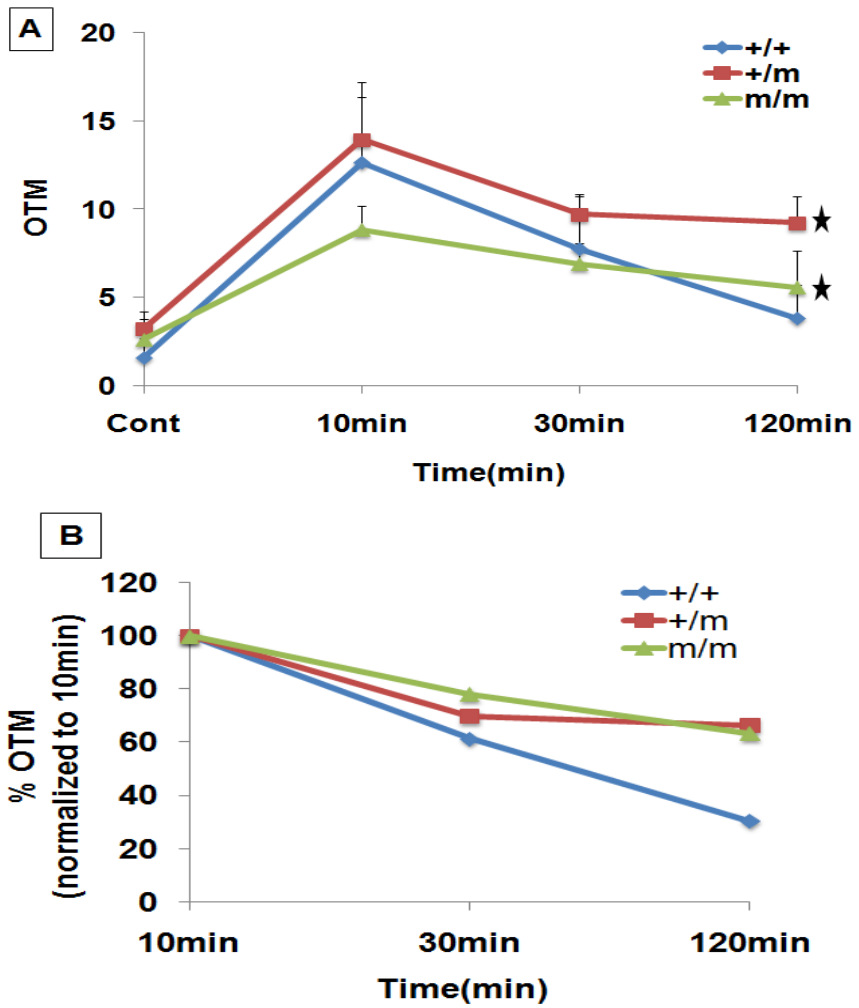

Figure 8.Role of Chd2 in repair of DNA damage

To analyze the repair of DNA damage, alkaline single-cell gel electrophoresis (SCGE, comet assay) was performed. **(A)** Wild-type (+/+), heterozygous mutant (+/m) and homozygous mutant (m/m) MEFs were exposed to 4Gy X-ray radiation and harvested at 10, 30 and 120minutes. At least 100 nuclei per experiment were quantified and the amount of DNA damage present in the individual nuclei was measured by Olive tail moment (OTM). OTM was calculated using the following formula: OTM=Tail length X (tail fluorescence / (head + tail fluorescence)]. **(B**) Percentage repair was evaluated by normalizing to OTM obtained after 10min exposure. Data 100 cells for each time point ±SD are shown for (A). *, p = < 0.0001(wild-type versus heterozygote; wild-type versus homozygote).

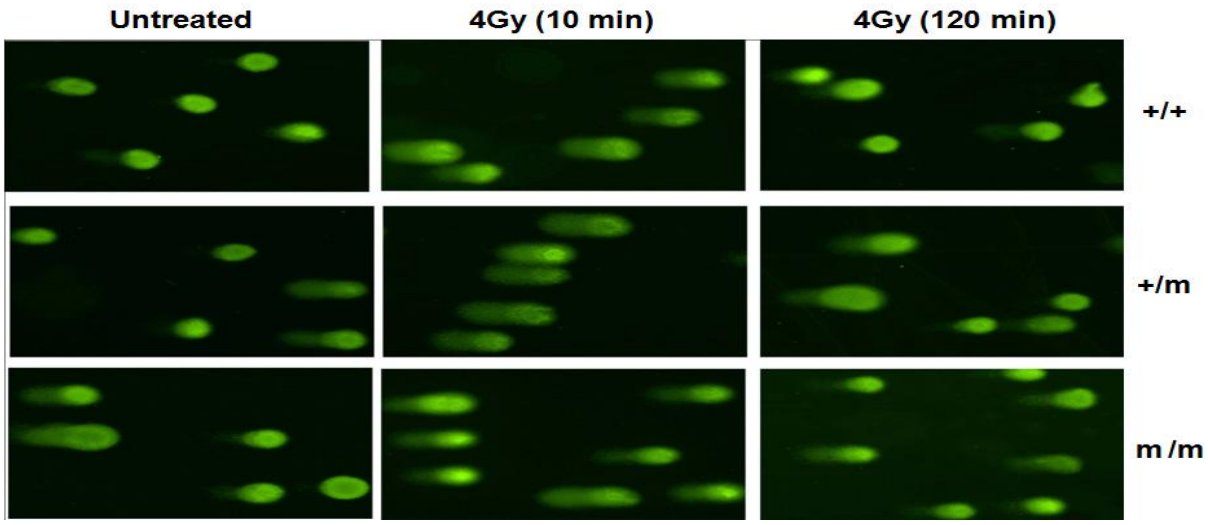

Figure 9.*Chd2* mutant cells have an impaired ability to repair damaged DNA

DNA damage (tail moment) detected by the Comet assay at 0 (untreated), 10 min, and 120 min in *NChd2* MEFs treated with 4Gy X-ray radiation

Of the 50 metaphases examined for each genotype, heterozygous and homozygous *NChd2* MEFs showed a slight increase in aneuploid cells and chromosome aberration in comparison with wild-type cells, but the increase was not statistically significant (Fig.11A). After X-ray treatment the heterozygous *NChd2* MEF cells showed a significant increase in chromosomal aberrations including chromosome breaks, chromatid breaks, fragments, and ring chromosomes when compared to the wild-type cells (Fig.11B, Fig.12). These results further suggest that Chd2 protein plays a critical role in maintaining genomic stability.

3.3. Metaphase analysis of spleenic and thymic lymphomas obtained from heterozygous mice.

Cancer results from the accumulation of a number of genetic changes. These changes include mutation as well as chromosomal aberrations.

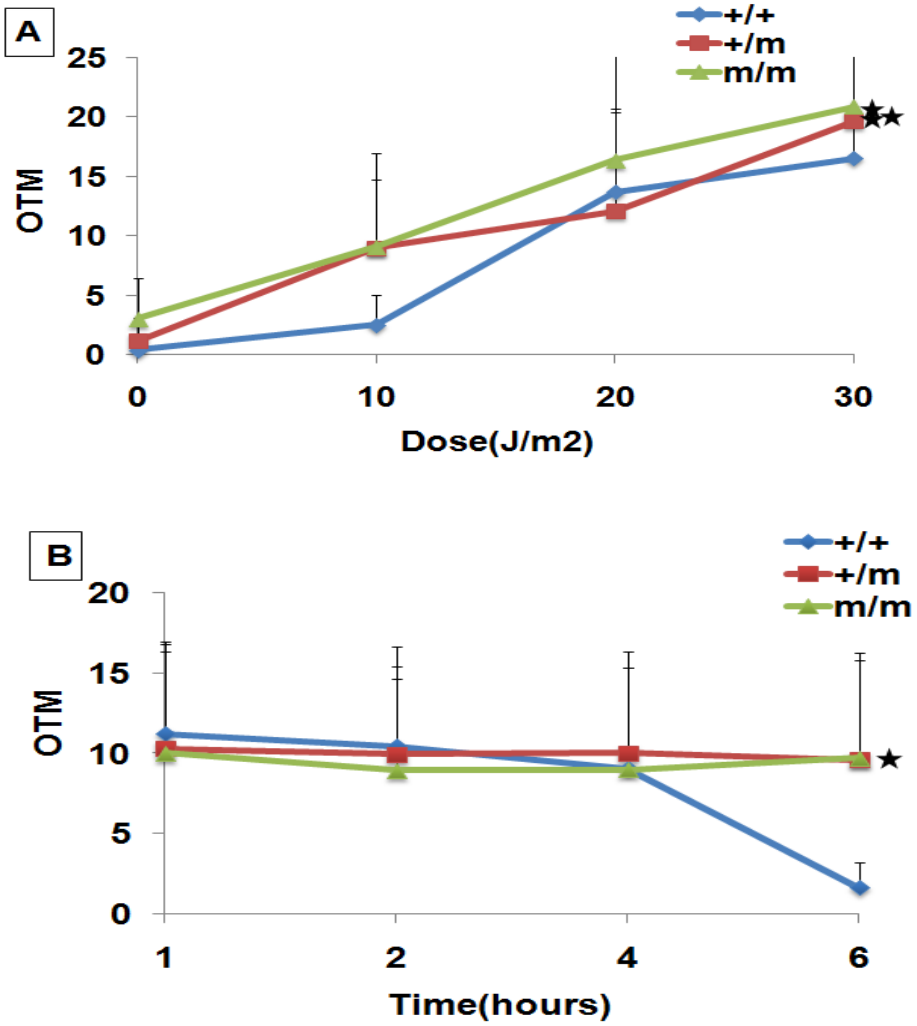

Figure 10.Repair of DNA damage induced by UV

To analyze repair of DNA damage, alkaline single-cell gel electrophoresis (SCGE, comet assay) was performed. **(A)** Wild-type (+/+), heterozygous mutant (+/m) and Homozygous mutant (m/m) MEFs were exposed to different UV-C doses and harvested after 6 h. * p = 0.0088 (wild-type versus heterozygote); ** p = 0.0016 (wild-type versus homozygote). **(B)** Cells were exposed to 10 J/m2 and subjected to SCGE after incubation times of 1, 2, 4 and 6 h. * p = < 0.0001 (wild-type versus heterozygote; wild-type versus homozygote). Data (OTM = Olive tail moment) of 100 cells for each time point & dose ±SD are shown.

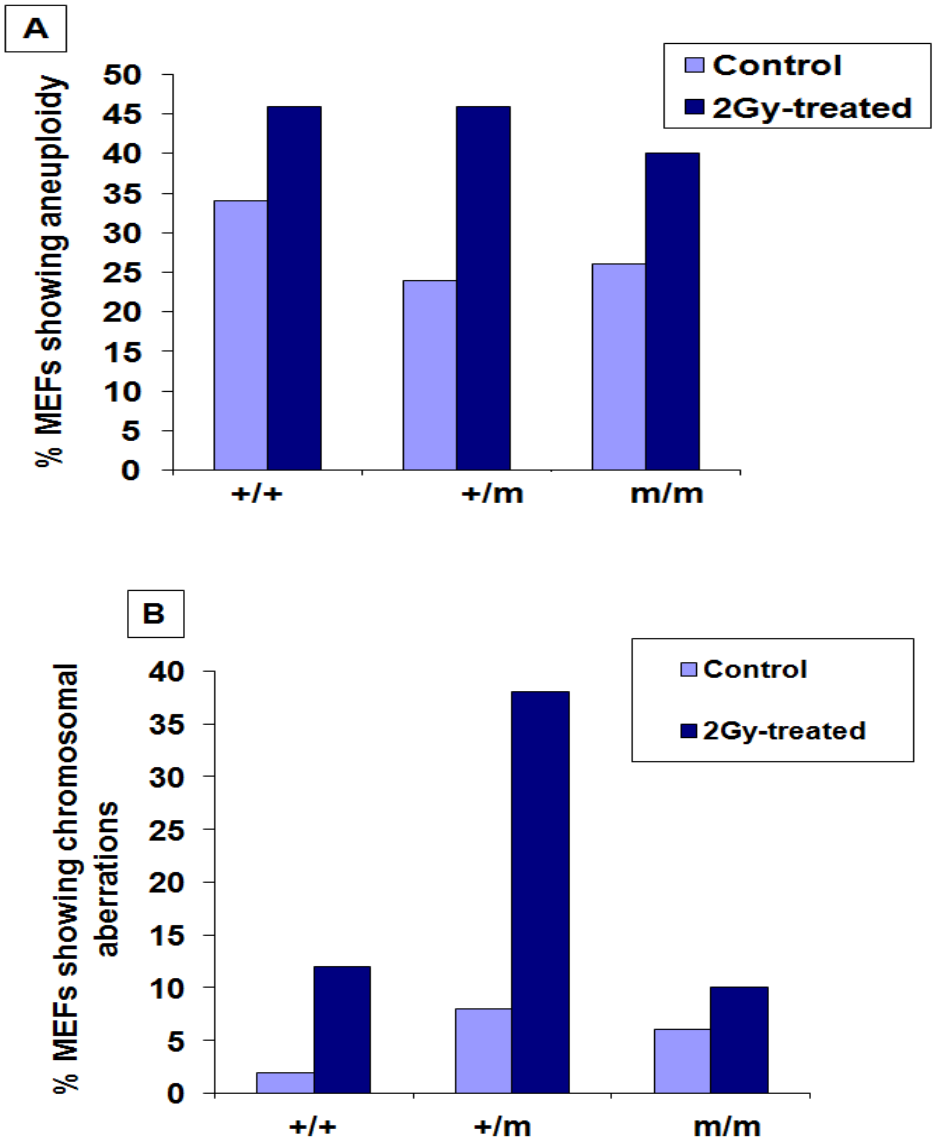

Figure 11.Role of Chd2 in genomic stability

Metaphase spreads from wild-type (+/+), heterozygous mutant (+/m) and homozygous mutant (m/m) Chd2 MEFs were scored for structural chromosomal abnormities [A] and numerical abnormality [B] (50 metaphases scored).

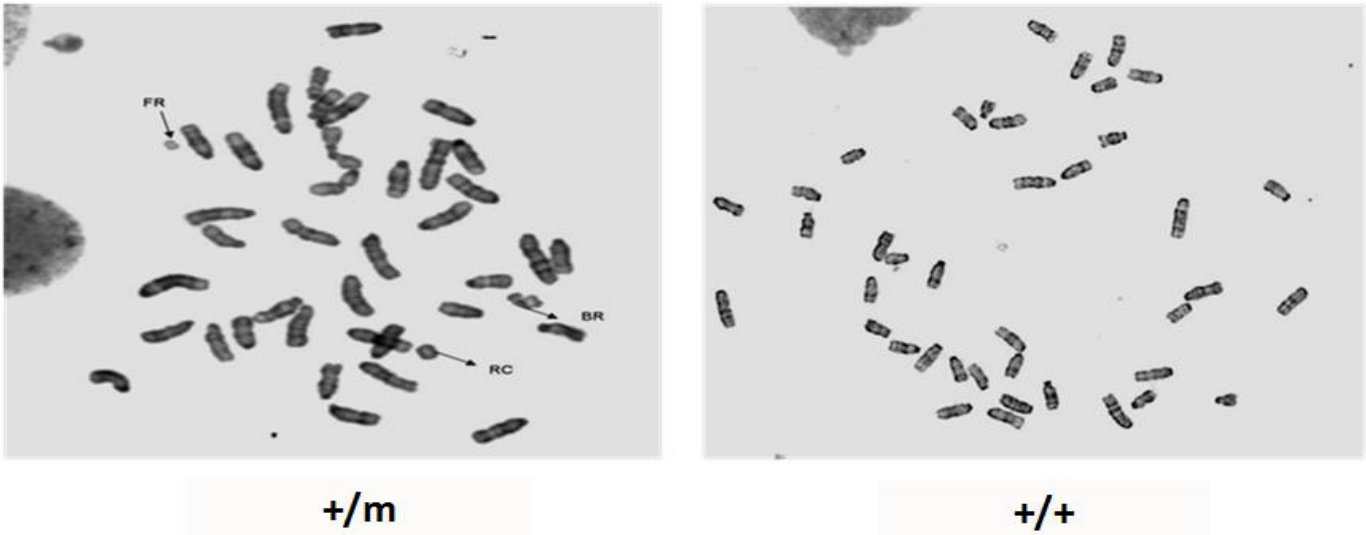

Figure 12. Mutation in *Chd2* promotes chromosomal instability
Representative photographs of metaphases from heterozygous mutant *NChd2* MEF (+/m) and wild-type *NChd2* MEF (+/+) showing chromosomal aberrations.

A number of chromosomal aberrations have been associated with different types of cancers, for example translocation between chromosome 8 and 14 is associated with Burkitt's lymphoma [145]. Thus in an effort to understand the molecular basis of the spleenic and thymic lymphomas seen in heterozygous *NChd2* mutant mice, metaphase spreads were made from these lymphomas and analyzed by spectral karyotyping. Eleven thymic lymphomas and eight spleenic lymphomas were obtained from heterozygous mice. Metaphase spreads were prepared from single cell suspensions of the lymphoma cells and sent for spectral karyotyping. Analysis of three thymic lymphomas showed presence of an extra chromosome 15 in two samples (data not shown).

3.4. Mutation in *Chd2* does not affect cell viability after DNA damage.

Defective DNA repair and genomic instability usually results either in apoptosis or growth arrest. Thus to determine the viability of *Chd2* mutant cells, an MTT (3-(4, 5-Dimethylthiazol-2-yl)-2, 5-diphenyltetrazolium bromide) assay was performed with low passage *NChd2+/+*, *NChd2+/m* and *NChd2m/m* MEFs. Cell survival was determined 48

hours later and expressed as a percentage by setting corresponding untreated controls as 100%. There were no differences in the viability of *NChd2+/+*, *NChd2+/m* and *NChd2m/m* MEFs after exposure to various doses of X-ray radiation. Interesting, the *NChd2+/m* cells showed a slight but significant increase in viability with 20Gy of X-ray radiation (Fig.13).

Treatment with UV did not show much difference in the viability between the wild-type and heterozygous cells. However the heterozygous MEFs showed slightly decreased viability at higher doses of UV radiation (Fig.14). And interestingly as seen in figure 15, homozygous *NChd2* mutant cells were significantly sensitive to both doses of UV radiation. To further determine the viability of Chd2 mutant cells in response to DNA damage by the alkylating agent, methyl methanesulfonate (MMS), we analyzed cell viability in wild type and *Chd2* mutant cells. Homozygous mutant *NChd2* cells exhibited a slightly reduced viability with both concentration of MMS treatment, whereas the heterozygous mutant cells exhibited reduced viability only with the higher concentration (0.05%) of MMS (Fig.15). However the difference was not statistically significant.

3.5. Clonogenic survival of SV40 immortalized Chd2 MEFs is affected after DNA damage.

The transformation of normal cells into tumorigenic cells requires several genetic events. The analysis of short term survival studies in primary mouse embryonic fibroblasts provide limited information on the role of proteins in cellular responses to DNA damage, thus a long term survival assay (clonogenicity assay) was performed with the *Chd2* mutant cells. To further investigate the role of Chd2 in affecting the clonogenic survival of cells, we used SV40 large T-antigen immortalized *NChd2+/+*, *NChd2+/m*, and *NChd2m/m* MEFs to examine their ability to survive DNA damage induction. The large T-antigen induces the transformation of primary rodent cells by interacting and inactivating the tumor suppressor proteins p53 and Rb [146]. We performed clonogenic survival assays with SV40 transformed *Chd2* proficient and mutant cells that were treated with UV and X-ray radiation.

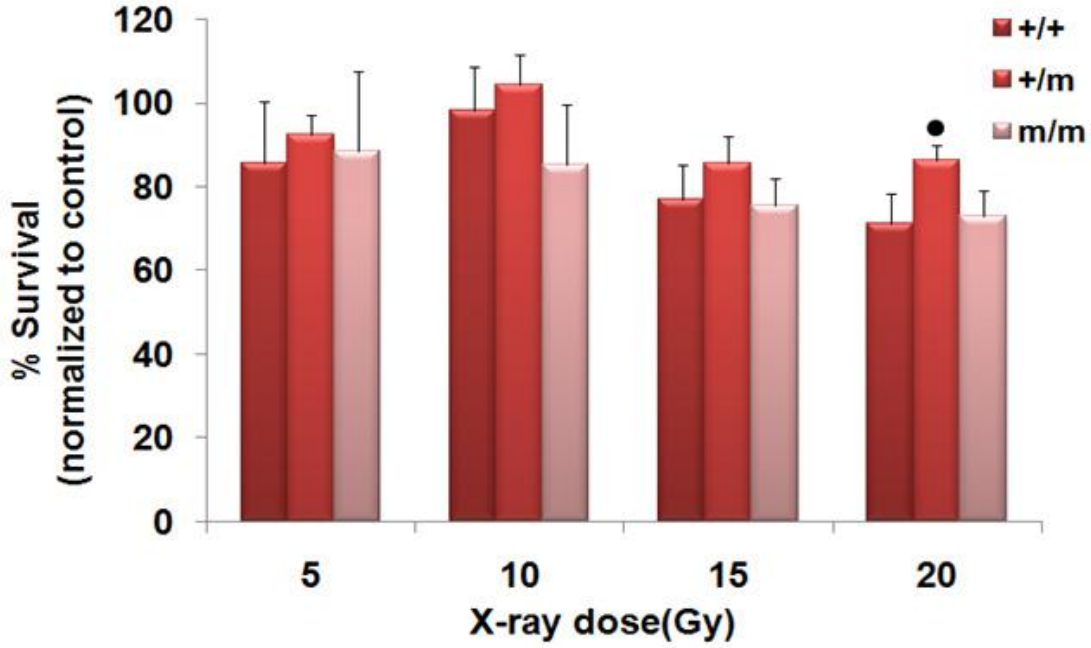

Figure 13.Cell viability of Chd2 MEFs after X-ray induced DNA damage

MTT assay of *NChd2+/+*, *NChd2+/m* and *NChd2m/m* MEFs following exposure to 5, 10, 15 and 20Gy dose of X-rays. Experiments were performed in quadruplets and results are normalized to control levels. Error bars represent SD values; ● p = 0.0161(wild-type versus heterozygote).

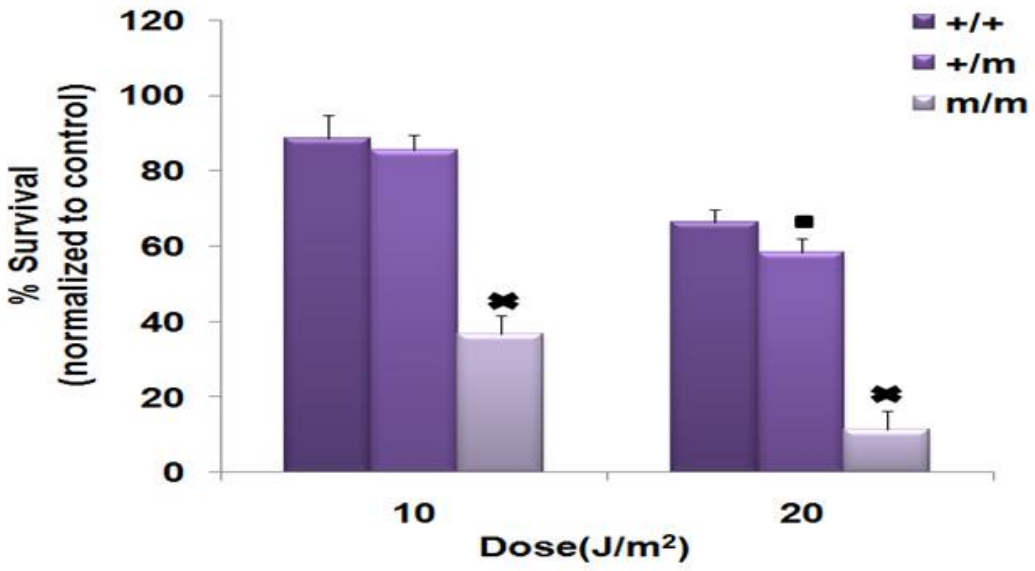

Figure 14.Cell viability of Chd2 MEFs after UV induced DNA damage

MTT assay of *NChd2+/+*, *NChd2+/m* and *NChd2m/m* MEFs following exposure to 10 and 20J/m2 of UV radiation. Experiments were performed in quadruplets and results are normalized to control levels. Error bars represent SD values; ■ p= 0.0198 (wild-type versus heterozygote); × p < 0.0001 (wild-type versus homozygote).

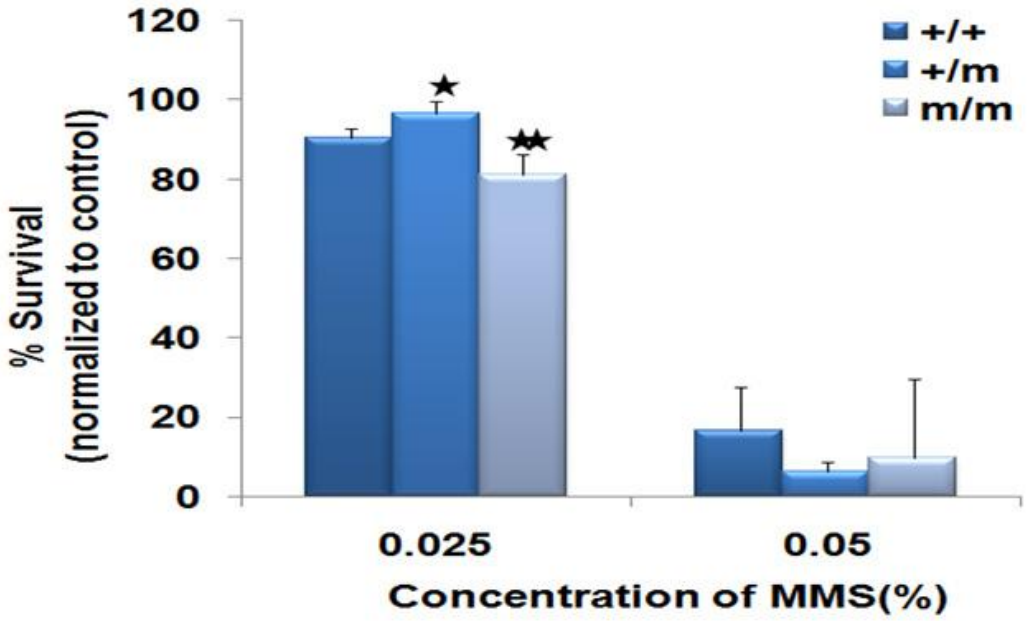

Figure 15. Cell viability of Chd2 MEFs after DNA damage with MMS
MTT assay performed with *NChd2+/+*, *NChd2+/m* and *NChd2m/m* MEFs following exposure to 0.025 % & 0.05% MMS. Experiments were performed in quadruplets and results are normalized to control levels. Error bars represent SD values; *p = 0.0127(wild-type versus heterozygote); ** p = 0.0163, (wild-type versus homozygote).

As shown in figure-16, SV40 immortalized *NChd2+/m* and *NChd2m/m* MEFs showed marked hypersensitivity to UV treatment compared to the wild-type. However the clonogenic survival of SV40 immortalized *NChd2+/m* MEFs was not affected with lower doses (2Gy) of X-ray radiation. But with an increased dose of 4Gy X-ray radiation, *NChd2+/m* MEFs became more sensitive than their wild-type counterparts. These observations indicate that immortalization of the heterozygous and homozygous mutant *Chd2* cell renders them susceptible to DNA damage induced by UV and X-ray, reducing their clonogenic survival.

Discussion

The data presented here demonstrate a potential role for Chd2 in maintaining genomic stability by affecting the efficiency of DNA repair.

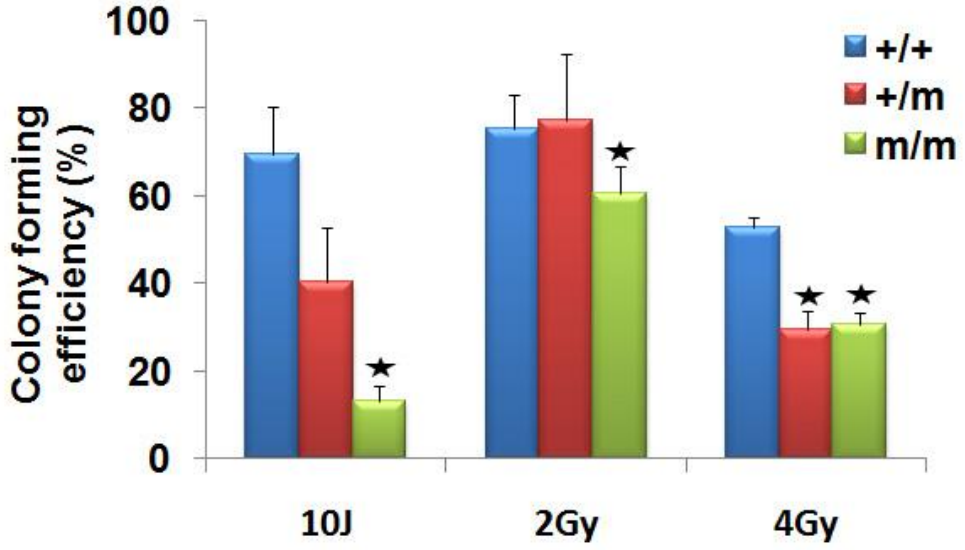

Figure 16. Clonogenicity assay of Chd2 MEFs
SV40 transformed wild-type (+/+) and Heterozygous (+/m) and homozygous (m/m) MEFs were seeded and treated with 10 & 20 J/m2 UV radiation or exposed to 2 & 4 Gy dose of IR. Colonies were counted after 7-10 days. The percentage of untreated cells was set at 100%. Error bars represent SD values for quadruplet's samples. * p = <0.0001(wild-type versus heterozygote; wild-type versus homozygote).

It has been well established that when cells fail to repair or inefficiently repair DNA damage it leads to cell death or chromosomal instability. The resultant chromosomal rearrangements or mutations contribute to tumorigenesis [147-148].

The *NChd2+/m* MEF displayed a delayed response to removal of DNA damage, as these cells showed high accumulation of DNA in their comet tail 2 hours post X-ray treatment and 6 hours post UV treatment. This finding was further supported by the observation that *NChd2+/m* MEFs showed a significant increase in chromosomal damage after exposure to X-ray radiation. However it was of interest to note that the short term viability of the *NChd2+/m was* not affected by the accumulated DNA damage. *NChd2+/m* MEFs were slightly more resistant to cytotoxicity by X-ray radiation, low doses of UV, and low concentrations of MMS than *NChd2+/+* cells. It has been reported

that measuring cell death using short-term viability assays such as the MTT assay is not an accurate measure to determine the role of DNA damage responses [149]. These assays have been shown to miscalculate the overall level of cell killing as cell death can take hours or days depending upon the cell type and the genotoxic agent used [149]. It has also been shown that primary mouse or human fibroblast cells are relatively more resistant to damage induced apoptosis [149-150].

The homozygous mutant cells demonstrated a decrease in the efficacy of DNA-repair in response to X-ray and UV radiations, but interestingly, they did not display extensive chromosomal instability post-crisis as the heterozygous mutant cells in metaphase analysis. This difference in observations between the *NChd2m/m* and *NChd2+/m* MEFs indicates that the loss of function of Chd2 due to mutation in both the copies of the gene may be compensated by another member of the same family (for example Chd1). This phenomenon known as functional compensation is not uncommon and has previously been reported in many studies [151-153]. In addition, the differences in the cell cycle phase of the homozygous mutant cells compared to the heterozygous mutant cells may be a reason for the reduced genomic instability in the homozygous cells. There are several reports which demonstrate that cells show a differential degree of sensitivity to DNA damage based on the phase of the cell cycle they are in [154-155]. The metaphase analysis of the wild type and Chd2 mutant cell lines were performed using asynchronous cells as synchronization of primary wild type MEFs leads to a substantial portion of the MEFs to arrest in the G0 phase of the cell cycle. Therefore the reduced chromosomal stability of the homozygous mutant is possibly related to differences in the cell cycle phase differences of the homozygous mutants in comparison to wild type and heterozygous mutant cells.

A direct correlation between *Chd2* mutation and aberrant DNA damage response was observed with SV-40 immortalized *NChd2+/+*, *NChd2+/m* and *NChd2m/m* MEFs. The colony forming capacity of the *NChd2m/m* and *NChd2+/m* MEFs was significantly compromised after treatment with DNA damaging agents. While, several studies have reported that presence of SV-40 large T-antigen in cells renders them more susceptible

to DNA damage [156-157]. The significant differences between the SV-40 transformed wild type, *NChd2m/m* and *NChd2+/m* MEFs after treatment with DNA damaging agents suggest that the Chd2 protein functions in DNA repair pathways.

It has been shown that ATP-dependent chromatin remodeling proteins like INO80 and SWR1 complexes perform critical functions in DNA repair by directly binding to the sites of DNA DSBs through their association with γ-H2AX. They bring about "nucleosome eviction" to facilitate the recruitment of DNA repair proteins and cell cycle check point proteins [158]. Other chromatin remodeling proteins like SWR1 are involved in the exchange of H2A-H2B dimers in nucleosomal arrays for H2AZ-H2B dimers. The presence of H2AZ histones loosen up the chromatin, increasing the accessibility to the DNA template. ATP-dependent chromatin remodeling proteins are not only required during the repair process but are also needed upon completion of the process to restore the native chromatin structure. The TIP60 histone acetyltransferase that also possesses ATPase activity, is known to catalyze the exchange of phosphorylated histone H2Av for unmodified H2Av to cease the DSB signal after the completion of the repair process [137]. TIP60 is also involved in regulation of DNA damaged induced acetylation of H2AX. Following DSB formation, TIP60 acetylates H2AX which results in the recruitment of the ubiquitin-conjugating enzyme UBC13. UBC13 promotes polyubiquitination of H2AX resulting in the release of H2AX from damaged chromatin [159]. Recently a haploinsufficient tumor suppressor gene, *HINT1*, which codes for a histidine triad nucleotide binding protein was shown to participate in ionizing radiation (IR) – induced DNA damage responses. HINT1 deficient cells exhibited an inability to displace γ-H2AX subsequent to DNA repair which was associated with impaired acetylation of γ-H2AX [160]. HINT1 deficient cells also showed inefficient DNA repair due to impaired acetylation of ATM [160]. It is of interest to note that, we have previously shown that *Chd2* mutant cells fail to remove γ-H2AX after DNA repair [109]. These results in conjunction with the defective repair phenotypes of the *Chd2* mutant cells suggest that CHD2 is potentially involved in facilitating acetylation of γ-H2AX once the repair process is complete , thus helping in restoration of the

chromatin structure. Alternatively CHD2 may function to remodel chromatin during the repair process by facilitating access to DNA repair proteins to sites of DNA damage. Additional studies to determine the functional binding partners of CHD2 would provide further insights into CHD2's function in the DDR pathway.

Chapter IV

Determination of molecular changes in CHD2 in response to DNA damage

Introduction

The DNA damage response (DDR) triggered by the cell consists of several interconnected pathways that include DNA repair, cell cycle arrest, and cell death. A variety of events in DDR are initiated through activating signals transmitted by checkpoint transducers. The transducers and their downstream targets are activated by different posttranslational modification events, such as phosphorylation, acetylation, methylation, and ubiquitylation, which influence their activity [161-162]. Central components of the kinase pathway are the phosphoinositide 3-kinase related kinases ATM, ATR, and DNA-PK. ATM (ataxia telangiectasia-mutated) and ATR (ATM and Rad3-related) are members of the phosphatidylinositol 3-kinase (PI-3) superfamily that are activated in response to DNA damage. Other members of the family include ATX/SMG-1, mTOR (mammalian target of rapamycin), FRAP (FK506binding protein 12-rapamycin associated protein 1), and DNA-PKcs (DNA-dependent protein kinase). Members of the PI-3 superfamily contain the PI3 kinase domain which is the catalytic site of the active protein kinase responsible for phosphorylating the key proteins involved in DNA damage response [116]. ATM and DNA-PK respond to DNA double strand breaks caused by ionizing irradiation (IR), while ATR and ATX respond to UV or stalled replication forks [14]. Studies have shown that the MRN complex is first recruited to the site of DSB and activates ATM by facilitating stable binding of ATM to its substrates and also promoting ATM's auto-phosphorylation [163]. The C-terminus of ATM harbors the FAT (FRAP/ATM/TRAP) domain, a PI3 kinase domain, and the FATC (FAT C-terminal) domain, all which regulate the kinase activity of ATM [164].

ATM exists as a dimer in its inactive state; upon sensing DSBs it undergoes auto-phosphorylation at serine 367, serine 1893, and serine 1981 residues leading to formation of active ATM monomers [164]. The ATM and ATR kinases, once activated,

phosphorylate H2AX, CHK2, CHK1 kinase, p53, MDM2, BRCA1, which then mediate downstream DDR [116]. Phosphosrylation of H2AX at serine 136 and 139 by ATM/ATR occurs within minutes of DNA double strand break (DSB) induction. Many additional substrates of ATM such as Rad17, p95, BRCA2, PTS, PhasI, WRN, DNA-5B and ligase IV have been identified and have been shown to play a role in DNA damage response pathway [115]. Consensus target sequences of ATM and ATR phosphorylation have been characterized which act as guidelines to determine whether a protein sequence is a potential target for phosphorylation by ATM/ATR kinase. These are: a) the presence of SQ/TQ motifs (serine or tyrosine residue that precede glutamine residue), b) the presence of hydrophobic amino acids at positions N-3 and N-1, and c) the presence of atleast three SQ/TQ motifs in a “core region of 100 amino acids” [115, 165]. Mutations in the ATM gene results in an autosomal recessive disorder known as Ataxia-telangiectasia (AT), characterized by cerebellar ataxia, telangiectasia, immunodeficiency, hypersensitivity to radiation induced cancers, defective cell cycle checkpoints, and chromosomal instability [164].

ATM/ATR and Chromatin remodeling proteins

It has been well established that the remodeling of chromatin takes place in the presence of DSBs and that this remodeling is necessary for efficient recruitment of DNA damage response proteins to the DSB site [166]. The decondensation of the chromatin takes place via an energy dependent manner suggesting that the initial sensors of DSBs have an ATP-dependent remodeling property [167]. The relaxation of chromatin is further enhanced by phosphorlyated H2AX (γ-H2AX) and ATM. Both of these proteins are involved in initiating the DNA damage response signal and recruitment of ATP-dependent remodeling complexes [167-168]. This fact is further supported by experimental evidence showing that ATM negative cells exhibit inefficient histone loss from the DSB site [168]. Furthermore, a study in yeast showed that the yeast Mec1/Tel1 kinases (ATM/ATR in mammals) phosphorylated the Ies4 subunit of the ATP-dependent remodeling protein complex-INO80 when the yeast cells were exposed to DNA

damaging agents. Phosphorylation of les4 influenced the checkpoint response following DNA damage. Additionally, the Mec1/Tel1 kinase phosphorylated H2AX, which then promoted the recruitment of INO80 to the region of DNA damage [169]. KAP-1(KRAB-associated protein), a corepressor of gene transcription, was shown to be an ATM effector protein. KAP-1 was phosphorylated by ATM upon DSB induction. Phosphorylated KAP-1 spreads throughout the chromatin and facilitates chromatin decondensation [170]. KAP-1 recruits heterochromatin protein 1(HP1) to histones. It also associates with the histone methyltransferase SETDB1 and Mi2-α. Assembly of these proteins coordinated by KAP-1 results in heterochromatization [171]. Protein interaction studies with ATM reveled its association with the histone deacetylase HDAC1, and the interaction was shown to increase with exposure to ionizing radiation [172]. A more recent study showed association of ATR with CHD4 and HDAC2 (histone deacetylase-2) in Hela cell lysates [142]. These studies demonstrate the functional importance of ATM/ATR dependent activation of ATP-dependent chromatin remodeling proteins in DNA damage responses.

In this section we show that CHD2 is a novel substrate of the ATM/ATR kinases. Analysis of the CHD2 protein sequence shows the presence of ten SQ motifs out which one motif has a hydrophobic amino acid at N-3 and N-1 and five motifs have a hydrophobic amino acid at either the N-3 or N-1 position. The presence of these SQ motifs in the CHD2 protein make CHD2 a potential target for ATM/ATR mediated phosphorylation. The SQ motifs were indeed phosphorylated upon damage, seen by immunoblot analysis using anti-phospho-SQ motif antibody. Immunoprecipitation studies were also conducted to determine whether ATM/ATR physically interact with CHD2 to bring about its phosphorylation. The findings of this objective and its biological relevance are discussed in this chapter.

Materials and Method

Generation of polyclonal Chd2 antibodies

Commercially available cDNA clones that contain various segments of Chd2 were used to generate an N-terminal portion of Chd2. cDNA fragment encoding the first 313 amino acids of *Chd2* were generated by restriction enzymes or PCR and then inserted into the Pet30A bacterial expression vector, which contains a histidine tag at the N-terminus. Synthesis of fusion protein was induced for 24 hrs at 20^0C with 1mM isopropyl-β-D-thiogalatoside. His-Chd2 fusion protein was isolated by affinity chromatography on a nickel column. A single rabbit was immunized with a His-Chd2 fusion protein encoding the first 183 amino acids of Chd2. The serum obtained from the rabbit was tested for its specificity against recombinant Chd2 peptides.

In addition to the generation of a polyclonal antibody to the first 183 amino acids of the mouse Chd2 protein, we also generated antibodies against specific peptides within the N-terminal region of the Chd2 protein. Rabbit anti-Chd2 antibody was generated by Open Biosystems (Huntsville, AL) to Chd2 peptides corresponding to the amino acid "RSNRSRQEPSRFNIKEEA" and "KQPKTQRGKRKKQDSSDEDD" were synthesized along with a 5'cystine and conjugating to KLH using the Maelimide kit (Pierce).

Gel Electrophoresis and Immunoblots for detection of CHD2

Normal human diploid fibroblasts- OSU2 cells were treated with 8Gy X-ray radiation and whole cell extracts were prepared by harvesting cells at 1, 1.5,3, and 5 hours. Whole cell extracts were prepared by resuspending cell pellets in 4X packed volume of lysis buffer (50mM Tris pH 8.0, 150mM NaCl, 0.1% NP-40, 10 mM β-mercaptoethanol, and 10% glycerol and protease inhibitors) and incubating on ice for 15 min. The cell lysates were sonicated for 10 seconds in ice. The sonicated lysates were spiked with 3mM MgSO4 and 1mM CaCl2 and treated with 1µl of 50units/µl of micrococcal nuclease for 20 min at room temperature. Protein concentrations were determined using a BCA kit (Pierce). Western blot samples were then prepared by adding an equal

volume of 2× SDS-gel loading dye to the lysates and boiled for 3 minutes. The supernatant obtained was electrophoresed on an 8% SDS-polyacrylamide gel. The samples were transferred onto a PVDF membrane overnight at 4^0C, 14 V. The membrane was probed with rabbit anti- Chd2 primary antibody, 1: 5000 for 1.5 hours at room temperature followed by peroxidase conjugated mouse anti-rabbit light chain IgG, 1: 3000 for 1 hour at room temperature. The immunoblots were developed using chemiluminescence by the addition of Supersignal West Pico (Pierce).

cDNA synthesis and reverse transcriptase (RT)- polymerase chain reaction (PCR)

OSU2 cells were treated with 8Gy X-ray radiation and harvested at 1, 1.5,3, and 5 hours after treatment. RNA was isolated from these cells by using TRIzol reagent (Invitrogen) according to the manufacturer's protocol. Genomic DNA was removed by incubating RNA samples with 2U of RNase-free deoxyribonuclease I (Promega) per 3µg of RNA for 30 minutes at 37^0C. First strand cDNA synthesis was performed with 3µg of total RNA using random hexamers and M-MLV reverse transcriptase (Promega). As a negative control, samples containing RNA but no reverse transcriptase were also included. 2µl of cDNA was used for PCR. The primer sequences for *Chd2* are: GGTGGTGATGGCAAGTCTTCAAGT (exon 33); AGGCAAATGAGGCTTCTGAGGATG (exon 36). The primer sequences for housekeeping gene ribosomal protein L38 (*RPL38*) are: TTCGGTTCTCATCGCTGTGAGTGT (forward); TCTTGACAGACTTGGCATCCTTCC (reverse). The PCR conditions for *Chd2* exons 33-36 were initial denaturation at 94^0C for 2 min, followed by 30 cycles at: 94^0C for 30 sec, 58^0C for 30 sec, and 720C for 40 sec with a final extension at 72^0C for 5 mins. The conditions for *Rpl38* were 94^0C for 2 min, followed by 30 cycles at: 94^0C for 30 sec, 58^0C for 30 sec, and 72^0C for 10 sec. PCR products were resolved by agarose gel electrophoresis and stained with ethidium bromide.

Generation of Chd2 with a hemagglutinin epitope tag (HA tag) at the c-terminus

Chd2 cDNA encoding the first 1395 amino acids and first 447 amino acids were tagged with a HA tag at the c-terminus using the PCR /restriction enzyme based cloning strategy into the vector pSport6. The clones were designated as PChdKHACT and PChd1KHA respectively. The constructs were expressed in U2OS cells and expression efficiency of the construct was measured by performing western blot using anti-HA antibody. An Immunflourescence study was performed with 1:500 dilution of mouse anti-HA antibody (Covance) and 1:250 dilution of fluorescein conjugated anti-mouse IgG (Jackson ImmunoResearch) to assess the localization pattern of the construct. PChdKHACT stable cell lines were created by co-transfecting the Chd2 plasmid with a puromycin-resistant plasmid (kind gift from Dr.Yisong Wang, Oak Ridge National Lab).

Generation and expression of Tandem affinity purification (TAP) tagged Chd2

Tandem affinity purification (TAP) tags were added to Chd2 using the Gateway system. A cDNA fragment of *Chd2* encoding the first 447 amino acids and the first 1395 amino acids with flanking attB1 and attB2 was generated by restriction enzymes or PCR. Chd2 clones with flanking attB sites were recombined with a donor vector (pDONOR221) to create an entry clone. The entry clone was then recombined with a destination vector (pcDNA-DEST40) to create an expression clone of Chd2 with C-terminal TAP tags (Chd1KSH and ChdkthRR respectively). Donor vector and modified pcDNA-DEST40-destination vectors were provided by Dr.Yisong Wang. The modified pcDNA-DEST40-destination vector contains the following tag at its c-terminus: 2strep2tev6His. Stable cell lines for both Chd1KSH and ChdkthRR were created by co-transfecting the Chd2 plasmids with a puromycin-resistant plasmid (kind gift from Dr.Yisong Wang, Oak Ridge National Lab). Expression efficiency and localization of the constructs were tested by immune blotting using rabbit anti-6X His tag (1:1000, Rockland) antibody and immunofluorescence using rabbit anti-Chd2 antibody (1:3000).

Transfection and Immunoprecipitation

U2OS cells at 90% confluency were either transfected with control or the expression plasmid construct containing 1395 amino acid Chd2 recombinant peptide with the tandem affinity (TAP) tag (ChdkthRR). Forty-eight hours after transfection, the cells were treated with different DNA damaging agents – U.V rays (50 J – 30minutes, 2hours), X-rays (40 Gy -30 minutes, 2 hours), and methyl methanesulfonate (MMS – 0.01% - 30 minutes, 2 hours). The cells were harvested and whole cell lysates were prepared using the appropriate volume of lysis buffer (50mM Tris pH 8.0, 150mM NaCl, 0.1% NP-40, 10 mM β-mercaptoethanol, 50mM NaH2PO4, and 10% glycerol and protease inhibitor). The lysates were sonicated for 10 seconds and spiked with 3mM $MgSO_4$ and 1mM $CaCl_2$, and then treated with 1µl of 50units/µl of micrococcal nuclease and 1µl of 2mg/ml of DNase for 20 min at room temperature. Total protein concentration was determined using a BCA protein assay kit (Pierce).

For immunoprecipitation, 40µl of 50% slurry of Ni-NTA beads (IBA, St. Louis, MO) were washed with 100µl of Net gel buffer (50mM Tris pH 8.0, 0.1% NP-40,1mM EDTA and 0.25% gelatin), resuspended in 50µl of Net gel buffer and added to 200µg of lysates. Lysates were immunoprecipitated with rotation at 4^0C for 2hours. The beads were washed with three times with 500µl of Net gel buffer. To examine the resulting protein complex, the beads were mixed with 1X SDS gel-loading dye (50mM Tris-Cl pH 6.8, 100mM dithiothreitol, 2%SDS, 0.1% bromophenol blue, and 10% glycerol) and boiled for 5 min at 90^0C. The samples were centrifuged at 2000 rpm for 5 sec to pellet the beads and the supernatant was electrophoresed on an 8% Tris-Glycine gel. The samples were then transferred to a PVDF (Polyvinylidene Difluoride) membrane (Thermo scientific) using Tris-glycine transfer buffer containing 20% methanol (25mM Tris, 200mM glycine, 0.2% SDS, and 20% methanol).

Immuno blot analysis of phosphorylated SQ/TQ motifs

The PVDF membrane was washed 2X for 5 min in TBS/Tween (20mM Tris pH 7.4, 0.15 M NaCl, and 0.1% Tween) and blocked for 1hour at room temperature with 5%

milk/TBS/Tween. For detection of phosphorylated SQ/TQ motifs, the PVDF blot was incubated with phosphorylated SQ/TQ motif antibody (Cell Signaling Technology) in a 1:690 v/v dilution at 4^0C overnight. The dilution was done with 5% BSA in 1X TBS and 0.1% Tween-20. Immunoblots were washed 3X with TBS/Tween followed by incubation with HRP-conjugated secondary antibody anti-rabbit (Pierce) in a 1: 2000 dilution v/v at room temperature for 1hour. The dilution of the secondary antibody was done with 5% milk/TBS/Tween. The blot was washed 3X for 15 min with TBS/Tween. The immunoblot was then subjected to chemiluminescence by the addition of Supersignal West Pico (Pierce), according to manufacturer's instructions, and exposed on CXS X-ray film (CXS, Omaha, NE).

Co-immunoprecipitations of CHD2 and ATR from nuclear extracts

75-80% confluent cultures of U2OS cells were treated with 10 and 20J/m^2 doses of UV radiation. Untreated and treated U2OS cells were washed with PBS and cells were collected by scraping. Nuclear pellets were obtained by lysing the cells with cytoplasmic buffer (10mM Tris HCl pH 7.9, 0.34M sucrose, 3mM $CaCl_2$, 2mM Mg-Acetate, 0.1mM EDTA, and protease inhibitors) and by centrifugation at 3,500 X g for 15 min at 4^0C. Nuclei were lysed with modified lysis buffer (50mM Tris pH 7.5, 150mM NaCl, 1mM EDTA, 1% Triton X100, 3mM $MgSO_4$, 1mM $CaCl_2$, and 5% glycerol and protease inhibitor) followed by sonication. The lysates were digested with 50units of micrococcal nuclease and 2µg of DNase for 20 min at room temperature. Total protein concentration was determined using the BCA protein assay kit (Pierce). 400 µg of extracts were pre-cleared with 10µl of 50% slurry of protein A sepharose beads for 20min at 4^0C. The pre-cleared extracts were then incubated with antibodies against ATR, Chd2 or with normal IgG for 4h at 4^0C. The protein complex was immunoprecipitated by incubating with 20µl of 50% slurry of protein A-sepharose beads overnight at 4^0C. The immunoprecipitated fractions were washed 3X with wash buffer (20mM HEPES pH 7.9, 150mM KCl, 0.5mM EDTA, 0.1% Triton X-100 and 10% glycerol). The washed fractions were subjected to SDS-PAGE and immunoblotting with

rabbit anti-Chd2 (1:20,000) or goat anti-ATR (1:500, Santa Cruz Biotechnology) antibodies were done.

Results

4.1. X-ray induced DNA damage increases endogenous CHD2 protein levels

Many proteins are activated and stabilized rapidly after DNA damage. Post-translational modifications of the DSB response/repair proteins facilitate damage-specific interactions to enhance the repair process [173]. For example, induction of p53 in response to DNA damage results in the up-regulation of its downstream targets (e.g. WAF1/p21, GADD45, cyclin G, Bax, and Mdm2) and leads to initiation of cell-cycle arrest or apoptosis [174]. To determine if DNA damage leads to changes in the stability of CHD2 protein levels experiments were performed with normal human diploid fibroblasts exposed to 8Gy X-ray radiation. CHD2 protein levels were examined at various time intervals using an anti-Chd2 antibody developed in our laboratory. CHD2 protein expression reached its maximum by 1-3hours after X-ray exposure and then started to decline by 5 hours after exposure (Fig.17).

4.1.1 Induction of CHD2 post DNA damage regulated by posttranslational events

In order to determine whether the induction of CHD2 after DNA damage was due to post-translational modification or due to an increase in transcription, reverse transcriptase (RT) coupled PCR was performed using RNA isolated from untreated and X-ray treated cells. RT-PCR analysis of *CHD2* expression in OSU2 cells after exposure to 8Gy dose of X-ray radiation at the indicated time intervals failed to show a concomitant elevation in *CHD2* mRNA levels (Fig.18). This indicates that the X-ray triggered induction of CHD2 is regulated by posttranslational events.

4.2. CHD2 is a potential ATM/ATR substrate

The rapid activation and stabilization of DNA damage response proteins usually occurs via post-translational modifications that involve phosphorylation of specific

residues. Earlier studies have shown that the ATM/ATR kinases phosphorylate a variety of proteins involved in the regulation of cell cycle responses induced by DNA damage [175-178]. ATM/ATR substrates have a common S/TQ (serine residue that precede glutamine residue) motif and the ATM/ATR kinase preferentially phosphorylate these motifs. The p53 tumor suppressor, BRCA1, and CHK2 are among the well known targets of ATM kinase to name a few [179-186].

While the role of ATM in signal transduction events leading to cell cycle arrest or apoptosis have been well established, its effect on the regulation of events (DNA repair as well as DNA-damage signaling) in the context of chromatin are not completely understood. In an effort to determine if CHD2 is a substrate for ATM we analyzed the human CHD2 peptide sequence and found the presence of ten SQ sites and a single TQ site (QPKT197QR) within the protein.

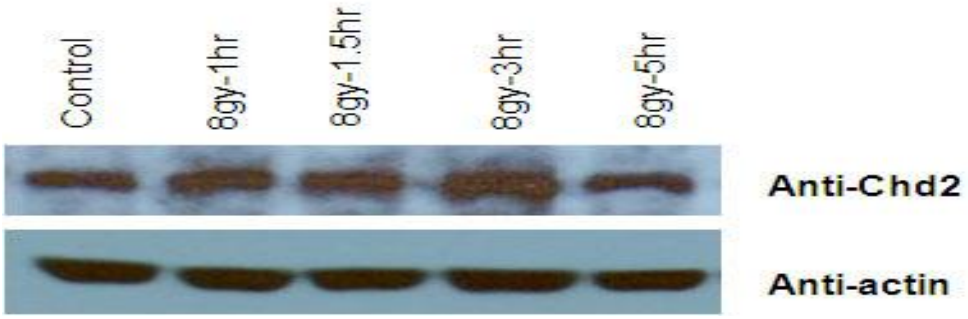

Figure 17.Induction of CHD2 in OSU2 cells following DNA damage
Cells extracts were prepared at the time points indicated after exposure to 8Gy X-ray radiation and processed for western blot analysis using Chd2 and actin antibodies. Actin levels show equal amount of protein loading.

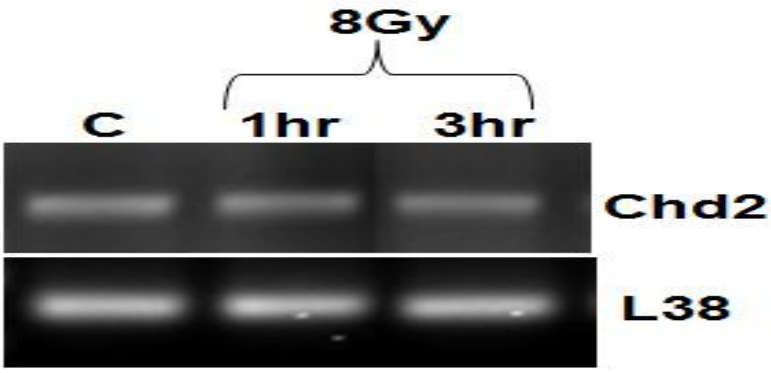

Figure 18.Effect of X-ray treatment on *CHD2* mRNA expression determined by RT-PCR

Upper panel: RT-PCR products of *CHD2* expression (exons33-36) in OSU2 cells after exposure to 8Gy dose of X-ray radiation at the indicated time intervals. Lower panel: RT-PCR products of the internal control housekeeping gene *RPL38*.

The relative locations of the SQ sites within the CHD2 sequence are shown in figures 19A and B. Among the ten SQ sites, four sites (S^{582}, S^{814}, S^{1019}, and S^{1560}) contain hydrophobic amino-acids either in the N-1 and N-3 which is indicative of a positive ATM substrate specificity [115, 165].

4.3. Phosphorylation of CHD2 by ATM/ATR kinase in response to DNA damage

To determine if CHD2 is phosphorylated after DNA damage, we expressed histidine tagged recombinant Chd2 encoding the first 1395 amino acids (ChdkthRR) in U2OS cells and analyzed the phosphorylation of 6X-His-Chd2 using an anti-phosho-(SQ/TQ) antibody (Cell Signaling Technology). As shown in figure 20A, X-ray and UV irradiation led to an increase in the phosphorylation of recombinant Chd2 (1-1395) indicated by the presence of an intense band around ~168kDa.

Authenticity of the band was confirmed by stripping and reprobing the membrane with anti-6X His antibody, which showed a band around ~ 168kDa, the predicted size of the recombinant Chd2 peptide. Figure 20B shows the expression efficiency of the two Chd2 recombinant constructs: Chd1KSH and ChdkthRR.

To further determine if ATM is involved in the phosphorylation of CHD2, we determined the phosphorylation status of CHD2 in AT proficient (U2OS) and deficient (AT) cells. AT cells are negative for ATM expression and thus serve as a control. U2OS and AT cells were transfected with HA-tagged clone of Chd2 plasmid (PChdKHACT). Localization of the construct was tested by immunofluorescence. As shown in Figure 21, the recombinant HA-tagged Chd2 localized to the nucleus. The transfected cells were treated with 40Gy X-ray for 30 minutes. Straight cell lysates were immunoblotted using antibodies against phosphorylated SQ/TQ motif. Western blot results showed a ~168KDa band in U2OS cells transfected with Chd2, whereas no band was seen around the same region in Chd2 transfected AT cells (Fig.22).

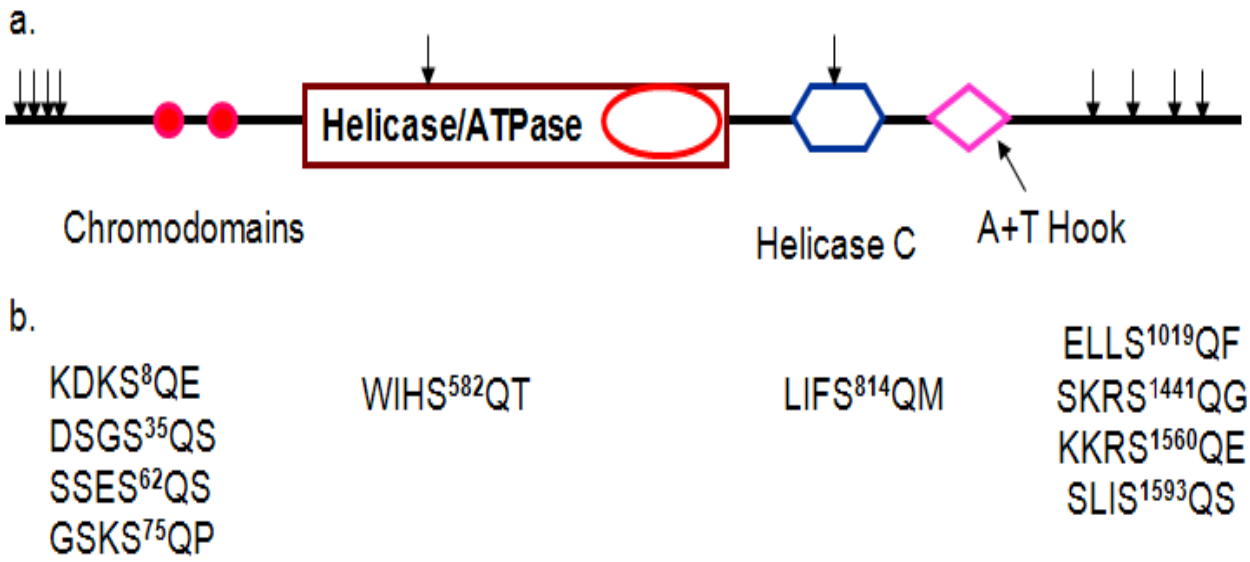

Figure 19.Potential ATM target sequences in Chd2

(A).The relative locations of the SQ sites within the Chd2 protein sequence are shown. **(B)**.The sequences of SQ motifs present in Chd2 showing presence of a hydrophobic amino acid at either N-3 or N-1 position or a hydrophobic amino acid at both N-3 and N-1 position.

4.4. Physical interaction between ATR and CHD2

ATP-dependent remodeling proteins have been identified as “novel and functional components in the ATM/ATR DNA damage checkpoint signaling pathway” [169]. For example the INO80 complex is a functional component in the Mec1/Tel1 kinase signaling pathway in yeast and CHD4 is part of the ATR- HDAC2 complex [142, 169]. Thus, we sought to determine whether the endogenous ATR and CHD2 proteins can physically interact by co-immunoprecipitation. CHD2 was immunoprecipitated from treated (10J and 20J) and untreated (control) U2OS cells using an anti-Chd2 antibody bound to protein A beads. Western blot analysis with the anti-ATR antibody showed the presence of ATR in the CHD2 immunoprecipitated beads from U2OS cells treated with 20J. Longer exposure showed a very faint band in control and in samples treated with 10J. No ATR bands were seen when the immunoprecipitation was done with normal IgG bound to protein A beads (Fig.23A). The interaction between ATR and CHD2 was confirmed by a reciprocal immunoprecipitation. Immunoblot analysis of CHD2 with the ATR immunoprecipitated beads showed a robust interaction of CHD2 with ATR in both control and U.V treated samples and this interaction increased in response to UV induced DNA damage (Fig.23B).

Discussion

The CHD family of proteins belong to the class of ATP-dependent chromatin-remodeling factors [187]. The CHD proteins are characterized by the presence of the Swi2/Snf2-like helicase/ATPase domain and two chromodomains (chromatin organization modifier) [34]. These proteins have previously known to be involved in the regulation of gene expression as transcription activators or repressors [34]. Recently, there have been several studies where some of the members such as CHD8, CHD5, CHD7 and CHD1 of this family have been reported to be involved in other processes such as apoptosis, tumorigenesis, mammalian development, and maintaining centrosome integrity via their chromatin specific interactions and activities [64, 70, 83, 89, 105, 188].

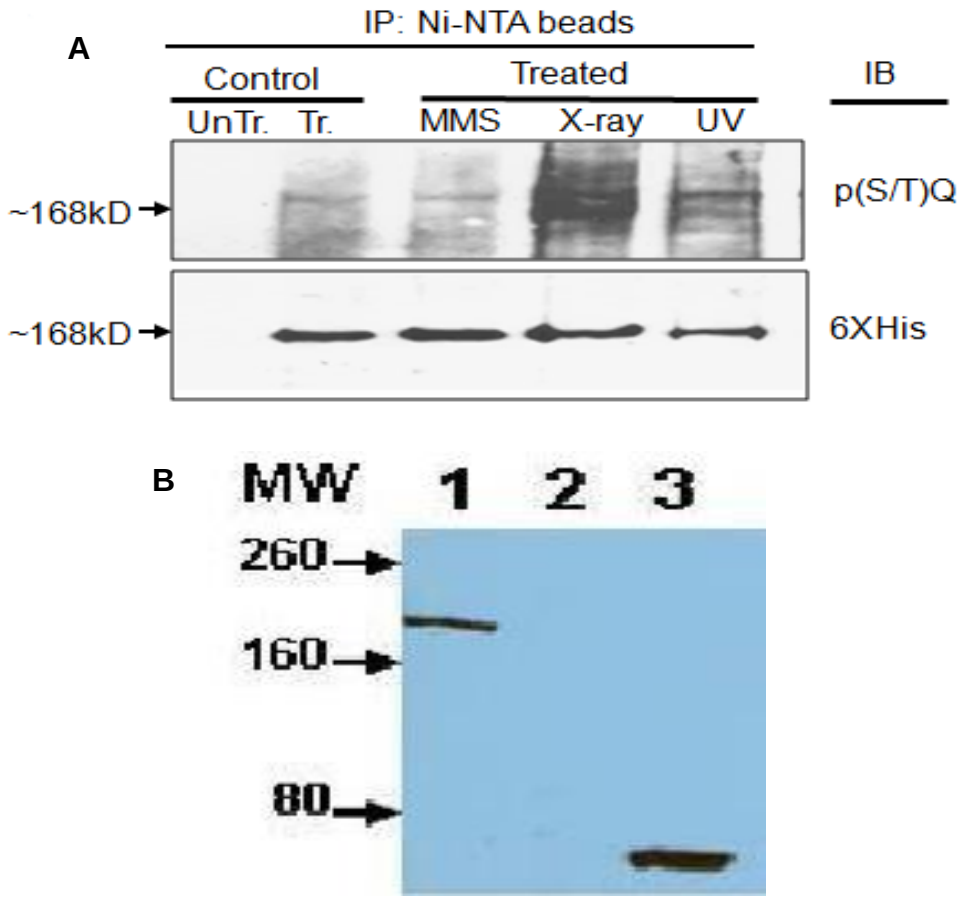

Figure 20.CHD2 is phosphoylated at the SQ site

(A) CHD2 phosphorylation by ATM/ATR kinase(s). U2OS cells were transfected with TAP-tagged clone of Chd2 plasmids and treated with different DNA damaging agents – U.V rays (50 J – 30minutes), X-rays (40 Gy -30 minutes) and methyl methanesulfonate (MMS – 0.01% - 30 minutes). TAP tagged Chd2 was immunoprecipitated from cell lysate using Ni-NTA beads after 48 hours of transfection. The beads were washed and the immunoprecipitated CHD2 protein was analyzed by western blot. Western blot was performed to determine the phosphorylation of Chd2 by ATM/ATR kinase using antibody against phosphorylated SQ/TQ motif. The same membrane was reprobed for 6X His tag (lower panel). **(B) Expression of Chd2 peptides containing tandem affinity tag.** Cell lysates were prepared from U2OS cell lines expressing the two Chd2 recombinant peptides (lane 1: ChdkthRR, lane2: empty lane and lane 3: Chd1KSH) and analyzed by anti-6X His antibodies in western blot assays. The molecular weight markers are indicated on the left.

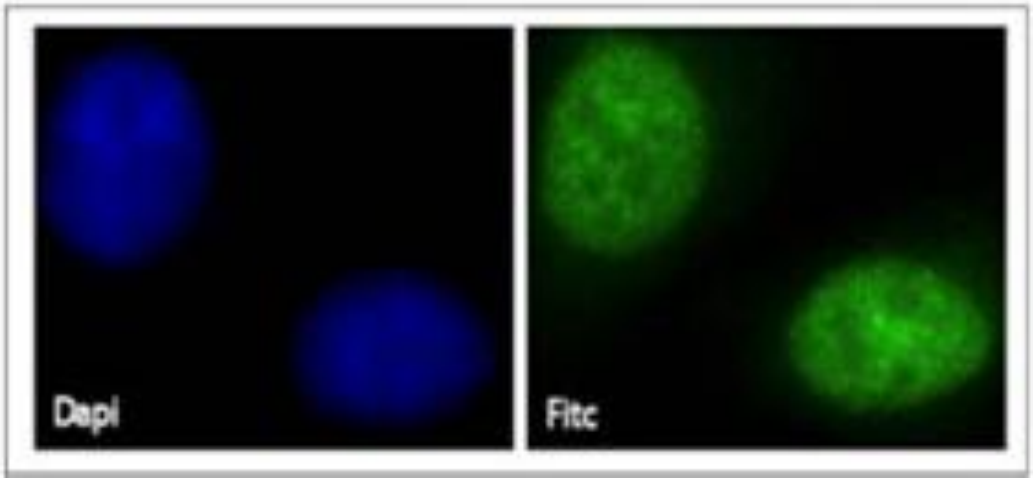

Figure 21.Generation of recombinant HA tagged Chd2 peptide

Nuclear localization of recombinant Chd2 peptide. Detection of HA tagged Chd2 with anti-HA antibodies in transfected U2OS cells by immunofluorescence staining.

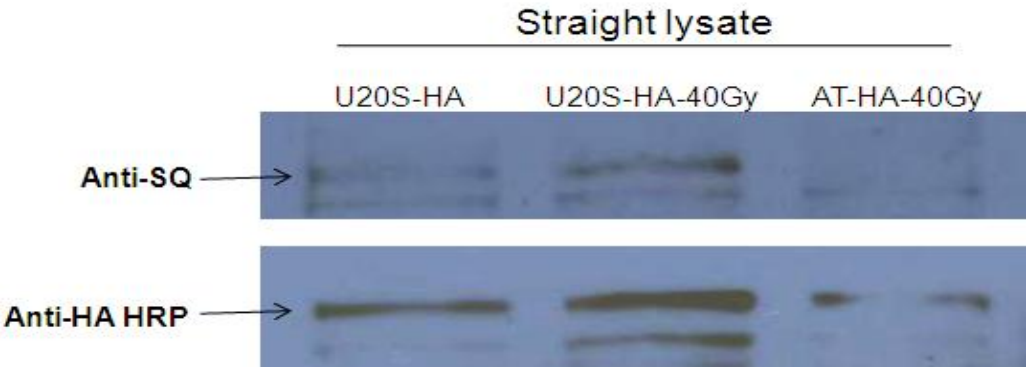

Figure 22. CHD2 phosphorylation by ATM/ATR

U2OS/AT cells were transfected with HA-tagged Chd2 and treated with 40Gy X-ray radiation, lysed after 30 minutes and analyzed by immunoblotting with anti-phosho –(SQ/TQ) antibody. The membrane was reprobed for HA-tag (lower panel).

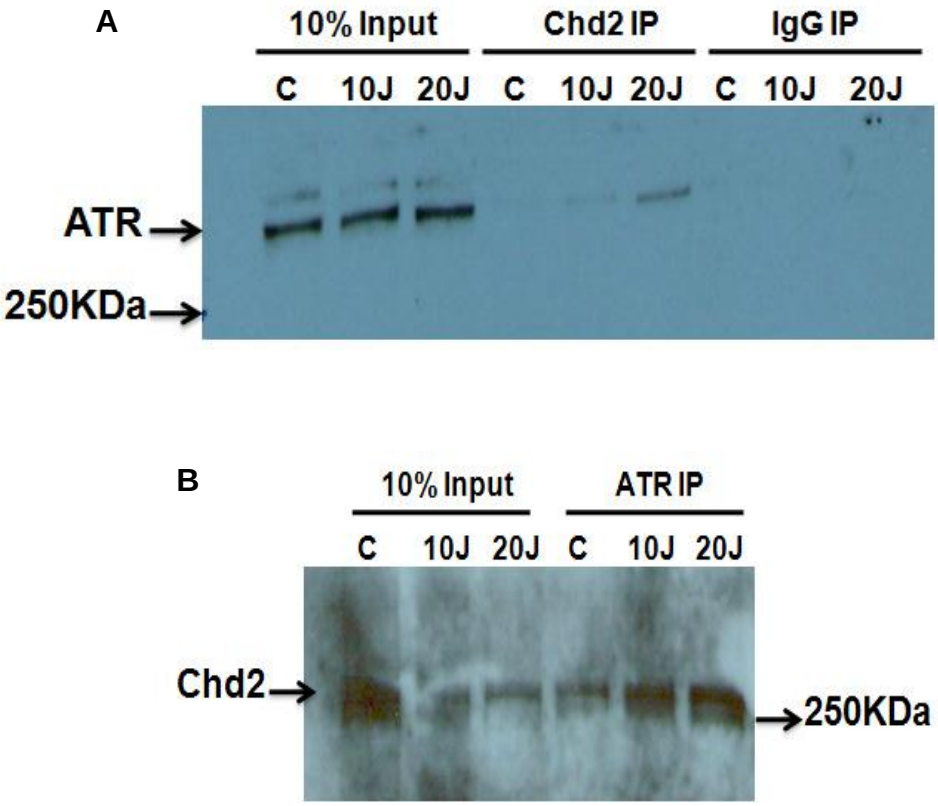

Figure 23. Interaction of CHD2 and ATR
(A) Cell extracts from untreated and treated (10J-2hr & 20J-2hr) U2OS cells were immunoprecipitated (IP) with anti-Chd2 antibody or normal rabbit IgG and immunoblotted with anti-ATR antibody. **(B)** Reciprocal immunopreciptation was performed with anti-ATR antibody and the membrane probed with anti-Chd2 antibody.

These studies highlight the important role played by the CHD proteins in diverse nuclear processes. Our studies were aimed at elucidating the role of CHD2 in DDR based on the following observations; (i) presence of putative ATM/ATR motifs in the Chd2 protein, ii) aberrant gamma-H2AX removal in *Chd2* mutant cells, and (iii) the high lymphoma susceptibility of the *Chd2* mutant mouse model generated in our laboratory to spontaneous lymphomas. The DNA damage response trigged by the cells is a complex pathway and the key coordinators are the ATM/ATR kinases. ATM and ATR belong to the phosphatidylinositol 3-kinase-like kinase (PIKK) family of protein kinases. These protein kinases are involved in phosphorlyation of crucial checkpoint signalling proteins and DNA repair proteins that activate the DNA repair response pathway [189]. Interestingly, the recent large-scale identification of ATM/ATR substrates in 293T cells indicates the presence of four CHD family members (CHD4, CHD5, CHD6, and CHD7) that are phosphorylated by ATM/ATR [190]. Furthermore, one of the CHD proteins,CHD4 has been reported to be an ATR-associated protein [142]. In addition, the S/TQ motifs are present in the subunits of many chromatin-modifying complexes such as SWI/SNF, RSC, and SWR1 [165, 169]. Additionally, two ATP-dependent chromatin remodeling proteins, Ies4 subunit of the INO80 complex and BAF170 subunit of the SWI–SNF complex have been reported to be phosphorylated by the ATM/ATR kinase in response to DNA damage [169, 191].

In this study we show that CHD2 is a potential substrate for ATM/ATR kinases. Protein sequence analysis of Chd2 reveled presence of ten ATM/ATR consensus (S/T) Q motifs. Immunoblot analysis indicated a specific band around 168 KDa with phospho-S/TQ (p-S/TQ) antibody when cells expressing the recombinant Chd2 peptides were treated with 40Gy dose of X-ray radiation. However this band was not seen when the recombinant Chd2 peptides were expressed in the cells negative for ATM expression. This data provides evidence that ATM/ATR kinases mediate the phosphorylation of CHD2 in response to DNA damage. This post translational modification (PTM) of CHD2 may help modulate its activity in response to DNA damage. Additionally, our immunoblot results show that CHD2 is stabilized in vivo in response to DNA damage.

There is a rapid induction of CHD2 protein levels after 3hours of DNA damage and the basal protein levels return 5hours post DNA damage. Furthermore, induction in CHD2 is mediated by posttranslational modifications as no difference was observed in the mRNA levels of the *CHD2* gene in human cell lines.

Our data also suggest that CHD2 interacts with ATR. The endogenous ATR and CHD2 co-precipitated efficiently, especially after DNA damage with 20J. However the amount of ATR detected in the CHD2 immunoprecipitates was low. This may be due the low abundance of ATR in the cells and also that CHD2 may be binding to only a small proportion of the ATR in UV treated cells. Similar observations were reported for the ATR and CHD4 molecular association study [142]. In addition to ATR, CHD2 may also possibly interact with ATM kinase. But since the immunoblot analysis with two different commercially available ATM antibodies did not work in our hands, further interaction studies with ATM were not pursued.

The above results provide initial clues to the role of CHD2 in modulating DNA damage responses in mammalian cells. The phosphorylation status of CHD2 would facilitate direct interaction of CHD2 with checkpoint proteins or DNA repair proteins. For instance, an enhanced interaction between the DNA response protein BRIT1 and SWI–SNF in response to DNA damage has been reported. This DNA-damage-enhanced binding affinity is mediated through an ATM/ATR-dependent phosphorylation of BAF170 subunit of SWI-SNF complex [191]. Alternatively, it is also possible that CHD2 phosphorylation status may activate its function as a chromatin remodeler by altering the chromatin environment surrounding DNA damage. The altered chromatin structure may facilitate rapid recruitment of checkpoint proteins or DNA repair proteins to the damaged site. Studies illustrating the effect of phosphorylation on the functions of chromatin remodeling proteins such as hSWI/SNF complex[192], dMi-2 chromatin remodeling complex [32] and INO80 complex [169] have been reported. In conclusion, the induction of CHD2 and its phosphorylation after DNA damage suggests a potential role for the protein in mediating DNA damage responses. However, the effect of phosphorylation on CHD2 function remains to be ascertained.

Chapter V

Determination of interaction of Chd2 with p53 and other proteins involved in genomic stability and DNA repair

Introduction

Chromatin remodelers alter the chromatin structure either through nucleosome displacement or histone exchange, increasing the access for the regulatory factors to perform various cellular processes. Various studies have shown the importance of chromatin remodeling for p53 to function as a transcription factor. Histone-modifying cofactors such as histone acetyltransferases- p300/CBP, Histone deacetylases (HDAC), protein arginine methyltransferases -CARM1, and PRMT1 are known to be important for p53 to regulate the expression of its target genes [193]. Studies have also provided links between p53 induced chromatin relaxation and DNA repair as part of the process of nucleotide excision repair. Treatment with UV irradiation resulted in recruitment of p300 and p53-dependent acetylation of lysine 9 of histone H3, leading to chromatin relaxation and efficient NER [194].

Persistent DNA damage and its erroneous resolution lead to genomic instability, tumorigenesis or cell death. Cells respond to DNA damage by activating a “signaling cascade known as the DNA damage response (DDR)” [117]. The key player in this cascade is the tumor suppressor protein- p53. p53 is a 53 kilodalton(Kda) nucleophosphoprotein which functions as a transcription factor [195]. The protein was identified in 1979 as SV40 large T antigen interacting peptide and postulated to be regulator of T-antigen functions [196]. Further elaborate studies designed to analyze the functions of p53 revealed its important role as a tumor suppressor [197]. The p53 protein contains a sequence-specific DNA binding domain which interacts with specific target double-stranded DNA sequences made up of two copies of **5'**-PuPuPu-C(A/T)(T/A)GPyPyPy-3**'**separated by 0-13 nucleotide. A vast majority of p53 mutations which occur in human cancers involve this DNA binding region [195]. Physiologically altered stress conditions such as DNA damage, heat shock, hypoxia, hyperoxia,

cytokines, growth factors, metabolic changes and oncogenes increase p53 levels, which otherwise is expressed in very low levels [195]. Autoregulatory negative feedback loops ensure low levels of p53 under normal circumstance. Three ubiquitin ligases, MDM2, Pirh2 and Cop-1 are involved in ubiquitination of p53, which leads to proteasomal degradation [198]. The exposure to stress conditions leads to stabilization and activation of p53 via a series of post-translational modification, mainly phoshorylation and acetylation [179, 198-200].

Phosphorylation of p53 is brought by activated phosphoinositide 3-kinase-related kinases (PIKK) after DNA damage [116]. Histone acetylases, p300/CBP and PCAF bring about acetylation of p53 [198]. Activated p53 stimulates the transcription of target genes required for cell growth arrest as well as for efficient DNA repair. p53 brings about cell cycle arrest in the G1 and G2 phase via activation of genes $p21^{CIP1/WAF1}$ and Gadd45, respectively [195]. If the damage is unrepairable then p53 activates transcription of target genes involved in apoptosis such as *PUMA* [p53 up-regulated modulator of apoptosis], *NOXA* [phorbol-12-myristate-13-acetate-induced protein 1] *and BAX* [BCL2-associated X protein] [117]. According to the International Agency for Research on Cancer TP53 database, about 24,785 somatic mutations and 423 germline mutations in the p53 gene have been associated with human cancers to date (http://www-p53.iarc.fr/). About 75% of these somatic mutations are missense substitutions, 9% are frameshift insertions and deletions, 7% nonsense mutations, 5% silent mutations and other infrequent alterations [201]. Early-onset cancers in Li-Fraumeni (LFS) and Li-Fraumeni-like syndromes (LFL) result from p53 germline mutations [201].

Loss of proliferation control, an important characteristic of cancer cells, can arise due to aberrant cell cycle regulation and/or a reduced ability to undergo apoptosis. The spontaneous lymphoma susceptibility of the *Chd2* mutant mice may underlie a defect in either cell cycle arrest and/or apoptosis due to a defective signal transduction at the chromatin level. Consistent with this, *Chd2* mutant cells show an increased proliferation potential in comparison to wild type counterparts (data not shown). In addition,

unpublished results from our lab show a defective induction of the pro-apoptotic gene *Puma* in *Chd2* mutant thymocytes. These results suggest that the *Chd2* mutant lymphoid cells may have a defective apoptotic response due to an aberrant p53 response and a potential role for CHD2 in regulating the p53 transcriptional activity. To address this possibility, we have performed studies to determine the interaction of CHD2 and p53.

While the CHD2-p53 interaction studies provide evidence for the role of Chd2 in the regulation DNA damage induced transcriptional activation of stress response genes, the identity of the CHD2 basal complex remains to be determined. Furthermore, the biochemical purification of other CHD proteins has shown that the CHD3 and CHD4 proteins are components of the NuRD complex while the yeast Chd1 protein co-purifies with the SAGA-SLIK complex in yeast [46, 57]. To identify CHD2 interacting proteins and its potential interaction with DNA damage response proteins (DNA repair and checkpoint proteins) and to understand the functional pathways regulated by CHD2, a tandem affinity purification approach coupled with mass spectrometry (MS) was performed for the identification of CHD2 interacting partners.

In recent years, mass spectrometry is emerging as a valuable tool for identifying proteins present in large complexes. Affinity purification followed by mass spectrometry analysis of the protein complexes is the method of choice because of its high sensitivity and specificity [202]. Some common approaches used for protein complex isolation are affinity chromatography, immunoprecipitation, epitope-tagging, GST-pulldown and tandem affinity purification [202-203]. Approaches such as affinity chromatography, immunoprecipitation, epitope-tagging, and GST-pulldown usually generates high background, results in identification of cross-reactive contaminating proteins and failure to isolate low stoichiometry interacting partners. The method of dual purification- TAP-tagging (tandem affinity purification) has been designed to overcome some of the aforementioned drawbacks. The TAP-tagging strategy makes use of a tag comprised of two affinity components with a protease cleavage site in-between the two components [204]. The original TAP tag consists of a calmodulin-binding peptide followed by a

tobacco etch virus (TEV) protease cleavage site and a IgG binding moiety of *S.aureus* protein A (Protein A) [204]. The TAP approach helps in efficient reduction of non-specific background and isolation of protein complex under physiological conditions [202]. The basic steps of this approach are, fusing the protein of interest in-frame with an N- or C-terminal TAP tag, expressing the recombinant protein in a particular cell line and then isolating the protein of interest and its interacting partners via tandem affinity purification. Tandem affinity purification involves immunoprecipiting the complex first using Protein A- IgG sepharose beads and then isolating the protein of interest along with its binding partners by cleaving the complex using TEV protease. This process ensures that the proteins which bind to the resin non-specifically are not isolated along with the protein complex of interest. The protein complex of interest is further purified by immobilizing to calmodulin coated beads and eluting via calcium chelation [203, 205]. The purified protein complex is separated via any of the following techniques, SDS-PAGE, isoelectric focusing or other two-dimensional approaches. The proteins are then digested into shorter peptides with a proteolytic enzyme such as trypsin or Lys-C and separated using reversed-phase capillary liquid chromatography to be injected into the mass spectrometry via electrospray ionization [203, 206]. The mass/charge ratio of the peptides are measured and then subjected to collision-induced fragmentation to generate a tandem (MS/MS) mass spectrum. The tandem mass spectra obtained are analyzed using computer algorithms such as SEQUEST or Mascot. The algorithm generates a theoretical fragmentation pattern for amino acid sequences in the database and matches to the observed tandem MS [206-207]. This method has lead to identification of the components of the important protein complexes from bacteria, yeast, plants and mammalian cells [205, 208-210]. In this study we have used a modified version of the original TAP tag, developed by Dr. Yisong Wang's laboratory, Oak Ridge National Laboratory. The modified version consists of a Strep-Tactin binding peptide followed by the TEV protease recognition site and then a 6X histidine (His) tag [210]. Dr. Wang's group has generated five dual-tag purification vectors, each with different sets of affinity tags. They have used these vectors to successfully identify

known interacting partners of human telomeric repeat binding factor 2(TRF2) protein [210]. The results described in this chapter includes, the list of CHD2 interacting proteins obtained from the mass spectrometric analysis done by Dr. Hayes McDonald (Oak Ridge National Laboratory) following the TAP purification protocol and the mass spectrometric analysis done by Applied Biomics following single step elution protocol.

Materials and Methods

Co-immunoprecipitations of CHD2 and p53 from whole cell lysate

Identification of endogenous CHD2 and p53 interaction: Actively growing culture of U2OS were irradiated with 10Gy dose of X-ray and harvested 2hrs later. Untreated and treated pelleted cells were resuspended in 4X packed volume of lysis buffer (50mM Tris pH 8.0, 150mM NaCl, 0.1% NP-40, 10 mM β-mercaptoethanol, and 10% glycerol and protease inhibitor) and incubated on ice for 15 min. The cell lysates were sonicated for 10 seconds in ice. The sonicated lysates were spiked with 3mM $MgSO_4$ and 1mM $CaCl_2$ and treated with 1µl of 50units/µl of micrococcal nuclease for 20 min at room temperature. Protein concentrations were determined using a BCA kit (Pierce). 300 µg of extracts were pre-cleared with 15µl of 50% slurry of protein A sepharose beads pre-equilibrated with modified Net gel buffer (50mM Tris pH 8.0, 0.1% NP-40,1mM EDTA, 0.25% gelatin, 2% BSA and protease inhibitors) for 20min at 4^0C. The pre-cleared extracts were then incubated with an antibody against Chd2 overnight at 4^0C. The protein complex was immunoprecipitated by incubating with 30µl of 50% slurry of pre-equilibrated protein A-sepharose beads at 4^0C for 2hrs. The immunoprecipitated fractions were washed 3X with Net gel buffer containing no BSA. The washed fractions were subjected to SDS-PAGE and immunoblotted with 1:1200 dilution of anti-p53 antibody [mouse monoclonal Ab-4(NeoMarkers)].

Identification of exogenous CHD2 and p53 interaction: 90% confluent culture of U2OS cells were either mock transfected (control) or co-transfected with the expression plasmid construct containing 1395 amino acid Chd2 recombinant peptide with HA tag at

the c-terminus (PChdKHACT) and/or with plasmid containing Flag tagged p53. PChdKHACT stable cell lines were also used for the experiment and were transfected with plasmid containing Flag tagged p53. The following day, cells were treated with 10Gy X-ray radiation and incubated for 2hrs. Extracts from transfected/untransfected U2OS and PChdKHACT stable cells were then prepared as described above. 200µg of the total protein extract was incubated with 5µl of 50% slurry of anti-HA affinity matrix (Roche) pre-equilibrated with modified Net gel buffer (50mM Tris pH 8.0, 0.1% NP-40,1mM EDTA, 0.25% gelatin, 2% BSA and protease inhibitors) 4^0C overnight. The immunoprecipitated fractions were washed 3X with wash buffer (20mM Tris pH 8.0, 100mM NaCl, and 0.05% Tween-20). The washed fractions were subjected to SDS-PAGE and immunoblotted with anti-p53 antibody, 1:1200 dilution [mouse monoclonal Ab-4(NeoMarkers)] and with 1:500 dilution of anti-HA-peroxidase high affinity rat monoclonal antibody (Roche).

Generation of full length recombinant Chd2

Chd2 cDNA encoding the last 432 amino acids was synthesized from thymus RNA obtained from a wild type mouse using Phusion® RT-PCR kit (NEB) according to manufacturer's protocol. The cDNA was amplified using a Pst1 restriction site containing forward primer and a reverse primer containing a Not1 restriction site and a FLAG tag sequence. The purified PCR product was double digested with PstI and NotI (Roche, NEB) and cloned into PChdKHACT plasmid previously digested with PstI and Not1. The construct was recloned into a pcDNA 3.1 vector. This construct was named as "YP2". YP2 was expressed in U2OS cells and expression efficiency of the construct was tested by performing western blot using rat anti-FLAG antibody (1:4000) (BioLegend).

Tandem affinity purification (TAP) of CHD2 protein complex

Exponentially growing cells of RR3 (stable cell line expressing the first 1395 amino acid Chd2 recombinant peptide with the dual affinity tags (Strep-TEV-6XHis) and PDYM

(stable cell line established by transfecting with empty vector) were treated with different DNA damaging agents such as 10Gy IR-1hr, 10Gy IR-4hr and 10J U.V-4hrs and harvested after the indicated incubation time. Untreated/control and treated cells were scraped and the cell pellets were resuspended in a 4X volume (of the cell pellet) of cold TAP lysis buffer (50mM Tris pH 8.0, 150mM NaCl, 0.1% NP-40, 10 mM β-mercaptoethanol, 50 µg/ml avidin, 50mM NaH2PO4, 10mM imidazole and protease inhibitors) . The cell lysates were sonicated for 20 seconds in ice. The sonicated lysates were spiked with 3mM $MgSO_4$ and 1mM $CaCl_2$ and treated with 1µl of 50units/µl of micrococcal nuclease for 20 min at room temperature. Protein concentrations were determined using a BCA kit (Pierce). TAP purification were performed as described by Giannone et al. [210] with some modification. Ten milligram of total protein extract was incubated for 1 h at 4°C under gentle rotation with 25µl of solid Ni-NTA beads (Qiagen), pre-equilibrated with 500µl wash buffer-I (50 mM Tris, 50 mM NaH2PO4, 150 mM NaCl, 40 mM imidazole, 1 mM DTT and 0.1% NP-40, pH 8). The supernatant was reapplied to 25µl of fresh pre-equilibrated solid Ni-NTA beads and rotated for 1h at 4°C. The beads were transferred to 15ml falcon tube and washed three times with 5 ml of wash buffer-I and once with 4ml of TEV cleavage buffer(TCB: 50 mM Tris, 150 mM NaCl, 0.5 mM EDTA, 0.1% NP-40, 1 mM DTT, pH 8). The beads were transferred into a clean 1.5ml eppendorf tube and resuspended in 50µl of TCB. The bound complexes were eluted via AcTEV digest (3x 80U; Invitrogen) for 30min at 37°C. The TEV elutes were combined and incubated 2hrs at 4°C under gentle rotation with 40µl of solid Strep-Tactin beads (Qiagen), pre-equilibrated with 500µl wash buffer-II (100 mM Tris pH 8.0, 150 mM NaCl, 1 mM EDTA, 1 mM DTT). The doubly purified protein complex was recovered by 2 X 100 µl additions of elution buffer (StrepII-tag: 100 mM Tris
pH 8.0, 150 mM NaCl, 1 mM EDTA, 1 mM DTT, 40 mM Desthiobiotin [IBA]) with 5 min of agitation between each elution. Samples collected at each step were analyzed by western blot (rabbit anti-Chd2 antibody [1:4000]) to monitor purification progress and yield.

2D-LC/MS/MS analysis: Sample preparation for mass spectrometry analysis was performed according to the protocol established by Organic and Biological Mass Spectrometry group at Dr. Hayes McDonald's laboratory, Oak Ridge National Laboratory. Briefly, the affinity purified protein complex was concentrated by trichloroacetic acid (TCA) precipitation and denatured by resuspending the concentrated protein in 50mM Tris buffer containing 8M urea and 15mM DTT. The denatured samples will be diluted to make the final concentration of urea 1M, followed by trypsin digestion of the samples added at 1:20(w/w) at 37^0C overnight (Connelly et al., 2006). The samples were desalted with an Omics 100µl solid phase extraction pipette tip (Phenomenex, Torrance, CA, USA) [211]. 2D-LC/MS/MS analysis of the samples was performed with a reverse-phase HPLC (high performance liquid chromatography) system coupled to a linear trapping quadrupole (LTQ) mass spectrometer (Thermo Electron Finnigan, San Jose, CA, USA) with a nano-electrospray ionization source. The mass spectrometer was operated in data-dependent mode to generate a tandem (MS/MS) mass spectrum [211].

Data analysis: The tandem mass spectra obtained were analyzed using computer algorithm – SEQUEST. SEQUEST correlates the tandem mass spectra of peptides with amino acid sequences from protein and nucleotide databases. The algorithm generates a theoretical fragmentation pattern for amino acid sequences in the database and matches to the observed tandem MS [212]. The MS data obtained from SEQUEST were sorted and filtered at one-peptide level using DTASelect software to obtain a list of potential interacting proteins of CHD2 [213]. The proteins were further classified based on their biological functions using the program-The Protein Information and Property Explorer.

Single step purification of CHD2 protein complex using Ni-NTA beads

Exponentially growing cells of ChdkthRR3 [stable cell line expressing the first 1395 amino acid Chd2 recombinant peptide with the dual affinity tags (Strep-TEV-6XHis)],1KSH [stable cell line expressing the first 447 amino acid Chd2 recombinant

peptide with the dual affinity tags (Strep-TEV-6XHis)] and PDYM (stable cell line established by transfecting with empty vector) were harvested and re-suspended in a 3X volume (of the cell pellet) of cold cytoplasmic buffer (10mM Tris HCl pH 7.9, 0.34M sucrose, 3mM $CaCl_2$, 2mM Mg-Acetate, 0.1mM EDTA, and protease inhibitors) and centrifuged at 3,500 X g for 15 min at 4^0C. The nuclear pellet obtained was re-suspended in 3X volume of cold TAP lysis buffer. The cell lysates were sonicated for 20 seconds in ice. The sonicated lysates were spiked with 3mM $MgSO_4$ and 1mM $CaCl_2$ and treated with 1µl of 50units/µl of micrococcal nuclease for 20 min at room temperature. Protein concentrations were determined using a BCA kit (Pierce). Five milligram of nuclear extract was incubated for 2hrs at 4°C under gentle rotation with 25µl of solid Ni-NTA beads (Qiagen), pre-equilibrated with 500µl wash buffer-I. The beads were transferred to 15ml falcon tube and washed three times with 3 ml of wash buffer-I. Bound protein complex was eluted with 2X 125µl of imidazole elution buffer (100 mM Tris, 150 mM NaCl, and 200 mM imidazole). The eluted samples were dialyzed overnight with DPBS [Dulbecco's phosphate buffered saline (HyClone)] and precipitated with TCA (6% [v/v]). The protein pellet was redissolved in 1X SDS-gel loading buffer (50mM Tris-HCl pH 6.8, 2% SDS, 0.1% bromophenol blue, 10% glycerol, and 100mM DTT) and separated on 4-15% gradient Criterion Tris-HCl gels (BioRad). Proteins were visualized with GelCode Blue Stain Reagent (Thermo Scientific). Protein bands not seen in control (PDYM) pull-down lane but seen in the lanes containing the ChdkthRR3 and 1KSH elutes were cut and collected in 1.5 ml eppendorf tubes with 30µl sterile dH_2O. The protein gel bands were sent to Applied Biomics (Hayward, CA) for Matrix-assisted laser desorption/ionization (MALDI) mass spectrometry analysis. The tandem mass spectra obtained were analyzed using computer algorithm – Mascot.

Co-immunoprecipitations of CHD2 and PSP1 from whole cell lysate

Actively growing culture of U2OS were treated with 10Gy radiation of X-ray dose and harvested 2hrs later. Untreated and treated pelleted cells were resuspended in 4X packed volume of lysis buffer (50mM Tris pH 8.0, 150mM NaCl, 0.1% NP-40, 10 mM β-

mercaptoethanol, and 10% glycerol and protease inhibitor*)* and incubated on ice for 15 min. The cell lysates were sonicated for 10 seconds in ice. The sonicated lysates were spiked with 3mM $MgSO_4$ and 1mM $CaCl_2$ and treated with 1µl of 50units/µl of micrococcal nuclease for 20 min at room temperature. Protein concentrations were determined using a BCA kit (Pierce). 400 µg of extracts were pre-cleared with 5µl of 50% slurry of protein A sepharose beads pre-equilibrated with modified Net gel buffer (50mM Tris pH 8.0, 0.1% NP-40,1mM EDTA, 0.25% gelatin, 2% BSA and protease inhibitors) for 20min at 4^0C. The pre-cleared extracts were then incubated with an antibody against CHD2 and PSP1 (Paraspeckle Protein 1: gift from Dr. Yasuyuki Kurihara, Yokohama National University, Japan) overnight at 4^0C. The protein complex was immunoprecipitated by incubating with 10µl of 50% slurry of pre-equilibrated protein A-sepharose beads at 4^0C for 2hrs. The immunoprecipitated fractions were washed 3X with wash buffer (20mM Tris pH 8.0, 100mM NaCl, and 0.05% Tween-20). The washed fractions were subjected to SDS-PAGE and immunoblotted with 1:2000 dilutions of anti-Psp1 antibody (mouse monoclonal) and/or rabbit anti-Chd2 antibody (1:4000).

***In vivo* splicing assay**

The assay was performed as previously described [214]. The pMTE1A minigene plasmid (3µg) (kind gift from Dr. A.Krainer, Cold Spring Harbor Laboratory) was transfected either alone or together with an increasing amount (2, 4, 6, 8 µg) of YP2 into U2OS cells. The empty parental vector pcDNA 3.1 was added to ensure equal DNA concentration in each transfection. RNA was isolated after 48hrs of transfection using TRizol according to manufacturer's protocol (Invitrogen). Genomic DNA was removed by incubating RNA samples with 2U of RNase-free deoxyribonuclease I (Promega) per 5µg of RNA for 30 minutes at 37^0C. First strand cDNA synthesis was performed with 2.5µg of total RNA using random hexamers and M-MLV reverse transcriptase (Promega).

The PCR was performed with 2.5µl of the reverse transcription reaction using primers; 5'-ATTATCTGCCACGGAAGGTGT-3' (sense) 5'-

GGATAGCAGGCGCCATTTTA-3' (antisense) [214]. The PCR conditions were; initial denaturation at 94^0C for 2min followed by 28 cycles of 94^0C for 1min, 58^0C for 2min and 72^0C for 2min and then final extension at 72^0C for 5mins. The bands were visualized and quantified using EpiChem^3 darkroom gel documentation (UVP, CA) and LabWorks acquisition & analysis software respectively. Three independent experiments were performed.

Results

5.1. CHD2 interacts with p53

To detect association of endogenous CHD2 with endogenous p53, U2OS cells were exposed to 10Gy X-ray radiation, incubated for 2hrs and immuno precipitated with anti-Chd2 antibody. Immunoblot analysis with anti-p53 antibody showed an interaction of p53 with Chd2. This interaction was greatly enhanced after X-ray treatment (Fig.24).

Figure 24. Endogenous interaction of CHD2 with p53
U20S cells were either mock treated (−IR, control) or exposed to 10Gy IR (+IR), immunoprecipitated with anti-Chd2 and immunoblotted with anti-p53 antibodies.

To verify the interaction, recombinant HA-tagged Chd2 (1-1395 a. acids) and Flag-tagged p53 were expressed in U2OS cells and were immunoprecipitated with HA beads. Western blot analysis with anti-p53 antibody showed robust association between the recombinant proteins (Fig.25).

5.2. Tandem affinity purification (TAP) of CHD2 complex and mass spectrometric analysis

To identify CHD2 interacting proteins and its potential interaction with DNA damage response proteins (DNA repair and checkpoint proteins), to understand the functional pathways regulated by CHD2, a tandem affinity purification approach coupled with mass spectrometry (MS) was performed for the identification of CHD2 interacting partners. Stable cell lines expressing a recombinant clone consisting of the first 1395 amino acid Chd2 recombinant peptide with the dual affinity tags (ChdkthRR3 :6X His and Strep tags with a TEV cleavage site in between[TAP tag]) was used for the experiment. Stable cell lines expressing the empty TAP vector (PDYM) were used as controls for the experiment. To verify if CHD2 associated with a different set of proteins after DNA damage, cells were exposed to different DNA damaging agents such as 10Gy IR-1hr, 10Gy IR-4hr and 10J U.V-4hrs and the cell lysates obtained were then preceded with the purification.

The protein complex containing CHD2 and its interacting partners was purified using the TAP purification protocol provided by Dr. Yisong's laboratory. Aliquots collected prior to the purification, during purification steps and the final eluted protein complex were analyzed by western blot using anti-Chd2 antibody to ascertain the recovery of tagged Chd2 (Fig.26). The strep elutes for each of the sample was analyzed by silver staining also (Fig.27).

The purified strep elutes were sent for two-dimensional liquid chromatography nano-electrospray ionization tandem mass spectrometry (2D-LC/MS/MS) analysis to Dr. Hayes McDonald (Oak Ridge National Laboratory).

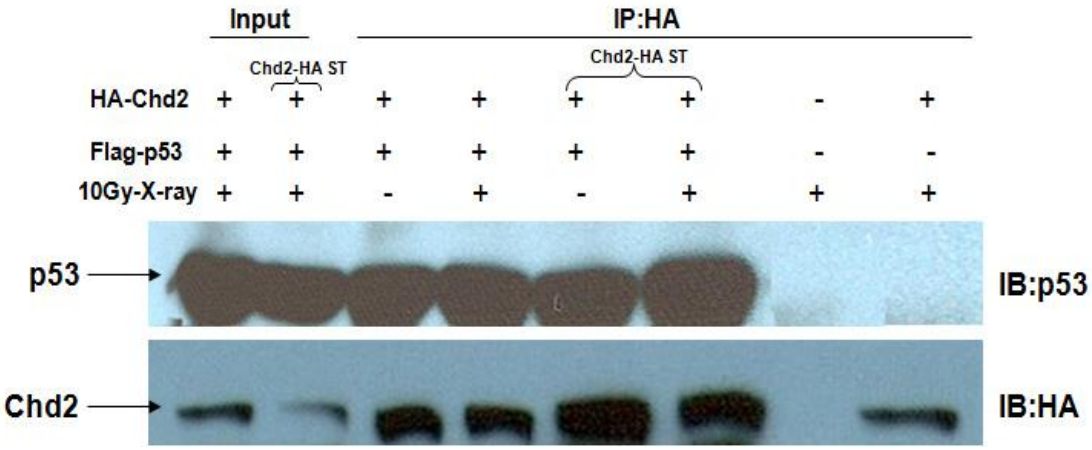

Figure 25. Interaction of recombinant p53 and CHD2

Co-immunoprecipitation experiments using lysates prepared from U2OS cells transfected with HA-tagged Chd2 and Flag-tagged p53, followed by immunoblot analysis with anti-p53 and anti-HA antibodies. Chd2-HA ST = U2OS cells stably transfected with HA-tagged Chd2, IB= Immunoblot, IP= Immunoprecipitation

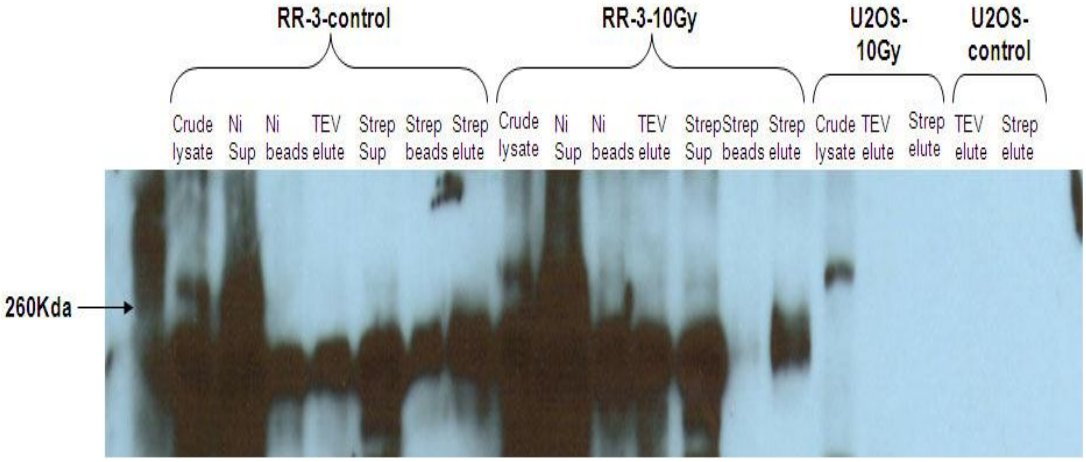

Figure 26. TAP purification of ChdkthRR-3 (1395 a.a clone) stable clone

Aliquots collected during the purification were resolved on a 10% SDS-PAGE and probed using 1:4000 diluted anti-Chd2 antibody.

The tandem mass spectra obtained were analyzed using computer algorithm – SEQUEST against the human database and then sorted using DTASelect software to obtain a list of potential CHD2 interacting proteins. The proteins were further classified based on their biological functions using the program-The Protein Information and Property Explorer (Table-3).

5.3 Identification of CHD2 interacting proteins through single step purification using Ni-NTA beads

Although TAP protocol is the most efficient way of obtaining purified protein complexes under physiological conditions, single step purification has its own advantages. Single step purification is simple, less time consuming and prevents the loss of transiently and weakly interacting proteins [215]. Single step purification of nuclear extracts obtained from ChdkthRR3, 1KSH and PDYM were performed as described in materials and methods.

TCA precipitated samples were thereafter separated by 4-15% Tris-HCl gradient gel and stained with GelCode Blue Stain Reagent. Several protein bands were identified to specifically co-purify with CHD2 protein, as they did not appear in the control lane (elute from PDYM) (data not shown). The protein bands of interest were excised from the gel and sent to Applied Biomics for mass spectrometric analysis.

Applied Biomics analyzed the resulting peptide fragment spectra using MASCOT and identified three proteins with high confidence: chromodomain helicase DNA binding protein 2 isoform CRA_a [Homo sapiens] , SFPQ protein [Homo sapiens] , and non-POU domain containing, octamer-binding isoform 1(p54NRB/NONO) [Homo sapiens] . SFPQ protein [Homo sapiens], and non-POU domain containing, octamer-binding isoform 1(p54NRB/NONO) belong to the DBHS (Drosophila melanogaster behavior, human splicing) family of proteins. These proteins are found in the paraspeckle of the nucleus and are known to involved in an array of functions specifically in transcription and RNA processing [216].

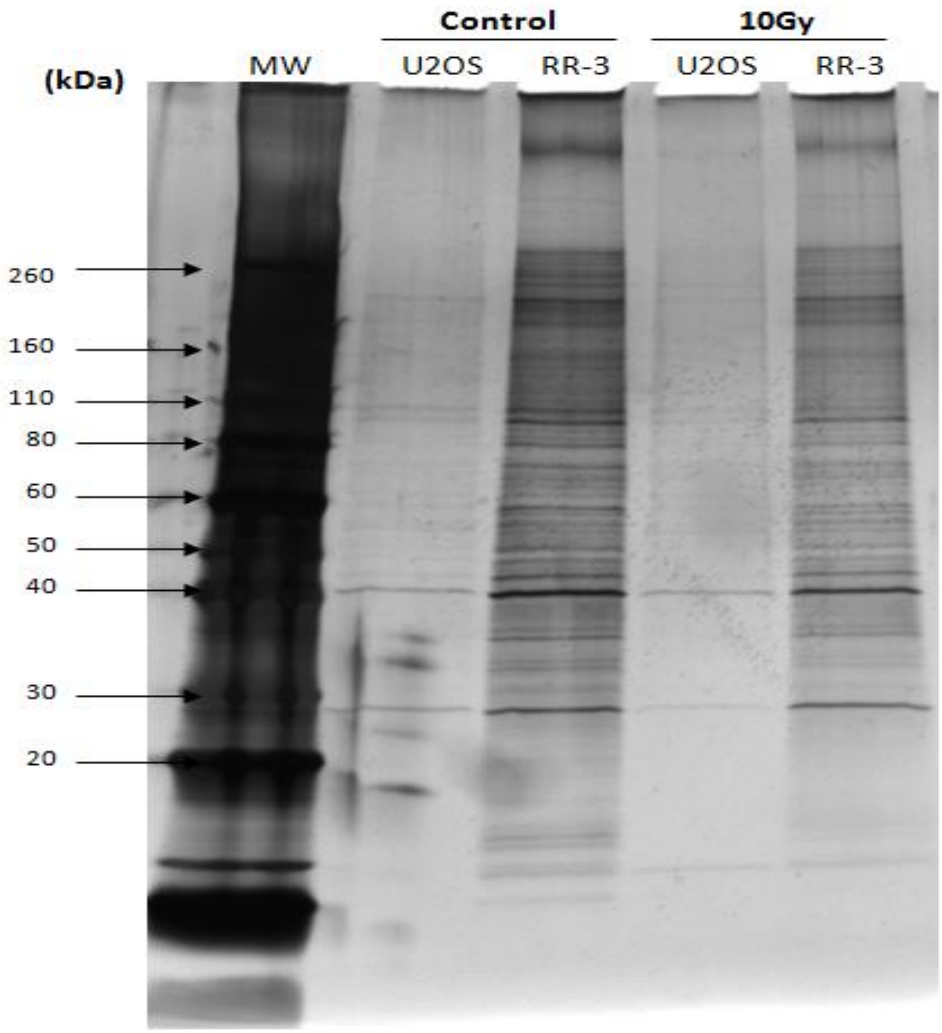

Figure 27. Identification of CHD2 associated proteins
Proteins interacting with CHD2 were isolated by tandem affinity purification of untransfected U2OS cells and cells stably transfected with recombinant Chd2 peptide (RR3) , resolved on a 4-20%SDS-PAGE gel and visualized by silver staining. 20µls of the final strep elutes were loaded on the gel. Strep elutes obtained from the purification of the cells (U2OS and RR3) treated with 10Gy radiation were also loaded.

Table-3: GO classification of the CHD2 interacting nuclear proteins based on biological function using The Protein Information and Property Explorer program.

Biological Function	Number of proteins
RNA metabolism, processing, regulation	9
Protein metabolism, synthesis	1
Nuclear organization and biogenesis	5
Immune Responses	1
Neuroblast differentiation	1

3.4 Effect of CHD2 on alternative splicing

The mass spectrometric analysis of CHD2 interacting protein partners obtained through tandem affinity purification and single step purification showed potential interaction of CHD2 with proteins involved in pre-mRNA processing events [217-219]. One of the interacting proteins, p54nrb is specifically shown to influence the splicing pattern of collagen, type II, α 1 (Col2a1) mRNA [220]. Furthermore, the CHD1 protein that is closely related to CHD2 has been show to interact with the splicing components [51-52]. The mass spectropmetry data suggested that the CHD2 protein plays a potential role in regulation of pre-mRNA splicing. To test this possibility, an *in vivo* splicing assay based on the alternative splicing of the adenoviral E1A gene was utilized. The concentration of the splicing proteins, constitutive signals, and other regulatory proteins in a cell is known to affect the alternative splicing pattern of many genes [221]. The E1A pre-mRNA of adenovirus utilizes three alternative 5'-splice site and a common 3'-splice site to form different mRNAs 13S, 12S, 11S, 10S, and 9S [222-223]. The E1A minigene system has been successfully used to demonstrate the role of many proteins in pre-mRNA splicing. These proteins have been shown to affect the splicing pattern of the E1A mRNA in a dose dependent manner [214, 221, 223-225]. In our experiments, transfection of E1A minigene plasmid into Hela cells resulted in four alternative splice

forms of E1A 13S, 12S, 10S and 9S. When the cells were co-transfected with increasing amounts of YP2 plasmid (plasmid expressing the full length FLAG tagged Chd2) along with constant amount of E1A, a modification in the splicing pattern was observed. Addition of YP2 resulted in an increase of the 9S form from 2.2 % to 4.5% and a slight decrease in the 13S forms from 59.4% to 58.4% in a dose-dependent manner (Fig.28A and B). There was also an increase in 10S form from 5.8% to 7% and decrease in 12S forms from 32.4% to 29.9% (Fig.28A and B). These results demonstrate that over expression of Chd2 appears to favor use of distal (9S) 5′ splice site in the E1A gene, thus, confirming that CHD2 is engaged in alternative splicing modulation.

5.5 Interaction of CHD2 and PSP1

Isoform 1 of Paraspeckle component 1 was identified as the protein with maximum high scoring peptides assigned to it from the MS data analysis of the tandem affinity purified CHD2 complex. Paraspeckle protein 1(PSP1/PSPC1) is a component of a nuclear body known as paraspeckle. It contains a DBHS (Drosophila behavior, human splicing) motif also found in PSF (Polypyrimidine tract-binding protein-associated splicing factor) and p54nrb/Nono (non-POU domain containing, octamer-binding) proteins. Both PSF and p54nrb/Nono are known to bind to RNA sequences in premRNA. These are known to play an important role in transcription as well as in RNA processing [219]. Mouse paraspeckle protein 1 was identified as a RNA-binding protein and was shown to dimerize with PSF and p54nrb/Nono [226]. To confirm the specificity of the interaction between PSP1 and CHD2, an *in vivo* co-immunoprecipitation study was performed. The results show that endogenous PSP1 is not co-immunoprecipitated by the rabbit polyclonal Chd2 antibody. Reciprocal immunoprecipitation confirmed these results as Chd2 would not be immunoprecipitated using a mouse monoclonal Psp1 antibody (Fig.29).

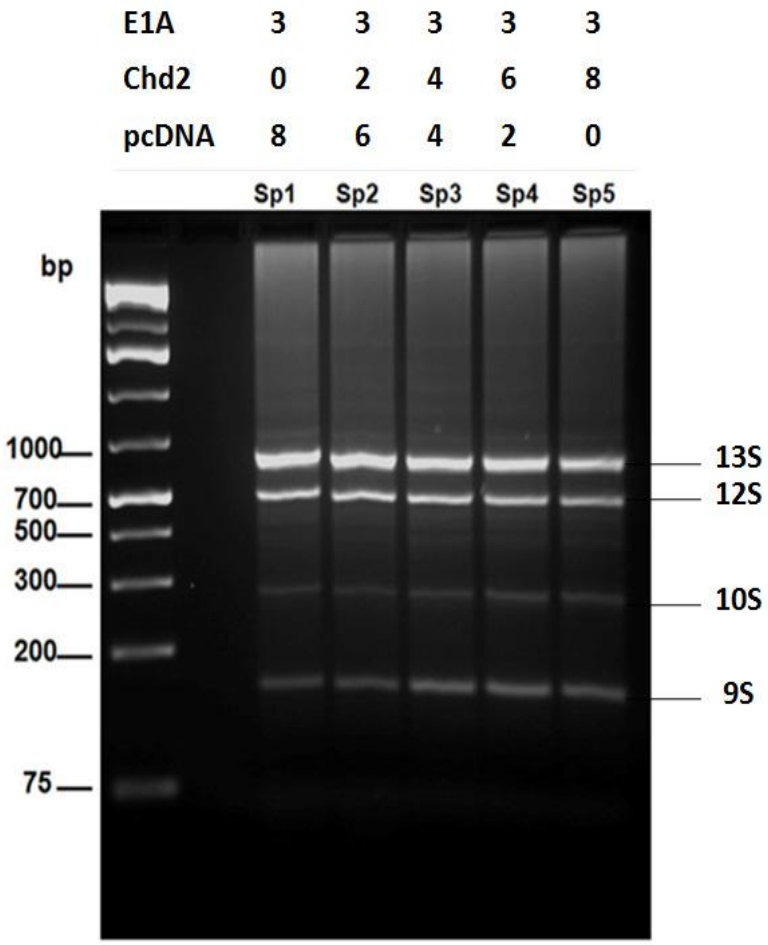

Figure 28. CHD2 affects the splicing pattern of E1A minigene

(A) Pattern of E1A alternative splicing in Hela cells upon transfection of the E1A minigene and cotransfection of increasing amounts Chd2 (YP2) plasmid. Top panel shows agarose gel picture of the PCR products of one experiment. The lanes Sp1, Sp2, Sp3, Sp4 and Sp5 represent different reactions in the experiment. Each reaction contains cells transfected with constant amount of E1A plasmid but different amounts of the Chd2 (YP2) plasmid. The total amount of transfected DNA was kept constant by the addition of the empty parental vector pcDNA 3.1. The upper panel shows the amounts of E1A, Chd2 (YP2) and the empty vector pcDNA 3.1 present in each reaction. **(B)** Quantification of the alternatively spliced forms of E1A mRNA (13S, 12S, 10S and 9S) upon cotransfection with increasing amounts of Chd2 (Sp1, Sp2, Sp3, Sp4 and Sp5). Three independent experiments were performed. Average percentage with std.dev of each isoform is shown.

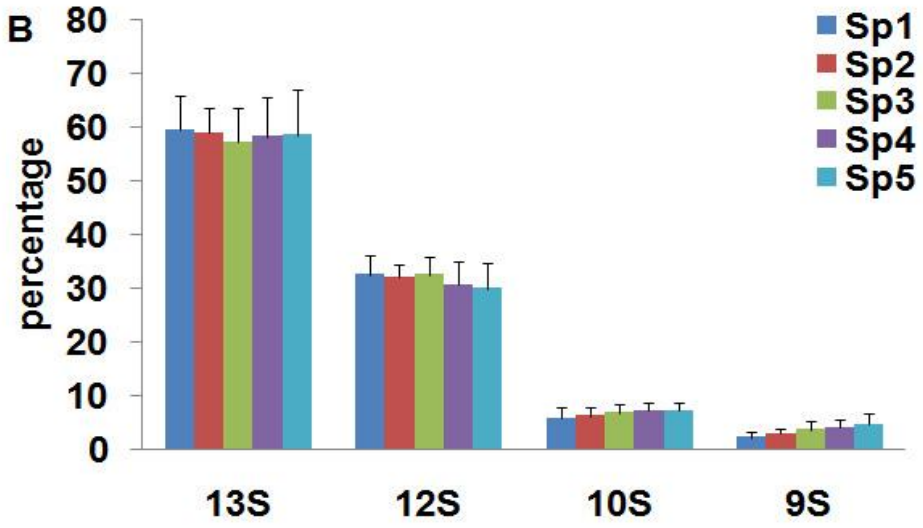

"Figure [figure number 28] continued"

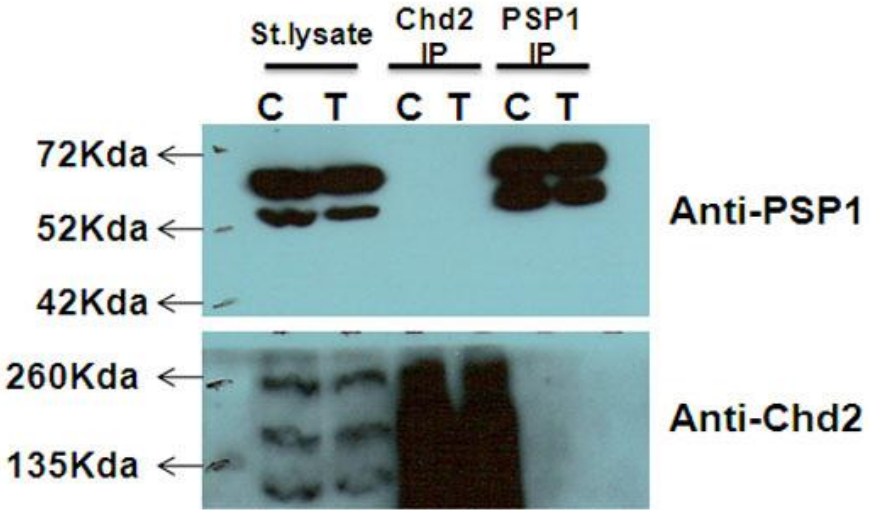

Figure 29. Co-immunoprecipitation of PSP1 and CHD2

To test the interaction of endogenous CHD2 and PSP1 protein, U2OS lysates were incubated with rabbit anti-Chd2 antibody, mouse anti-PSP1/PSPC1 antibody or no antibody control and pulled down by Protein A beads. Immunoprecipitated proteins were separated by SDS-PAGE gel and blotted by a mouse anti-PSP1 or rabbit anti-Chd2 antibody. IP = Immunoprecipitation.

Discussion

The CHD family of proteins is a novel class of chromatin remodeling proteins that contain not only a Swi/Snf-like helicase-ATPase but also two chromodomains as well as a DNA-binding domain. These proteins are reported to play an important role in regulating development, gene expression and oncogenesis [34, 187, 227]. Recently, one of the CHD family members, the CHD8 protein was reported to bind to histone H1 and p53 resulting in the recruitment of histone H1 by CHD8 to the promoter of p53 target genes(*p21*and *Noxa*) to downregulate their transcription [89]. Interestingly, *Chd2* mutant thymocytes and MEF were found to be defective in their ability to induce the pro-apoptotic gene, PUMA and p21, a gene involved in cell cycle arrest (George Samaan and Venkatachalam, unpublished observations). *p21* and *PUMA* [p53 up-regulated modulator of apoptosis] are transcriptional targets of p53 and induce cell cycle arrest and apoptosis respectively [228]. Thus we sought to determine whether CHD2 directly interacts with p53 and modulates the activity of p53 target genes. In order to investigate the possibility of direct interactions of CHD2 with p53, we performed immunoprecipitation using antibodies to p53 or CHD2 on U2OS cell lysates. Our results show that anti-Chd2 antibody was able to effectively pull-down the p53-CHD2 complex. This interaction was enhanced when the cells were exposed to IR. These results were validated by performing pull-down assays with cells expressing recombinant p53 and Chd2 peptides. These results show that CHD2 play an essential role both in the early and late stages of DDR pathway. CHD2 can affect the p53 transcriptional activity by two mechanisms. CHD2 can facilitate post-translational modifications on p53 through recruitment of co-activators to p53, which would lead to stabilization and activation of p53. For example, co-activators such as CBP/p300 (cAMP response element binding protein (CREB)-binding protein) and PCAF (p300/CBP associated factor) have been demonstrated to bring about acetylation of p53 which enhances its transcriptional activity [229-230]. Interestingly, in the absence of genotoxic damage, CBP has been shown to destabilize p53 through interaction with a chromatin remodeler protein BRG1 (component of Swi/Snf complex) [231]. The second mechanism would be that CHD2

modulates the acetylation patterns of the chromatin structure on the promoter regions of p53-target genes or remodels the chromatin, enabling easy access for p53. Consistent with this model, recent studies have demonstrated the role of some ATP-dependent chromatin remodeling proteins such as SWI/SNF complex, CHD8 and NuRD complex in regulating the transcriptional activity of p53 [89, 118, 232]. Further studies into how CHD2 affects the transcriptional activity of p53 will be of great importance and interest.

In addition to interacting with specific proteins, some of the CHD proteins are known to be critical for the functioning of multiprotein complexes involved in transcriptional regulation. For instance, yeast Chd1 is reported to be a component of yeast SAGA (Spt-Ada-Gcn5 acetyltransferase) and SLIK (SAGA-like) complex involved in regulation of transcription activity [46]. CHD1 was also shown to associate with HMG box-containing protein, SSRP1, component of FACT complex [42]. CHD3 and CHD4 are part of the nucleosome remodeling and deacetylating (NuRD) complex involved in transcription repression[142]. CHD4 was shown to coimmunoprecipitate with ATR, HDAC2 and centrosomal protein pericentrin [64, 142]. These data suggest that CHD2 might also function as a component of a multiprotein complex. Thus a tandem affinity purification approach combined with mass spectrometry was adopted to identify the protein partners of CHD2 to dissect the biological pathways in which CHD2 functions.

The tandem affinity purification approach combined with mass spectrometry is a powerful approach to identifying the composition of protein complexes [233]. It is a rapid, easy technique which helps to identify true interacting protein partners under physiological conditions with minimum background [234]. Application of this technique in mammalian cells has lead to identification of many novel interactions. Some examples include, the interaction between SMAD3 and HSP70 [235] and protein partners of telomeric repeat binding factor 2 (TRF2) [210]. In this study, the *Chd2* gene encoding all the structural domains was cloned into a 6X histidine-TEV-Streptavidin tagged vector and expressed in U2OS cells. Tandem affinity purification followed by mass spectrometric analysis was performed on CHD2 protein complex. We identified proteins that are involved in various cellular processes such as proteins involved in RNA

metabolism, processing, regulation, protein metabolism, nuclear organization, immune responses and neuroblast differentiation. These results highlight the functional diversity of CHD2 protein. Isoform 1 of Paraspeckle component 1 was one of the 'high-confidence' proteins obtained from the MS data analysis of TAP purified CHD2 complex. Paraspeckle component 1is a RNA-binding protein and was shown to play a role in RNA processing [219].

Mass spectrometric analysis of single step purified CHD2 protein complex showed presence of two paraspeckle proteins, SFPQ/PSF and p54NRB/NONO in the complex. There are three proteins in the paraspeckle family-PSF/SFPQ, P54nrb/NONO, and PSPC1 [paraspeckle protein 1]. P54nrb/NONO and PSP1/PSPC1 have been shown to form a heterodimer and localize to the paraspeckle in the nucleus [236]. The paraspeckle proteins along with the long nonprotein-coding RNA NEAT1 (MEN-epsilon/beta) form the paraspeckle structure [216]. PSF/SFPQ and P54nrb/NONO are known to be involved in nuclear retention of RNA as they prevent A to I hyperedited RNA from leaving the nucleus [216]. PSF and p54nrb were initially identified as essential pre-mRNA splicing factors needed for spliceosome formation [217, 219, 237]. Interestingly, some CHD proteins have also been reported to play roles in RNA processing. For example the CHD1 protein that is closely related to CHD2 has been shown to have a role in pre-mRNA splicing [51-52]. CHD1 interacts with splicing proteins mKIAA0164, Srp20 and Saf-B and affects the pre-mRNA splicing pattern of *Clk1* minigene. Overexpression of CHD1 resulted in 20% shift towards exclusion of the alternatively spliced exon in *Clk1* mRNA [51]. CHD6 has been shown to colocalizes with phorsphorylated forms of RNA polymerase II (RNAPII) and is present in loci of mRNA synthesis [76]. CHD8 has also been shown to associate with the elongating form of RNAPII and is involved in expression regulation of cyclin E2 gene [90].

The paraspeckle proteins are now known as "multifunctional proteins" involved in transcription initiation, coactivation, and corepression, constitutive and alternative splicing and transcriptional termination and DNA repair [216, 238]. A biochemical study demonstrated that PSF-p54/nrb complex binds to the DNA substrates of the non-

homologous end joining reaction and helps Ku protein to form a functional preligation complex [239]. Interestingly, PSF has also been shown to bind to both single-stranded (ss) and double-stranded (ds) DNA and promote homologous pairing [240]. More direct evidence of PSF's role in homologous pairing was shown in which purified human PSF was able to bind with RAD51 and promote RAD51-mediated homologous pairing [241]. Recently, an *in vivo* study with p54nrb in human cells has highlighted its important role in DNA double-strand break repair [242]. Cells negative in p54nrb displayed a significant delay in recovery from DNA damage as these showed persistence of γ-H2AX foci 2hrs post treatment with gamma radiation. p54nrb attenuated cells also showed increased chromosomal aberrations and increased radiosensitivity after treatment with gamma radiation [242]. The authors of this article speculate that p54nrb may function with specific protein partners to bring about the repair of DNA double strand break [242]. Additionally, it has been shown previously that DNA topoisomerase I directly interacts with PSF-p54nrb complex [243].

Collectively, these observations by other groups and our results lead us to hypothesze that CHD2 associates with the paraspeckle proteins to facilitate their function in pre-mRNA splicing and DNA double-strand break repair. Experiments conducted in the first aim of this thesis show that CHD2 plays a vital role in maintaining genomic stability by affecting the efficiency of DNA repair. *Chd2*-mutant cells treated with X-ray radiation exhibited a delay in DSB repair in a comet assay. These cells also showed a significant increase in X-ray radiation induced chromosomal aberrations. Thus it is possible that CHD2 brings about remodeling of chromatin near the DNA damaged sites and also facilitates recruitment of the paraspeckle proteins to the damaged sites. It would be interesting to see if the levels of any of the paraspeckle proteins-PSF, p54nrb/NONO or PSP1/PSPC1 are low or completely absent in the Chd2 mutant cells.

To investigate whether CHD2 could modulate the pre-mRNA splicing event, we performed an *in vivo* splicing assay. An *in vivo* assay performed with E1A minigene showed that overexpression of CHD2 strongly activated distal 5' splice site of the E1A

gene, giving rise to an increase in the amount of 9S and decrease in 13S. These results implicated that CHD2 would regulate alternative splicing events. Interestingly, recent studies have demonstrated that changes in chromatin structure affect RNA splicing process [244-245]. Splicing is shown to be tightly coupled to transcription as introns are removed while the nascent transcript is still attached to the transcribed gene. This process is carried out by RNA pol II via association with many splicing factors [246]. The transcription rate of RNA pol II have also been shown to affect splicing [247]. Furthermore, recent studies have shown that the ATP-dependent chromatin remodeler, Brahma (hBrm), subunit of SWI/SNF complex delays the transcription rate of RNA pol II and associates with the splicing machinery proteins such as U1 and U5 snRNPs, resulting in modulation of alternative splicing pattern of several SWI/SNF target genes via favoring inclusion of variant exons [248-249]. Additionally, nucleosome positioning and post-translational modifications on histones have been shown to affect the rate of RNAPII elongation [244]. Interestingly as mentioned before, CHD1 has been shown to affect the pre-mRNA splicing pattern of *Clk1* minigene. [51-52]. And CHD6 and CHD8 have been shown to associate with RNA polymerase II [76, 90].

CHD2 seems to play a role in modulating both pre-mRNA splicing and repair of DNA damage as the paraspeckle proteins. Additionally, the mass spectrometric analysis shows that the paraspeckle proteins could be potential interacting partners of CHD2. Thus, co-immunoprecipitation studies were performed to test whether Chd2 directly interacts with any of the paraspeckle proteins. However, co-immunoprecipitation study of CHD2 with PSP1/PSPC1 failed to show any direct interaction of CHD2 with PSP1/PSPC1. Since there is paucity of commercial reagents available for the PSP1/PSPC1 protein and the antibody used in this study was generated by another lab, it may not be efficient for IP. Alternatively, as CHD2 possibly interacts with the second member of the paraspeckle protein family-p54nrb/NONO (data from the second mass spectrometric run; see result section), and since PSP1/PSPC1 forms a heterodimer with p54nrb/NONO [236], it is possible that PSP1 is present in the CHD2-p54nrb complex, but does not directly interact with CHD2. Additionally, it is also possible that the

interaction between CHD2 and the paraspeckle proteins is transient and would need better biochemical approaches to test the direct association. Nevertheless, analysis of CHD2 binding proteins using MS is a very feasible and constructive approach to gain insight into the biological importance and functions of this protein.

Conclusion: "CHD2 a multi-function protein?"

ATP-dependent remodeling proteins are essentially regarded as transcriptional regulators. These proteins utilize the energy from ATP hydrolysis to modulate and reposition nucleosomes so that the transcription machinery can access the DNA template [250-252]. However, recent studies have shown that the ATP-dependent chromatin remodeling proteins function much more diversely than just as transcriptional regulators. ATP-dependent remodeling proteins like INO80 and SWR1 have been shown to play critical role in processes such as DNA repair, checkpoint regulation, DNA replication, telomere maintenance, and chromosome segregation [28, 158]. Similarly the SWI/SNF chromatin remodeling complex have been demonstrated to be involved in an array of functions such as in differentiation, in tumor suppression, in the control of cell proliferation, in DNA repair, in cellular adhesion, in immune responses, T-cell development and recombination events [253-255]. The CHD family of chromatin remodelers have also been implicated in diverse cellular functions (described in chapter I of this thesis). Though the ATP-dependent chromatin remodeling proteins have been shown to be involved in various cellular processes, it is not still clear whether these diverse functions are dependent or independent of the chromatin remodeling activity of these proteins. Thus the roles of CHD2 in DNA repair, cellular responses to DNA damage and tumor suppression elucidated in this thesis may be due to the direct chromatin remodeling activity of CHD2 or indirect effects on the transcriptional regulation of specific target genes. Based on our observations relating to the DNA repair defects, DNA damage induced phosphorylation and interaction of CHD2 with ATR (and paraspeckle proteins) we propose that CHD2 is a multi-functional protein that potentially facilitates both the pre-mRNA splicing process and the initial DNA repair process. A schematic model for the role of CHD2 in DNA repair is shown in figure 30. Briefly, upon DNA damage induction, activated ATM/ATR catalyzes the post-translational modification of CHD2. This modification could either aid in enhancing the interaction of CHD2 with the paraspeckle proteins or could help in activating CHD2's function as a chromatin remodeler. The activated CHD2 remodels the chromatin around the

damaged site and facilities recruitment of the paraspeckle proteins. The paraspeckle proteins interact with the NHEJ proteins to bring about the repair of the DNA DSB.

At the transcriptional level, our data show that CHD2 plays a role in the downstream process of the DDR pathway. The interaction of CHD2 with p53 and the loss of the p53 transcriptional target *PUMA* in thymocytes suggests that the CHD2 protein facilitates p53 transcriptional activity either by enhancing the post-translational modifications on p53 or by remodeling the chromatin around the promoter regions of p53-target genes to facilitate the interaction of p53 to its cognate sites. A schematic representation of the role of CHD2 in facilitating p53 transcativation is shown in Figure 31. Interestingly, our studies also show that the CHD2 protein has a potential role in mRNA splicing of exogenously expressed E1A minigene. However, the functions of CHD2 in pre-mRNA splicing of endogenous genes remain to be ascertained. Future studies as to how Chd2 is involved in the regulation of the vital cellular processes of pre-mRNA splicing, DNA repair and DNA damage induced transcriptional activation of stress response genes would be of great importance to dissect the functions of CHD2 at the molecular and cellular levels. Finally, the knowledge regarding CHD2 function as a chromatin remodeler comes from implications derived from bioinformatics analysis of its structural domains and comparative functional analysis of other CHD members. Thus, it would be valuable to demonstrate its chromatin remodeling activity experimentally to provide direct evidence for the role of CHD2 in chromatin remodeling.

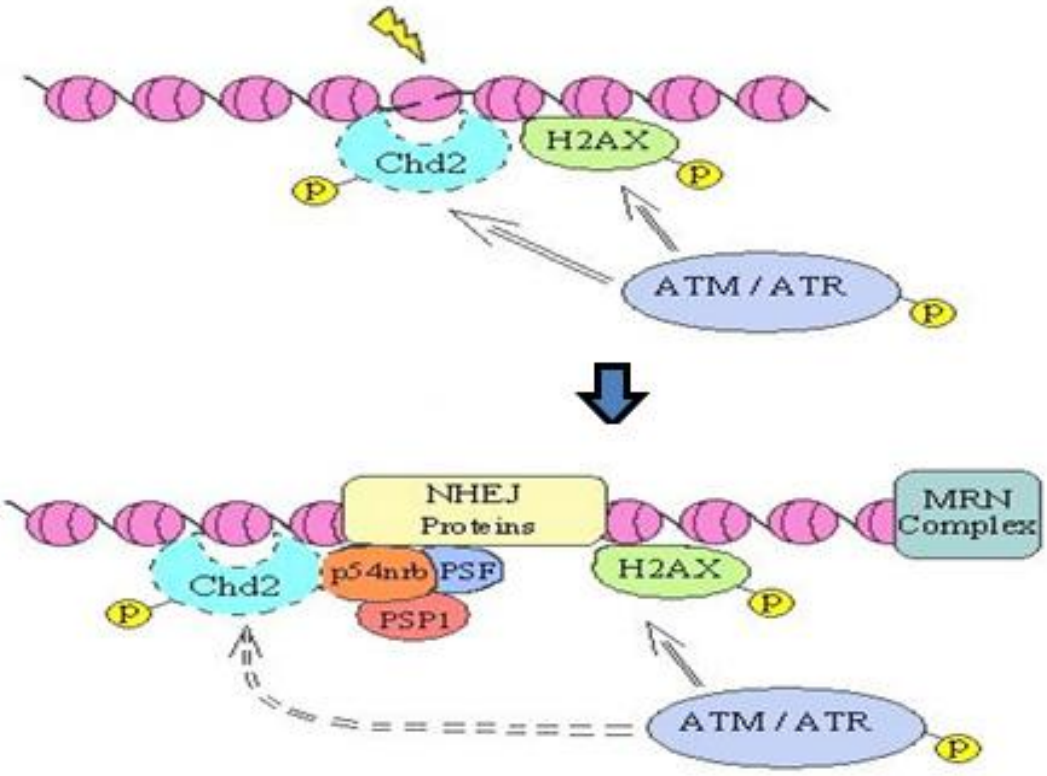

Figure 30. A model illustrating a role of CHD2 in DNA damage response

CHD2 can be phoshorylated by ATM/ATR kinase upon DNA damage. Phosphorylated CHD2 facilitates chromatin remodeling and recruitment of the paraspeckle proteins to damaged site. The paraspeckle proteins associate with NHEJ proteins to bring about repair of damaged DNA.

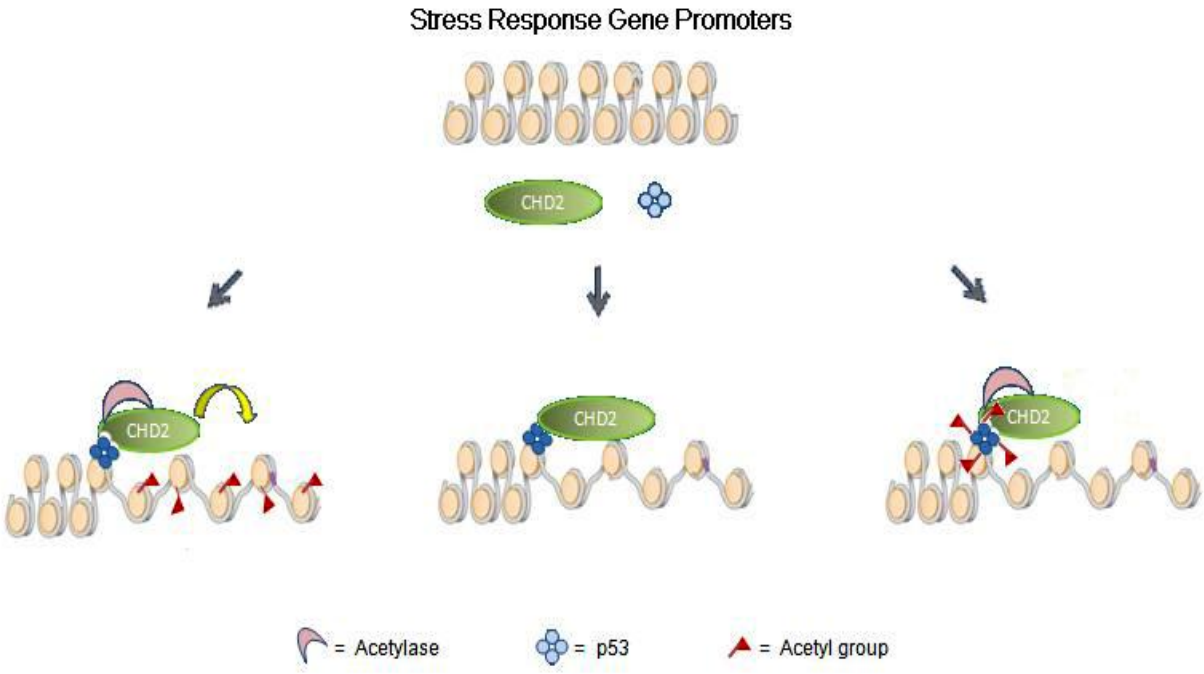

Figure 31.Role of CHD2 in transactivation of p53 dependent target genes
CHD2 can have a potential role in the downstream process of DDR by modulating p53's transcriptional activity. It can do this by either facilitating post-translational modifications on p53 through recruitment of co-activators to p53 or by modulating the acetylation patterns of the chromatin structure on the promoter regions of p53-target genes or remodel the chromatin around the promoter region.

References

1. Ehrenhofer-Murray, A.E., *Chromatin dynamics at DNA replication, transcription and repair.* Eur J Biochem, 2004. **271**(12): p. 2335-49.
2. Margueron, R., P. Trojer, and D. Reinberg, *The key to development: interpreting the histone code?* Curr Opin Genet Dev, 2005. **15**(2): p. 163-76.
3. Marino-Ramirez, L., et al., *Histone structure and nucleosome stability.* Expert Rev Proteomics, 2005. **2**(5): p. 719-29.
4. Ito, T., *Role of histone modification in chromatin dynamics.* J Biochem, 2007. **141**(5): p. 609-14.
5. Bhaumik, S.R., E. Smith, and A. Shilatifard, *Covalent modifications of histones during development and disease pathogenesis.* Nat Struct Mol Biol, 2007. **14**(11): p. 1008-16.
6. Zhang, K. and S.Y. Dent, *Histone modifying enzymes and cancer: going beyond histones.* J Cell Biochem, 2005. **96**(6): p. 1137-48.
7. Kusch, T., et al., *Acetylation by Tip60 is required for selective histone variant exchange at DNA lesions.* Science, 2004. **306**(5704): p. 2084-7.
8. Eberharter, A. and P.B. Becker, *Histone acetylation: a switch between repressive and permissive chromatin. Second in review series on chromatin dynamics.* EMBO Rep, 2002. **3**(3): p. 224-9.
9. Bauer, U.M., et al., *Methylation at arginine 17 of histone H3 is linked to gene activation.* EMBO Rep, 2002. **3**(1): p. 39-44.
10. Strahl, B.D., et al., *Methylation of histone H4 at arginine 3 occurs in vivo and is mediated by the nuclear receptor coactivator PRMT1.* Curr Biol, 2001. **11**(12): p. 996-1000.
11. Peters, A.H., et al., *Partitioning and plasticity of repressive histone methylation states in mammalian chromatin.* Mol Cell, 2003. **12**(6): p. 1577-89.
12. Bannister, A.J. and T. Kouzarides, *Reversing histone methylation.* Nature, 2005. **436**(7054): p. 1103-6.
13. Eissenberg, J.C. and S.C. Elgin, *Molecular biology: antagonizing the neighbours.* Nature, 2005. **438**(7071): p. 1090-1.
14. Yang, J., et al., *ATM and ATR: sensing DNA damage.* World J Gastroenterol, 2004. **10**(2): p. 155-60.
15. Chowdhury, D., et al., *gamma-H2AX dephosphorylation by protein phosphatase 2A facilitates DNA double-strand break repair.* Mol Cell, 2005. **20**(5): p. 801-9.
16. Neely, K.E. and J.L. Workman, *The complexity of chromatin remodeling and its links to cancer.* Biochim Biophys Acta, 2002. **1603**(1): p. 19-29.
17. Tsukiyama, T., *The in vivo functions of ATP-dependent chromatin-remodelling factors.* Nat Rev Mol Cell Biol, 2002. **3**(6): p. 422-9.
18. Cote, J., C.L. Peterson, and J.L. Workman, *Perturbation of nucleosome core structure by the SWI/SNF complex persists after its detachment, enhancing subsequent transcription factor binding.* Proc Natl Acad Sci U S A, 1998. **95**(9): p. 4947-52.

19. Peterson, C.L., A. Dingwall, and M.P. Scott, *Five SWI/SNF gene products are components of a large multisubunit complex required for transcriptional enhancement.* Proc Natl Acad Sci U S A, 1994. **91**(8): p. 2905-8.
20. Peterson, C.L. and I. Herskowitz, *Characterization of the yeast SWI1, SWI2, and SWI3 genes, which encode a global activator of transcription.* Cell, 1992. **68**(3): p. 573-83.
21. Cairns, B.R., *Chromatin remodeling: insights and intrigue from single-molecule studies.* Nat Struct Mol Biol, 2007. **14**(11): p. 989-96.
22. Tsukiyama, T. and C. Wu, *Chromatin remodeling and transcription.* Curr Opin Genet Dev, 1997. **7**(2): p. 182-91.
23. Ng, H.H., et al., *Genome-wide location and regulated recruitment of the RSC nucleosome-remodeling complex.* Genes Dev, 2002. **16**(7): p. 806-19.
24. Bouazoune, K. and A. Brehm, *ATP-dependent chromatin remodeling complexes in Drosophila.* Chromosome Res, 2006. **14**(4): p. 433-49.
25. Mellor, J., *Imitation switch complexes.* Ernst Schering Res Found Workshop, 2006(57): p. 61-87.
26. Deuring, R., et al., *The ISWI chromatin-remodeling protein is required for gene expression and the maintenance of higher order chromatin structure in vivo.* Mol Cell, 2000. **5**(2): p. 355-65.
27. Mellor, J. and A. Morillon, *ISWI complexes in Saccharomyces cerevisiae.* Biochim Biophys Acta, 2004. **1677**(1-3): p. 100-12.
28. Conaway, R.C. and J.W. Conaway, *The INO80 chromatin remodeling complex in transcription, replication and repair.* Trends Biochem Sci, 2008.
29. Bao, Y. and X. Shen, *INO80 subfamily of chromatin remodeling complexes.* Mutat Res, 2007. **618**(1-2): p. 18-29.
30. Morrison, A.J., et al., *INO80 and gamma-H2AX interaction links ATP-dependent chromatin remodeling to DNA damage repair.* Cell, 2004. **119**(6): p. 767-75.
31. Woodage, T., et al., *Characterization of the CHD family of proteins.* Proc Natl Acad Sci U S A, 1997. **94**(21): p. 11472-7.
32. Bouazoune, K. and A. Brehm, *dMi-2 chromatin binding and remodeling activities are regulated by dCK2 phosphorylation.* J Biol Chem, 2005. **280**(51): p. 41912-20.
33. Flanagan, J.F., et al., *Double chromodomains cooperate to recognize the methylated histone H3 tail.* Nature, 2005. **438**(7071): p. 1181-5.
34. Hall, J.A. and P.T. Georgel, *CHD proteins: a diverse family with strong ties.* Biochem Cell Biol, 2007. **85**(4): p. 463-76.
35. Tajul-Arifin, K., et al., *Identification and analysis of chromodomain-containing proteins encoded in the mouse transcriptome.* Genome Res, 2003. **13**(6B): p. 1416-29.
36. Delmas, V., D.G. Stokes, and R.P. Perry, *A mammalian DNA-binding protein that contains a chromodomain and an SNF2/SWI2-like helicase domain.* Proc Natl Acad Sci U S A, 1993. **90**(6): p. 2414-8.

37. Hara, R. and A. Sancar, *The SWI/SNF chromatin-remodeling factor stimulates repair by human excision nuclease in the mononucleosome core particle.* Mol Cell Biol, 2002. **22**(19): p. 6779-87.
38. Stokes, D.G. and R.P. Perry, *DNA-binding and chromatin localization properties of CHD1.* Mol Cell Biol, 1995. **15**(5): p. 2745-53.
39. Stokes, D.G., K.D. Tartof, and R.P. Perry, *CHD1 is concentrated in interbands and puffed regions of Drosophila polytene chromosomes.* Proc Natl Acad Sci U S A, 1996. **93**(14): p. 7137-42.
40. Konev, A.Y., et al., *CHD1 motor protein is required for deposition of histone variant H3.3 into chromatin in vivo.* Science, 2007. **317**(5841): p. 1087-90.
41. McDaniel, I.E., et al., *Investigations of CHD1 function in transcription and development of Drosophila melanogaster.* Genetics, 2008. **178**(1): p. 583-7.
42. Kelley, D.E., D.G. Stokes, and R.P. Perry, *CHD1 interacts with SSRP1 and depends on both its chromodomain and its ATPase/helicase-like domain for proper association with chromatin.* Chromosoma, 1999. **108**(1): p. 10-25.
43. Kumari, A., et al., *A role for SSRP1 in recombination-mediated DNA damage response.* J Cell Biochem, 2009. **108**(2): p. 508-18.
44. Simic, R., et al., *Chromatin remodeling protein Chd1 interacts with transcription elongation factors and localizes to transcribed genes.* Embo J, 2003. **22**(8): p. 1846-56.
45. Lusser, A., D.L. Urwin, and J.T. Kadonaga, *Distinct activities of CHD1 and ACF in ATP-dependent chromatin assembly.* Nat Struct Mol Biol, 2005. **12**(2): p. 160-6.
46. Pray-Grant, M.G., et al., *Chd1 chromodomain links histone H3 methylation with SAGA- and SLIK-dependent acetylation.* Nature, 2005. **433**(7024): p. 434-8.
47. Xella, B., et al., *The ISWI and CHD1 chromatin remodelling activities influence ADH2 expression and chromatin organization.* Mol Microbiol, 2006. **59**(5): p. 1531-41.
48. Biswas, D., R. Dutta-Biswas, and D.J. Stillman, *Chd1 and yFACT act in opposition in regulating transcription.* Mol Cell Biol, 2007. **27**(18): p. 6279-87.
49. Biswas, D., et al., *A role for Chd1 and Set2 in negatively regulating DNA replication in Saccharomyces cerevisiae.* Genetics, 2008. **178**(2): p. 649-59.
50. Sims, R.J., 3rd, et al., *Human but not yeast CHD1 binds directly and selectively to histone H3 methylated at lysine 4 via its tandem chromodomains.* J Biol Chem, 2005. **280**(51): p. 41789-92.
51. Tai, H.H., et al., *CHD1 associates with NCoR and histone deacetylase as well as with RNA splicing proteins.* Biochem Biophys Res Commun, 2003. **308**(1): p. 170-6.
52. Sims, R.J., 3rd, et al., *Recognition of trimethylated histone H3 lysine 4 facilitates the recruitment of transcription postinitiation factors and pre-mRNA splicing.* Mol Cell, 2007. **28**(4): p. 665-76.
53. Papantonis, A., et al., *CHD1 assumes a central role during follicle development.* J Mol Biol, 2008. **383**(5): p. 957-69.

54. Gaspar-Maia, A., et al., *Chd1 regulates open chromatin and pluripotency of embryonic stem cells.* Nature, 2009.
55. Ge, Q., et al., *Molecular analysis of a major antigenic region of the 240-kD protein of Mi-2 autoantigen.* J Clin Invest, 1995. **96**(4): p. 1730-7.
56. Seelig, H.P., et al., *Two forms of the major antigenic protein of the dermatomyositis-specific Mi-2 autoantigen.* Arthritis Rheum, 1996. **39**(10): p. 1769-71.
57. Bowen, N.J., et al., *Mi-2/NuRD: multiple complexes for many purposes.* Biochim Biophys Acta, 2004. **1677**(1-3): p. 52-7.
58. Baker, L.A., C.D. Allis, and G.G. Wang, *PHD fingers in human diseases: disorders arising from misinterpreting epigenetic marks.* Mutat Res, 2008. **647**(1-2): p. 3-12.
59. Capili, A.D., et al., *Solution structure of the PHD domain from the KAP-1 corepressor: structural determinants for PHD, RING and LIM zinc-binding domains.* Embo J, 2001. **20**(1-2): p. 165-77.
60. Denslow, S.A. and P.A. Wade, *The human Mi-2/NuRD complex and gene regulation.* Oncogene, 2007. **26**(37): p. 5433-8.
61. Ahringer, J., *NuRD and SIN3 histone deacetylase complexes in development.* Trends Genet, 2000. **16**(8): p. 351-6.
62. Zhang, Y., et al., *The dermatomyositis-specific autoantigen Mi2 is a component of a complex containing histone deacetylase and nucleosome remodeling activities.* Cell, 1998. **95**(2): p. 279-89.
63. Fujita, N., et al., *MTA3 and the Mi-2/NuRD complex regulate cell fate during B lymphocyte differentiation.* Cell, 2004. **119**(1): p. 75-86.
64. Sillibourne, J.E., et al., *Chromatin remodeling proteins interact with pericentrin to regulate centrosome integrity.* Mol Biol Cell, 2007. **18**(9): p. 3667-80.
65. von Zelewsky, T., et al., *The C. elegans Mi-2 chromatin-remodelling proteins function in vulval cell fate determination.* Development, 2000. **127**(24): p. 5277-84.
66. Zhang, H., et al., *The CHD3 remodeler PICKLE promotes trimethylation of histone H3 lysine 27.* J Biol Chem, 2008. **283**(33): p. 22637-48.
67. Murawska, M., et al., *dCHD3, a novel ATP-dependent chromatin remodeler associated with sites of active transcription.* Mol Cell Biol, 2008. **28**(8): p. 2745-57.
68. Thompson, P.M., et al., *CHD5, a new member of the chromodomain gene family, is preferentially expressed in the nervous system.* Oncogene, 2003. **22**(7): p. 1002-11.
69. de la Cruz, J., D. Kressler, and P. Linder, *Unwinding RNA in Saccharomyces cerevisiae: DEAD-box proteins and related families.* Trends Biochem Sci, 1999. **24**(5): p. 192-8.
70. Bagchi, A. and A.A. Mills, *The quest for the 1p36 tumor suppressor.* Cancer Res, 2008. **68**(8): p. 2551-6.

71. Mulero-Navarro, S. and M. Esteller, *Chromatin remodeling factor CHD5 is silenced by promoter CpG island hypermethylation in human cancer.* Epigenetics, 2008. **3**(4): p. 210-5.
72. Gorringe, K.L., et al., *Mutation and methylation analysis of the chromodomain-helicase-DNA binding 5 gene in ovarian cancer.* Neoplasia, 2008. **10**(11): p. 1253-8.
73. Schuster, E.F. and R. Stoger, *CHD5 defines a new subfamily of chromodomain-SWI2/SNF2-like helicases.* Mamm Genome, 2002. **13**(2): p. 117-9.
74. Boyer, L.A., R.R. Latek, and C.L. Peterson, *The SANT domain: a unique histone-tail-binding module?* Nat Rev Mol Cell Biol, 2004. **5**(2): p. 158-63.
75. Nioi, P., et al., *The carboxy-terminal Neh3 domain of Nrf2 is required for transcriptional activation.* Mol Cell Biol, 2005. **25**(24): p. 10895-906.
76. Lutz, T., R. Stoger, and A. Nieto, *CHD6 is a DNA-dependent ATPase and localizes at nuclear sites of mRNA synthesis.* FEBS Lett, 2006. **580**(25): p. 5851-7.
77. Surapureddi, S., et al., *Identification of a transcriptionally active peroxisome proliferator-activated receptor alpha -interacting cofactor complex in rat liver and characterization of PRIC285 as a coactivator.* Proc Natl Acad Sci U S A, 2002. **99**(18): p. 11836-41.
78. Vissers, L.E., et al., *Mutations in a new member of the chromodomain gene family cause CHARGE syndrome.* Nat Genet, 2004. **36**(9): p. 955-7.
79. Kim, H.G., et al., *Mutations in CHD7, encoding a chromatin-remodeling protein, cause idiopathic hypogonadotropic hypogonadism and Kallmann syndrome.* Am J Hum Genet, 2008. **83**(4): p. 511-9.
80. Schnetz, M.P., et al., *Genomic distribution of CHD7 on chromatin tracks H3K4 methylation patterns.* Genome Res, 2009.
81. Allen, M.D., et al., *Solution structure of the BRK domains from CHD7.* J Mol Biol, 2007. **371**(5): p. 1135-40.
82. Bosman, E.A., et al., *Multiple mutations in mouse Chd7 provide models for CHARGE syndrome.* Hum Mol Genet, 2005. **14**(22): p. 3463-76.
83. Hurd, E.A., et al., *Loss of Chd7 function in gene-trapped reporter mice is embryonic lethal and associated with severe defects in multiple developing tissues.* Mamm Genome, 2007. **18**(2): p. 94-104.
84. Renda, M., et al., *Critical DNA binding interactions of the insulator protein CTCF: a small number of zinc fingers mediate strong binding, and a single finger-DNA interaction controls binding at imprinted loci.* J Biol Chem, 2007. **282**(46): p. 33336-45.
85. Ishihara, K., M. Oshimura, and M. Nakao, *CTCF-dependent chromatin insulator is linked to epigenetic remodeling.* Mol Cell, 2006. **23**(5): p. 733-42.
86. Yuan, C.C., et al., *CHD8 associates with human Staf and contributes to efficient U6 RNA polymerase III transcription.* Mol Cell Biol, 2007. **27**(24): p. 8729-38.

87. Thompson, B.A., et al., *CHD8 is an ATP-dependent chromatin remodeling factor that regulates beta-catenin target genes.* Mol Cell Biol, 2008. **28**(12): p. 3894-904.
88. Nishiyama, M., et al., *Early embryonic death in mice lacking the beta-catenin-binding protein Duplin.* Mol Cell Biol, 2004. **24**(19): p. 8386-94.
89. Nishiyama, M., et al., *CHD8 suppresses p53-mediated apoptosis through histone H1 recruitment during early embryogenesis.* Nat Cell Biol, 2009.
90. Rodriguez-Paredes, M., et al., *The chromatin remodeling factor CHD8 interacts with elongating RNA polymerase II and controls expression of the cyclin E2 gene.* Nucleic Acids Res, 2009.
91. Shur, I. and D. Benayahu, *Characterization and functional analysis of CReMM, a novel chromodomain helicase DNA-binding protein.* J Mol Biol, 2005. **352**(3): p. 646-55.
92. Shur, I., R. Socher, and D. Benayahu, *In vivo association of CReMM/CHD9 with promoters in osteogenic cells.* J Cell Physiol, 2006. **207**(2): p. 374-8.
93. Marom, R., et al., *Expression and regulation of CReMM, a chromodomain helicase-DNA-binding (CHD), in marrow stroma derived osteoprogenitors.* J Cell Physiol, 2006. **207**(3): p. 628-35.
94. Benayahu, D., N. Shacham, and I. Shur, *Insights on the functional role of chromatin remodelers in osteogenic cells.* Crit Rev Eukaryot Gene Expr, 2007. **17**(2): p. 103-13.
95. Wilson, G.N., et al., *Phenotypic delineation of ring chromosome 15 and Russell-Silver syndromes.* J Med Genet, 1985. **22**(3): p. 233-6.
96. Whiteford, M.L., et al., *A child with bisatellited, dicentric chromosome 15 arising from a maternal paracentric inversion of chromosome 15q.* J Med Genet, 2000. **37**(8): p. E11.
97. Cordin, O., et al., *The DEAD-box protein family of RNA helicases.* Gene, 2006. **367**: p. 17-37.
98. Linder, P., *Dead-box proteins: a family affair--active and passive players in RNP-remodeling.* Nucleic Acids Res, 2006. **34**(15): p. 4168-80.
99. Bustin, M. and R. Reeves, *High-mobility-group chromosomal proteins: architectural components that facilitate chromatin function.* Prog Nucleic Acid Res Mol Biol, 1996. **54**: p. 35-100.
100. Slavotinek, A.M., et al., *Array comparative genomic hybridization in patients with congenital diaphragmatic hernia: mapping of four CDH-critical regions and sequencing of candidate genes at 15q26.1-15q26.2.* Eur J Hum Genet, 2006. **14**(9): p. 999-1008.
101. Osman, I., et al., *Novel blood biomarkers of human urinary bladder cancer.* Clin Cancer Res, 2006. **12**(11 Pt 1): p. 3374-80.
102. Koch, J.G., et al., *Mammary tumor modifiers in BALB/cJ mice heterozygous for p53.* Mamm Genome, 2007. **18**(5): p. 300-9.

103. Feys, T., et al., *A detailed inventory of DNA copy number alterations in four commonly used Hodgkin's lymphoma cell lines.* Haematologica, 2007. **92**(7): p. 913-20.
104. Kessler-Becker, D., T. Krieg, and B. Eckes, *Expression of pro-inflammatory markers by human dermal fibroblasts in a three-dimensional culture model is mediated by an autocrine interleukin-1 loop.* Biochem J, 2004. **379**(Pt 2): p. 351-8.
105. Marfella, C.G., et al., *Mutation of the SNF2 family member Chd2 affects mouse development and survival.* J Cell Physiol, 2006. **209**(1): p. 162-71.
106. Marfella, C.G., et al., *A Mutation in the Mouse Chd2 Chromatin Remodeling Enzyme Results in a Complex Renal Phenotype.* Kidney Blood Press Res, 2009. **31**(6): p. 421-432.
107. Flanagan, J.F., et al., *Molecular implications of evolutionary differences in CHD double chromodomains.* J Mol Biol, 2007. **369**(2): p. 334-42.
108. Kulkarni, S., et al., *Disruption of chromodomain helicase DNA binding protein 2 (CHD2) causes scoliosis.* Am J Med Genet A, 2008. **146**(9): p. 1117-27.
109. Nagarajan, P., et al., *Role of chromodomain helicase DNA-binding protein 2 in DNA damage response signaling and tumorigenesis.* Oncogene, 2009. **28**(8): p. 1053-62.
110. Kulkarni, S., et al., *Disruption of chromodomain helicase DNA binding protein 2 (CHD2) causes scoliosis.* Am J Med Genet A, 2008. **146A**(9): p. 1117-27.
111. Osley, M.A., T. Tsukuda, and J.A. Nickoloff, *ATP-dependent chromatin remodeling factors and DNA damage repair.* Mutat Res, 2007. **618**(1-2): p. 65-80.
112. Khanna, K.K. and S.P. Jackson, *DNA double-strand breaks: signaling, repair and the cancer connection.* Nat Genet, 2001. **27**(3): p. 247-54.
113. Wang, G.G., C.D. Allis, and P. Chi, *Chromatin remodeling and cancer, Part II: ATP-dependent chromatin remodeling.* Trends Mol Med, 2007. **13**(9): p. 373-80.
114. Huen, M.S. and J. Chen, *The DNA damage response pathways: at the crossroad of protein modifications.* Cell Res, 2008. **18**(1): p. 8-16.
115. Kim, S.T., et al., *Substrate specificities and identification of putative substrates of ATM kinase family members.* J Biol Chem, 1999. **274**(53): p. 37538-43.
116. Shiloh, Y., *ATM and related protein kinases: safeguarding genome integrity.* Nat Rev Cancer, 2003. **3**(3): p. 155-68.
117. Rodier, F., J. Campisi, and D. Bhaumik, *Two faces of p53: aging and tumor suppression.* Nucleic Acids Res, 2007. **35**(22): p. 7475-84.
118. Lee, D., et al., *SWI/SNF complex interacts with tumor suppressor p53 and is necessary for the activation of p53-mediated transcription.* J Biol Chem, 2002. **277**(25): p. 22330-7.
119. Reed, S.H. and R. Waters, *DNA Repair*. ENCYCLOPEDIA OF LIFE SCIENCES. 2005: John Wiley & Sons, Ltd: Chichester http://www.els.net/ [doi:10.1038/npg.els.0005284].

120. Hakem, R., *DNA-damage repair; the good, the bad, and the ugly.* Embo J, 2008. **27**(4): p. 589-605.
121. Tannock, I., et al., *The basic science of oncology*. 4th ed. 2005: McGraw-Hill Professional.
122. Hsieh, P. and K. Yamane, *DNA mismatch repair: molecular mechanism, cancer, and ageing.* Mech Ageing Dev, 2008. **129**(7-8): p. 391-407.
123. Li, G.M., *Mechanisms and functions of DNA mismatch repair.* Cell Res, 2008. **18**(1): p. 85-98.
124. Hoeijmakers, J.H., *Nucleotide excision repair. II: From yeast to mammals.* Trends Genet, 1993. **9**(6): p. 211-7.
125. Hoeijmakers, J.H., *Nucleotide excision repair I: from E. coli to yeast.* Trends Genet, 1993. **9**(5): p. 173-7.
126. Costa, R.M., et al., *The eukaryotic nucleotide excision repair pathway.* Biochimie, 2003. **85**(11): p. 1083-99.
127. Baute, J. and A. Depicker, *Base excision repair and its role in maintaining genome stability.* Crit Rev Biochem Mol Biol, 2008. **43**(4): p. 239-76.
128. Cann, K.L. and G.G. Hicks, *Regulation of the cellular DNA double-strand break response.* Biochem Cell Biol, 2007. **85**(6): p. 663-74.
129. Shrivastav, M., L.P. De Haro, and J.A. Nickoloff, *Regulation of DNA double-strand break repair pathway choice.* Cell Res, 2008. **18**(1): p. 134-47.
130. van den Bosch, M., P.H. Lohman, and A. Pastink, *DNA double-strand break repair by homologous recombination.* Biol Chem, 2002. **383**(6): p. 873-92.
131. Lieber, M.R., *The mechanism of human nonhomologous DNA end joining.* J Biol Chem, 2008. **283**(1): p. 1-5.
132. Weterings, E. and D.J. Chen, *The endless tale of non-homologous end-joining.* Cell Res, 2008. **18**(1): p. 114-24.
133. Ma, Y., et al., *Repair of double-strand DNA breaks by the human nonhomologous DNA end joining pathway: the iterative processing model.* Cell Cycle, 2005. **4**(9): p. 1193-200.
134. Ray, A., et al., *Human SNF5/INI1, a component of the human SWI/SNF chromatin remodeling complex, promotes nucleotide excision repair by influencing ATM recruitment and downstream H2AX phosphorylation.* Mol Cell Biol, 2009. **29**(23): p. 6206-19.
135. Verger, A. and M. Crossley, *Chromatin modifiers in transcription and DNA repair.* Cell Mol Life Sci, 2004. **61**(17): p. 2154-62.
136. Bao, Y. and X. Shen, *Chromatin remodeling in DNA double-strand break repair.* Curr Opin Genet Dev, 2007. **17**(2): p. 126-31.
137. Sapountzi, V., I.R. Logan, and C.N. Robson, *Cellular functions of TIP60.* Int J Biochem Cell Biol, 2006. **38**(9): p. 1496-509.
138. Heyer, W.D., et al., *Rad54: the Swiss Army knife of homologous recombination?* Nucleic Acids Res, 2006. **34**(15): p. 4115-25.

139. Park, J.H., et al., *Mammalian SWI/SNF complexes facilitate DNA double-strand break repair by promoting gamma-H2AX induction.* Embo J, 2006. **25**(17): p. 3986-97.
140. Jin, Y.H., et al., *Isolation and characterization of hrp1+, a new member of the SNF2/SWI2 gene family from the fission yeast Schizosaccharomyces pombe.* Mol Gen Genet, 1998. **257**(3): p. 319-29.
141. Wang, H.P., et al., *Identification of differentially transcribed genes in human lymphoblastoid cells irradiated with 0.5 Gy of gamma-ray and the involvement of low dose radiation inducible CHD6 gene in cell proliferation and radiosensitivity.* Int J Radiat Biol, 2006. **82**(3): p. 181-90.
142. Schmidt, D.R. and S.L. Schreiber, *Molecular association between ATR and two components of the nucleosome remodeling and deacetylating complex, HDAC2 and CHD4.* Biochemistry, 1999. **38**(44): p. 14711-7.
143. Kobzdej, M., J. Matuszyk, and L. Strzadala, *Overexpression of Ras, Raf and L-myc but not Bcl-2 family proteins is linked with resistance to TCR-mediated apoptosis and tumorigenesis in thymic lymphomas from TCR transgenic mice.* Leuk Res, 2000. **24**(1): p. 33-8.
144. Aguilera, A. and B. Gomez-Gonzalez, *Genome instability: a mechanistic view of its causes and consequences.* Nat Rev Genet, 2008. **9**(3): p. 204-17.
145. Solomon, E., J. Borrow, and A.D. Goddard, *Chromosome aberrations and cancer.* Science, 1991. **254**(5035): p. 1153-60.
146. Ozer, H.L., et al., *SV40-mediated immortalization of human fibroblasts.* Exp Gerontol, 1996. **31**(1-2): p. 303-10.
147. Hartlerode, A.J. and R. Scully, *Mechanisms of double-strand break repair in somatic mammalian cells.* Biochem J, 2009. **423**(2): p. 157-68.
148. Liang, Y., et al., *DNA damage response pathways in tumor suppression and cancer treatment.* World J Surg, 2009. **33**(4): p. 661-6.
149. Brown, J.M. and B.G. Wouters, *Apoptosis, p53, and tumor cell sensitivity to anticancer agents.* Cancer Res, 1999. **59**(7): p. 1391-9.
150. Holt, S.E., et al., *Resistance to apoptosis in human cells conferred by telomerase function and telomere stability.* Mol Carcinog, 1999. **25**(4): p. 241-8.
151. Mulligan, G. and T. Jacks, *The retinoblastoma gene family: cousins with overlapping interests.* Trends Genet, 1998. **14**(6): p. 223-9.
152. Minkoff, R., et al., *Antisense oligonucleotide blockade of connexin expression during embryonic bone formation: evidence of functional compensation within a multigene family.* Dev Genet, 1999. **24**(1-2): p. 43-56.
153. Marschang, P., et al., *Normal development and fertility of knockout mice lacking the tumor suppressor gene LRP1b suggest functional compensation by LRP1.* Mol Cell Biol, 2004. **24**(9): p. 3782-93.
154. Tang, H., et al., *Influence of cell cycle phase on radiation-induced cytotoxicity and DNA damage in human colon cancer (HT29) and Chinese hamster ovary cells.* Radiat Res, 1994. **138**(1 Suppl): p. S109-12.

155. Terasima, T. and L.J. Tolmach, *Variations in several responses of HeLa cells to x-irradiation during the division cycle.* Biophys J, 1963. **3**: p. 11-33.
156. Digweed, M., et al., *SV40 large T-antigen disturbs the formation of nuclear DNA-repair foci containing MRE11.* Oncogene, 2002. **21**(32): p. 4873-8.
157. Popescu, N.C., S.C. Amsbaugh, and J.A. DiPaolo, *Human and rodent transformed cells are more sensitive to in vitro induction of SCE by N-methyl-N'-nitro-N-nitrosoguanidine (MNNG) than normal cells.* Hum Genet, 1983. **63**(1): p. 53-7.
158. Morrison, A.J. and X. Shen, *Chromatin remodelling beyond transcription: the INO80 and SWR1 complexes.* Nat Rev Mol Cell Biol, 2009. **10**(6): p. 373-84.
159. Ikura, T., et al., *DNA damage-dependent acetylation and ubiquitination of H2AX enhances chromatin dynamics.* Mol Cell Biol, 2007. **27**(20): p. 7028-40.
160. Li, H., et al., *The HINT1 tumor suppressor regulates both gamma-H2AX and ATM in response to DNA damage.* J Cell Biol, 2008. **183**(2): p. 253-65.
161. Branzei, D. and M. Foiani, *Regulation of DNA repair throughout the cell cycle.* Nat Rev Mol Cell Biol, 2008. **9**(4): p. 297-308.
162. Schleker, T., S. Nagai, and S.M. Gasser, *Posttranslational modifications of repair factors and histones in the cellular response to stalled replication forks.* DNA Repair (Amst), 2009. **8**(9): p. 1089-100.
163. Zhou, J., et al., *The role of NBS1 in the modulation of PIKK family proteins ATM and ATR in the cellular response to DNA damage.* Cancer Lett, 2006. **243**(1): p. 9-15.
164. Iijima, K., et al., *Dancing on damaged chromatin: functions of ATM and the RAD50/MRE11/NBS1 complex in cellular responses to DNA damage.* J Radiat Res (Tokyo), 2008. **49**(5): p. 451-64.
165. Traven, A. and J. Heierhorst, *SQ/TQ cluster domains: concentrated ATM/ATR kinase phosphorylation site regions in DNA-damage-response proteins.* Bioessays, 2005. **27**(4): p. 397-407.
166. Sidik, K. and M.J. Smerdon, *Nucleosome rearrangement in human cells following short patch repair of DNA damaged by bleomycin.* Biochemistry, 1990. **29**(32): p. 7501-11.
167. Kruhlak, M.J., et al., *Changes in chromatin structure and mobility in living cells at sites of DNA double-strand breaks.* J Cell Biol, 2006. **172**(6): p. 823-34.
168. Berkovich, E., R.J. Monnat, Jr., and M.B. Kastan, *Roles of ATM and NBS1 in chromatin structure modulation and DNA double-strand break repair.* Nat Cell Biol, 2007. **9**(6): p. 683-90.
169. Morrison, A.J., et al., *Mec1/Tel1 phosphorylation of the INO80 chromatin remodeling complex influences DNA damage checkpoint responses.* Cell, 2007. **130**(3): p. 499-511.
170. Ziv, Y., et al., *Chromatin relaxation in response to DNA double-strand breaks is modulated by a novel ATM- and KAP-1 dependent pathway.* Nat Cell Biol, 2006. **8**(8): p. 870-6.

171. White, D.E., et al., *KAP1, a novel substrate for PIKK family members, colocalizes with numerous damage response factors at DNA lesions.* Cancer Res, 2006. **66**(24): p. 11594-9.
172. Kim, G.D., et al., *Sensing of ionizing radiation-induced DNA damage by ATM through interaction with histone deacetylase.* J Biol Chem, 1999. **274**(44): p. 31127-30.
173. Riches, L.C., A.M. Lynch, and N.J. Gooderham, *Early events in the mammalian response to DNA double-strand breaks.* Mutagenesis, 2008. **23**(5): p. 331-9.
174. Lakin, N.D. and S.P. Jackson, *Regulation of p53 in response to DNA damage.* Oncogene, 1999. **18**(53): p. 7644-55.
175. Abraham, R.T., *Cell cycle checkpoint signaling through the ATM and ATR kinases.* Genes Dev, 2001. **15**(17): p. 2177-96.
176. Lavin, M.F. and S. Kozlov, *ATM activation and DNA damage response.* Cell Cycle, 2007. **6**(8): p. 931-42.
177. Kastan, M.B., et al., *ATM--a key determinant of multiple cellular responses to irradiation.* Acta Oncol, 2001. **40**(6): p. 686-8.
178. Rotman, G. and Y. Shiloh, *ATM: from gene to function.* Hum Mol Genet, 1998. **7**(10): p. 1555-63.
179. Siliciano, J.D., et al., *DNA damage induces phosphorylation of the amino terminus of p53.* Genes Dev, 1997. **11**(24): p. 3471-81.
180. Xu, B., et al., *Phosphorylation of serine 1387 in Brca1 is specifically required for the Atm-mediated S-phase checkpoint after ionizing irradiation.* Cancer Res, 2002. **62**(16): p. 4588-91.
181. Khanna, K.K., et al., *ATM associates with and phosphorylates p53: mapping the region of interaction.* Nat Genet, 1998. **20**(4): p. 398-400.
182. Canman, C.E., et al., *Activation of the ATM kinase by ionizing radiation and phosphorylation of p53.* Science, 1998. **281**(5383): p. 1677-9.
183. Banin, S., et al., *Enhanced phosphorylation of p53 by ATM in response to DNA damage.* Science, 1998. **281**(5383): p. 1674-7.
184. Chaturvedi, P., et al., *Mammalian Chk2 is a downstream effector of the ATM-dependent DNA damage checkpoint pathway.* Oncogene, 1999. **18**(28): p. 4047-54.
185. Matsuoka, S., M. Huang, and S.J. Elledge, *Linkage of ATM to cell cycle regulation by the Chk2 protein kinase.* Science, 1998. **282**(5395): p. 1893-7.
186. Barlow, C., et al., *Atm selectively regulates distinct p53-dependent cell-cycle checkpoint and apoptotic pathways.* Nat Genet, 1997. **17**(4): p. 453-6.
187. Marfella, C.G. and A.N. Imbalzano, *The Chd family of chromatin remodelers.* Mutat Res, 2007. **618**(1-2): p. 30-40.
188. Wang, X., et al., *CHD5 is down-regulated through promoter hypermethylation in gastric cancer.* J Biomed Sci, 2009. **16**: p. 95.
189. Tomimatsu, N., B. Mukherjee, and S. Burma, *Distinct roles of ATR and DNA-PKcs in triggering DNA damage responses in ATM-deficient cells.* EMBO Rep, 2009. **10**(6): p. 629-35.

190. Matsuoka, S., et al., *ATM and ATR substrate analysis reveals extensive protein networks responsive to DNA damage.* Science, 2007. **316**(5828): p. 1160-6.
191. Peng, G., et al., *BRIT1/MCPH1 links chromatin remodelling to DNA damage response.* Nat Cell Biol, 2009. **11**(7): p. 865-72.
192. Muchardt, C., et al., *The hbrm and BRG-1 proteins, components of the human SNF/SWI complex, are phosphorylated and excluded from the condensed chromosomes during mitosis.* Embo J, 1996. **15**(13): p. 3394-402.
193. An, W., J. Kim, and R.G. Roeder, *Ordered cooperative functions of PRMT1, p300, and CARM1 in transcriptional activation by p53.* Cell, 2004. **117**(6): p. 735-48.
194. Rubbi, C.P. and J. Milner, *p53 is a chromatin accessibility factor for nucleotide excision repair of DNA damage.* Embo J, 2003. **22**(4): p. 975-86.
195. Cheah, P.L. and L.M. Looi, *p53: an overview of over two decades of study.* Malays J Pathol, 2001. **23**(1): p. 9-16.
196. Lane, D.P. and L.V. Crawford, *T antigen is bound to a host protein in SV40-transformed cells.* Nature, 1979. **278**(5701): p. 261-3.
197. Mowat, M., et al., *Rearrangements of the cellular p53 gene in erythroleukaemic cells transformed by Friend virus.* Nature, 1985. **314**(6012): p. 633-6.
198. Lavin, M.F. and N. Gueven, *The complexity of p53 stabilization and activation.* Cell Death Differ, 2006. **13**(6): p. 941-50.
199. Sakaguchi, K., et al., *DNA damage activates p53 through a phosphorylation-acetylation cascade.* Genes Dev, 1998. **12**(18): p. 2831-41.
200. Liu, L., et al., *p53 sites acetylated in vitro by PCAF and p300 are acetylated in vivo in response to DNA damage.* Mol Cell Biol, 1999. **19**(2): p. 1202-9.
201. Petitjean, A., et al., *TP53 mutations in human cancers: functional selection and impact on cancer prognosis and outcomes.* Oncogene, 2007. **26**(15): p. 2157-65.
202. Bauer, A. and B. Kuster, *Affinity purification-mass spectrometry. Powerful tools for the characterization of protein complexes.* Eur J Biochem, 2003. **270**(4): p. 570-8.
203. Gingras, A.C., R. Aebersold, and B. Raught, *Advances in protein complex analysis using mass spectrometry.* J Physiol, 2005. **563**(Pt 1): p. 11-21.
204. Puig, O., et al., *The tandem affinity purification (TAP) method: a general procedure of protein complex purification.* Methods, 2001. **24**(3): p. 218-29.
205. Gregan, J., et al., *Tandem affinity purification of functional TAP-tagged proteins from human cells.* Nat Protoc, 2007. **2**(5): p. 1145-51.
206. Deutsch, E.W., H. Lam, and R. Aebersold, *Data analysis and bioinformatics tools for tandem mass spectrometry in proteomics.* Physiol Genomics, 2008. **33**(1): p. 18-25.
207. Goodlett, D.R. and E.C. Yi, *Proteomics without polyacrylamide: qualitative and quantitative uses of tandem mass spectrometry in proteome analysis.* Funct Integr Genomics, 2002. **2**(4-5): p. 138-53.
208. Gavin, A.C., et al., *Functional organization of the yeast proteome by systematic analysis of protein complexes.* Nature, 2002. **415**(6868): p. 141-7.

209. Rohila, J.S., et al., *Improved tandem affinity purification tag and methods for isolation of protein heterocomplexes from plants.* Plant J, 2004. **38**(1): p. 172-81.
210. Giannone, R.J., et al., *Dual-tagging system for the affinity purification of mammalian protein complexes.* Biotechniques, 2007. **43**(3): p. 296, 298, 300 passim.
211. Connelly, H.M., et al., *Characterization of pII family (GlnK1, GlnK2, and GlnB) protein uridylylation in response to nitrogen availability for Rhodopseudomonas palustris.* Anal Biochem, 2006. **357**(1): p. 93-104.
212. Eng, J.K., A.L. Mccormack, and J.R. Yates, *An Approach to Correlate Tandem Mass-Spectral Data of Peptides with Amino-Acid-Sequences in a Protein Database.* Journal of the American Society for Mass Spectrometry, 1994. **5**(11): p. 976-989.
213. Tabb, D.L., W.H. McDonald, and J.R. Yates, 3rd, *DTASelect and Contrast: tools for assembling and comparing protein identifications from shotgun proteomics.* J Proteome Res, 2002. **1**(1): p. 21-6.
214. Bressan, G.C., et al., *Functional association of human Ki-1/57 with pre-mRNA splicing events.* Febs J, 2009.
215. Junttila, M.R., et al., *Single-step Strep-tag purification for the isolation and identification of protein complexes from mammalian cells.* Proteomics, 2005. **5**(5): p. 1199-203.
216. Bond, C.S. and A.H. Fox, *Paraspeckles: nuclear bodies built on long noncoding RNA.* J Cell Biol, 2009. **186**(5): p. 637-44.
217. Patton, J.G., et al., *Cloning and characterization of PSF, a novel pre-mRNA splicing factor.* Genes Dev, 1993. **7**(3): p. 393-406.
218. Lutz, C.S., et al., *The snRNP-free U1A (SF-A) complex(es): identification of the largest subunit as PSF, the polypyrimidine-tract binding protein-associated splicing factor.* Rna, 1998. **4**(12): p. 1493-9.
219. Emili, A., et al., *Splicing and transcription-associated proteins PSF and p54nrb/nonO bind to the RNA polymerase II CTD.* Rna, 2002. **8**(9): p. 1102-11.
220. Hata, K., et al., *Paraspeckle protein p54nrb links Sox9-mediated transcription with RNA processing during chondrogenesis in mice.* J Clin Invest, 2008. **118**(9): p. 3098-108.
221. Caceres, J.F., et al., *Regulation of alternative splicing in vivo by overexpression of antagonistic splicing factors.* Science, 1994. **265**(5179): p. 1706-9.
222. Gattoni, R., et al., *Modulation of alternative splicing of adenoviral E1A transcripts: factors involved in the early-to-late transition.* Genes Dev, 1991. **5**(10): p. 1847-58.
223. Wen, X., et al., *Structural organization and cellular localization of tuftelin-interacting protein 11 (TFIP11).* Cell Mol Life Sci, 2005. **62**(9): p. 1038-46.
224. Stoss, O., et al., *The in vivo minigene approach to analyze tissue-specific splicing.* Brain Res Brain Res Protoc, 1999. **4**(3): p. 383-94.
225. Wang, P., et al., *Modulation of alternative pre-mRNA splicing in vivo by pinin.* Biochem Biophys Res Commun, 2002. **294**(2): p. 448-55.

226. Myojin, R., et al., *Expression and functional significance of mouse paraspeckle protein 1 on spermatogenesis.* Biol Reprod, 2004. **71**(3): p. 926-32.
227. Bagchi, A., et al., *CHD5 is a tumor suppressor at human 1p36.* Cell, 2007. **128**(3): p. 459-75.
228. Nakano, K. and K.H. Vousden, *PUMA, a novel proapoptotic gene, is induced by p53.* Mol Cell, 2001. **7**(3): p. 683-94.
229. Brooks, C.L. and W. Gu, *Ubiquitination, phosphorylation and acetylation: the molecular basis for p53 regulation.* Curr Opin Cell Biol, 2003. **15**(2): p. 164-71.
230. Barlev, N.A., et al., *Acetylation of p53 activates transcription through recruitment of coactivators/histone acetyltransferases.* Mol Cell, 2001. **8**(6): p. 1243-54.
231. Naidu, S.R., et al., *The SWI/SNF chromatin remodeling subunit BRG1 is a critical regulator of p53 necessary for proliferation of malignant cells.* Oncogene, 2009. **28**(27): p. 2492-501.
232. Luo, J., et al., *Deacetylation of p53 modulates its effect on cell growth and apoptosis.* Nature, 2000. **408**(6810): p. 377-81.
233. Gould, K.L., et al., *Tandem affinity purification and identification of protein complex components.* Methods, 2004. **33**(3): p. 239-44.
234. Kaiser, P., et al., *Tandem affinity purification combined with mass spectrometry to identify components of protein complexes.* Methods Mol Biol, 2008. **439**: p. 309-26.
235. Knuesel, M., et al., *Identification of novel protein-protein interactions using a versatile mammalian tandem affinity purification expression system.* Mol Cell Proteomics, 2003. **2**(11): p. 1225-33.
236. Fox, A.H., C.S. Bond, and A.I. Lamond, *P54nrb forms a heterodimer with PSP1 that localizes to paraspeckles in an RNA-dependent manner.* Mol Biol Cell, 2005. **16**(11): p. 5304-15.
237. Dong, B., et al., *Purification and cDNA cloning of HeLa cell p54nrb, a nuclear protein with two RNA recognition motifs and extensive homology to human splicing factor PSF and Drosophila NONA/BJ6.* Nucleic Acids Res, 1993. **21**(17): p. 4085-92.
238. Shav-Tal, Y. and D. Zipori, *PSF and p54(nrb)/NonO--multi-functional nuclear proteins.* FEBS Lett, 2002. **531**(2): p. 109-14.
239. Bladen, C.L., et al., *Identification of the polypyrimidine tract binding protein-associated splicing factor.p54(nrb) complex as a candidate DNA double-strand break rejoining factor.* J Biol Chem, 2005. **280**(7): p. 5205-10.
240. Akhmedov, A.T. and B.S. Lopez, *Human 100-kDa homologous DNA-pairing protein is the splicing factor PSF and promotes DNA strand invasion.* Nucleic Acids Res, 2000. **28**(16): p. 3022-30.
241. Morozumi, Y., et al., *Human PSF binds to RAD51 and modulates its homologous-pairing and strand-exchange activities.* Nucleic Acids Res, 2009. **37**(13): p. 4296-307.

242. Li, S., et al., *Involvement of p54(nrb), a PSF partner protein, in DNA double-strand break repair and radioresistance.* Nucleic Acids Res, 2009. **37**(20): p. 6746-53.
243. Straub, T., et al., *The RNA-splicing factor PSF/p54 controls DNA-topoisomerase I activity by a direct interaction.* J Biol Chem, 1998. **273**(41): p. 26261-4.
244. Schwartz, S., E. Meshorer, and G. Ast, *Chromatin organization marks exon-intron structure.* Nat Struct Mol Biol, 2009. **16**(9): p. 990-5.
245. Kornblihtt, A.R., *Chromatin, transcript elongation and alternative splicing.* Nat Struct Mol Biol, 2006. **13**(1): p. 5-7.
246. de Almeida, S.F. and M. Carmo-Fonseca, *The CTD role in cotranscriptional RNA processing and surveillance.* FEBS Lett, 2008. **582**(14): p. 1971-6.
247. de la Mata, M., et al., *A slow RNA polymerase II affects alternative splicing in vivo.* Mol Cell, 2003. **12**(2): p. 525-32.
248. Batsche, E., M. Yaniv, and C. Muchardt, *The human SWI/SNF subunit Brm is a regulator of alternative splicing.* Nat Struct Mol Biol, 2006. **13**(1): p. 22-9.
249. Tyagi, A., et al., *SWI/SNF associates with nascent pre-mRNPs and regulates alternative pre-mRNA processing.* PLoS Genet, 2009. **5**(5): p. e1000470.
250. Lusser, A. and J.T. Kadonaga, *Chromatin remodeling by ATP-dependent molecular machines.* Bioessays, 2003. **25**(12): p. 1192-200.
251. Becker, P.B. and W. Horz, *ATP-dependent nucleosome remodeling.* Annu Rev Biochem, 2002. **71**: p. 247-73.
252. Luo, R.X. and D.C. Dean, *Chromatin remodeling and transcriptional regulation.* J Natl Cancer Inst, 1999. **91**(15): p. 1288-94.
253. Reisman, D., S. Glaros, and E.A. Thompson, *The SWI/SNF complex and cancer.* Oncogene, 2009. **28**(14): p. 1653-68.
254. Muchardt, C. and M. Yaniv, *The mammalian SWI/SNF complex and the control of cell growth.* Semin Cell Dev Biol, 1999. **10**(2): p. 189-95.
255. Jeong, S.M., et al., *The SWI/SNF chromatin-remodeling complex modulates peripheral T cell activation and proliferation by controlling AP-1 expression.* J Biol Chem, 2010. **285**(4): p. 2340-50.

Vita

Sangeetha Rajagopalan was born on September 4th, 1979 in a small city in India. She moved to New Delhi in 1990 and graduated from high school in 1997. She then received her Bachelor of Science degree in Microbiology from Bharathidasan University in Tamil-Nadu, in the year 2000. After completing her Bachelor of Science degree with distinction, she joined Birla Institute of Technology (BITS), Pilani for Masters. During her Masters' she carried out her thesis work in the Department of Molecular Biology and Genetics at Sankara Nethralaya, Chennai. Her thesis work was on analyzing the molecular genetics of Glaucoma in Indian population. She was a co-author in a research article published in *Clinical Genetics*, highlighting the findings of this work.

After graduating from BITS she joined All India Institute of Medical Sciences, New Delhi as a Junior Research Associate in the department of Molecular Microbiology. Here she was a part of a research group that worked on novel molecular diagnostic for eye disease and vision enhancement devices. This research project was funded by Council of Scientific and Industrial Research (India). In 2004, she joined the PhD program in Genome Science and Technology at The University of Tennessee, Knoxville.